lek. Marcin Strojny

Novel Human Epineural Sheath Conduit Supported with Human Mesenchymal Stem Cells to Restore Long Nerve Defects in Rat Experimental Model

A thesis submitted for the degree of Doctor of Medical Sciences

Thesis Advisor: Maria Siemionow, M.D., Ph.D., D.Sc.

College of Medical Sciences
Poznań University of Medical Sciences

Poznań, 2021

I would like to sincerely thank:

Professor Maria Siemionow

For her advice, her patience, invaluable support, and help
at every stage of the preparation of this doctoral dissertation

Professor Krzysztof Słowiński

For his unwavering support
and allowing me to follow my dreams and ambitions

Microsurgery Laboratory Team

For their help in completing my experiments

To My Family

For their support during this process

I would like to dedicate this work
to my wife, daughter, parents
and the rest of my family

TABLE OF CONTENTS

ABBREVIATIONS

ANG: Advance Nerve Graft

BDNF: Brain-Derived Neurotrophic Factor

BMSC: Bone Marrow Stromal Cells

CNTF: Ciliary Neurotrophic Factor

ESC: Epineural Sheath Conduit

FDA: Food and Drug Administration

FGF Basic Fibroblast Growth Factor

GDNF: Glial Cell Line-Derived Neurotrophic Factor

GFAP: Glial Fibrillary Acidic Protein

GMI: Gastrocnemius Muscle Index

hESC: Human Epineural Sheath Conduit

HIV: Human Immunodeficiency Virus

hMSC: Human Mesenchymal Stem Cells

IED: Improvised Explosive Devices

IGF: Insulin-Like Growth Factor

IL-6: Interleukin 6

MCP: Monocyte Chemoattractant Protein

MHC: Major Histocompatibility Complex

MSCGM: Mesenchymal Stem Cell Growth Medium

MTF: Musculoskeletal Transplant Foundation

NGF: Nerve Growth Factor

NMNAT2: Nicotinamide/nicotinic acid mononucleotide adenylyltransferase 2

PNA: Peripheral Nerve Autograft

PNI: Peripheral Nerve Injury

SC: Schwann cells

TBS: Tris Buffered Saline

TEST: Turnover Epineural Sheath Tube

UIC: University of Illinois at Chicago

VEGF: Vascular Endothelial Growth Factor

vWF: von Willebrand factor

KEY WORDS: nerve injury, nerve gap, nerve repair, conduit, allograft, mesenchymal stem cells

SŁOWA KLUCZOWE: uraz nerwu, ubytek nerwu, naprawa nerwu, konduit, alograft, mezenchymalne komórki macierzyste

1. INTRODUCTION

1.1. Anatomy and Physiology of the Peripheral Nervous System

The knowledge of the peripheral nervous system's anatomy and physiology is essential for understanding the pathophysiology and treatment after nerve injuries. The peripheral nervous system is divided into the afferent and efferent nerves. Afferent nerves, also called sensory nerves, collect information from receptors and conduct impulses to the central nervous system for interpretation. Efferent nerves, also called motor nerves, conduct impulses from the central nervous system to the periphery, prompting a response. Efferent nerves are divided into the somatic nervous system - the voluntary impulses to skeletal muscles - and the autonomic nervous system - the involuntary impulses to the cardiac muscle, smooth muscles, and glands.

On a cellular level, the peripheral nervous system consists of neurons and neuroglia. The neuron is an electrically excitable cell, and its function is to communicate over long distances. Neuroglia, the supporting cells whose function is to provide homeostasis to the nervous system, cannot propagate action potentials; however, their role is essential to nerve function.[1,2]

A nerve cell has multiple dendrites that stem from the cell body and gather stimuli from either other cells or the surrounding. The cell body contains the nucleolus and provides the nerve with its functional needs through different organelles. A narrowing of the cell body is the axon's hillock, which joins with the cell's axon. The axons' role is to propagate the action potential to the terminal buttons, passing on the impulse to another nerve, muscle, or gland.[1]

Schwann cells, a neuroglia of the peripheral nervous system, provides essential support to maintain the proper function of the neuron. One of the critical physiological functions of Schwann cells is to create spiral layers of myelin by wrapping its plasma membrane around the axon. Each Schwann cell forms a single myelin. This allows for the formation of gaps of about 1 μm in length between the myelin, also called the nodes of Ranvier. In these areas, voltage-gated sodium channels accumulate, which allows for a significant increase in the speed of the action potentials by allowing the impulse to "skip" between the nodes.[3] Not all axons are myelinated.

This allowed Erlanger and Gasser, as the first, to categorize nerve fibers into three groups[4]:
Group A - myelinated fibers of size ranging between 1-22 μm and velocities from 5-120 m/s
Group B - myelinated fibers of size below 3 μm and velocities 3-15 m/s
Group C - unmyelinated fibers of size ranging between 0.1- 1.3 μm and velocities 0.6-2.0 m/s

Each axon, either myelinated or unmyelinated, is surrounded by a connective tissue layer called endoneurium or Henle's sheath. It is formed by two layers of connective tissue. The outer layer is composed of longitudinally oriented fibers called the sheath of Key and Retzius, while the inner layer of the interwoven thin fibrils is called the sheath of Plenk and Laidlaw.[5] The sheaths are mainly constructed by type I collagen, which is produced by the Schwann cells. Endoneurium is a permeable layer, which provides a nutritive and protective function.[6]

Multiple axons, surrounded by a fibrous layer called the perineurium, are called nerve fascicles. The perineurium is composed of multiple concentric layers of the perineurial cells. By means of tight junctions, this layer forms a metabolically active diffusion barrier of the nerve.[7]

The epineurium is the external layer of connective tissue, which constitutes the anatomical border of the nerve. It contains the vasa nervorum, which represents the microvasularization of the nerve penetrating to the perineurium. It also contains the nervi nervorum, the small nerve fibers that penetrate all the way to the endoneurium (Figure 1).

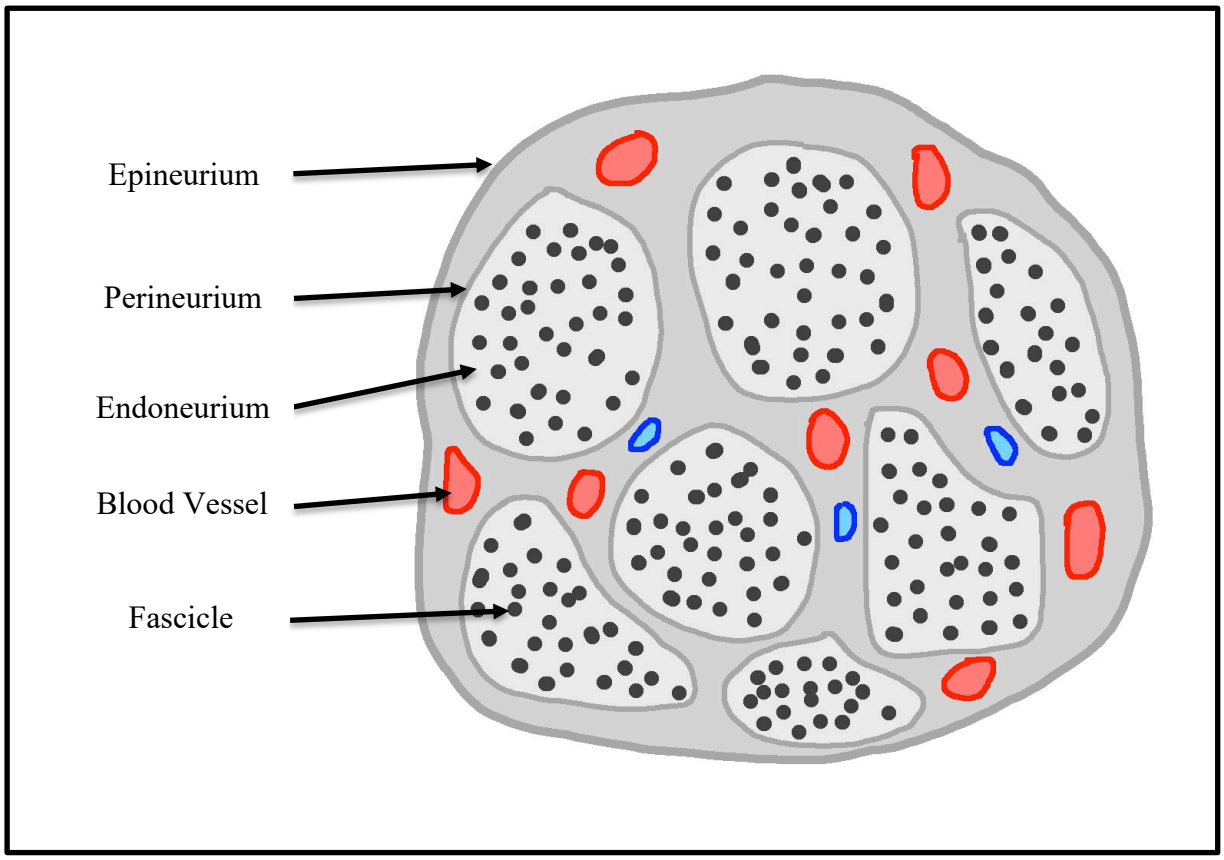

Figure 1. Diagram of the cross-section of a Peripheral Nerve. Authors own artwork.

1.2. Peripheral Nerve Injury

Peripheral nerve injuries (PNI) are most commonly caused by traumatic events, leading to functional loss in 2.8% of trauma patients.[8] They affect over 1 million people worldwide each year, leading to approximately 100,000 peripheral nerve surgery repairs in the US and Europe alone.[9,10] Although stretch-related injuries are the most common in the civilian setting, lacerations (glass, knife, fan, saw accidents) account for about 30% of all cases. In the military setting, PNI commonly occur in blast injuries caused by the improvised explosive devices (IED) or bombs.[11]

There are two classifications of peripheral nerve injuries which help to assess the timing of nerve repair and the potential of success following nerve injury. The simpler classification was developed by Seddon and was divided into three categories: neurapraxia, axonotmesis, and neurotmesis. Neurapraxia is the least severe with the continuity of the nerve maintained; however, the nerve cannot transmit impulses, which leads to transient functional loss. This is thought to be caused by the segmental demyelination of the nerve. In the case of axonotmesis, the axon is completely severed, while the connective tissue (perineurium, epineurium) surrounding the injured area remains intact. This can lead to spontaneous recovery as the regenerating axon is provided guidance by the uninjured connective tissue. Neurotmesis represents the most severe nerve injury where the entire cross-sectional area of the nerve becomes severed. This leads to fibrosis of the nerve stumps and loss of guidance, and regenerative axonal sprouting. In this case, surgical intervention is usually indicated to restore nerve function.

Sutherland's classification of nerve injury is divided into five degrees. First-degree and second-degree injuries correspond to Seddon's neurapraxia and axonotmesis, respectively. Third-degree injury is classified when axonotmesis occurs with damage to the endoneurium. Functional recovery may take place, depending on the degree of endoneurial damage. Fourth-degree occurs when all portions of the nerve except the epineurium are interrupted. Finally, a fifth-degree injury is diagnosed when the entire nerve is severed. Both the fourth and fifth-degree injuries require surgical intervention for nerve recovery (Table 1).[11,12]

Table 1. Sunderland's and Seddon's Classification of Peripheral Nerve Injury [11,12]

Sunderland	Seddon	Injury	Outcome
First degree	Neurapraxia	Segmental Demyelination (Transient functional loss)	Spontaneous Recovery
Second degree	Axonotmesis	Axon is completely severed, while the connective tissue (perineurium, epineurium) surrounding the injured area is in intact	Prospect of spontaneous recovery is excellent
Third degree	Axonotmesis	Axon is completely severed, with injury to the endoneurium	Functional recovery depends on the degree of damage
Fourth degree	Axonotmesis	All portions of the nerve severed except the epineurium	Surgical intervention
Firth degree	Neurotmesis	Complete severance of the nerve	Surgical intervention

1.3. Pathophysiology of Peripheral Nerve Injury and Regeneration

Unlike other cells, peripheral nerve response to injury does not involve mitosis or cellular proliferation.[12] Transection nerve injuries can either recover through collateral branching of the uninjured axons or by axonal regeneration.[13] If only 20-30% of the axons are damaged, nerve recovery occurs through the non-injured axons' collateral branching.[14] However, if more than 90% of the axons are severed, recovery of the nerve may be achieved through the regeneration of the injured axon.[15]

Regeneration of the injured axon is a multifaceted process that differs between the proximal and distal stump. The changes in the proximal stump differ based on the location of the injury. Proximal injury near the cell body can lead to apoptosis, while the axon's distal injury can lead to degradation to the nearest node of Ranvier.[16]

To prepare for axonal regeneration, the cell body goes through the process known as chromatolysis in the first 6 hours postinjury. The nucleus is relocated to the edge of the cell, and Nissl granules, rough endoplasmic reticulum, break up and disperse.[12,14] This process indicates a shift in metabolic priority from the creation of neurotransmitters to the production of the components necessary for axonal repair.[17]

Essential elements of the cytoskeleton, such as actin, tubulin, and neurofilament proteins, are transferred down by anterograde transport.[18] The upregulation of multiple regenerative-associated genes such as c-Jun[19], ATF-3[20], Sox-11[21] is essential in the regeneration process.[22]

Axonal regeneration begins with the forming of a growth cone at the distal tip of the proximal end of the injury. The growth cone plays an essential role in axon guidance and is believed to respond to contact guidance clues afforded by laminin and fibronectin, two major glycoprotein components of the basal lamina of the Schwann cell and other portions of the extracellular matrix.[17] Further guidance of the regenerating neurites is achieved through neurotrophic factors, such as NGF, which is also produced by Schwann cells. NGF promotes the growth and proliferation of Schwann cells and is also found on the receptors of Schwann cell lining bands of Büngner to provide trophism to the outgrowing axon.[15]

Just hours after injury, the failure to deliver adequate amounts of the essential axonal protein Nicotinamide/nicotinic acid mononucleotide adenylyltransferase 2 (NMNAT2) to the distal end of the injured nerve will stimulate the process known as Wallerian (or anterograde) degeneration, which creates the microenvironment for nerve recovery.[23,24] Axonal fragmentation begins within hours after sustaining injury. This is followed soon by the degradation of the myelin sheath. Schwann cells become activated in the first 24 hours through

a sudden inflow of Ca+ and Na+, displaying nuclear and cytoplasmic enlargement as well as an increased mitotic rate.[14] Its initial role is to remove the degenerated axonal and myelin debris and then pass it on to macrophages. Both these cells work together for phagocytosis and clear the injured site. This process is supported by endoneurial mast cells, which release histamine and serotonin, enhancing capillary permeability to macrophages.[12] Later in the process, stacks of Schwann cell processes representing collapsed endoneurial tubes form columns known as the bands of Büngner and become essential guides for sprouting axons during reinnervation (Figure 2).[12,15]

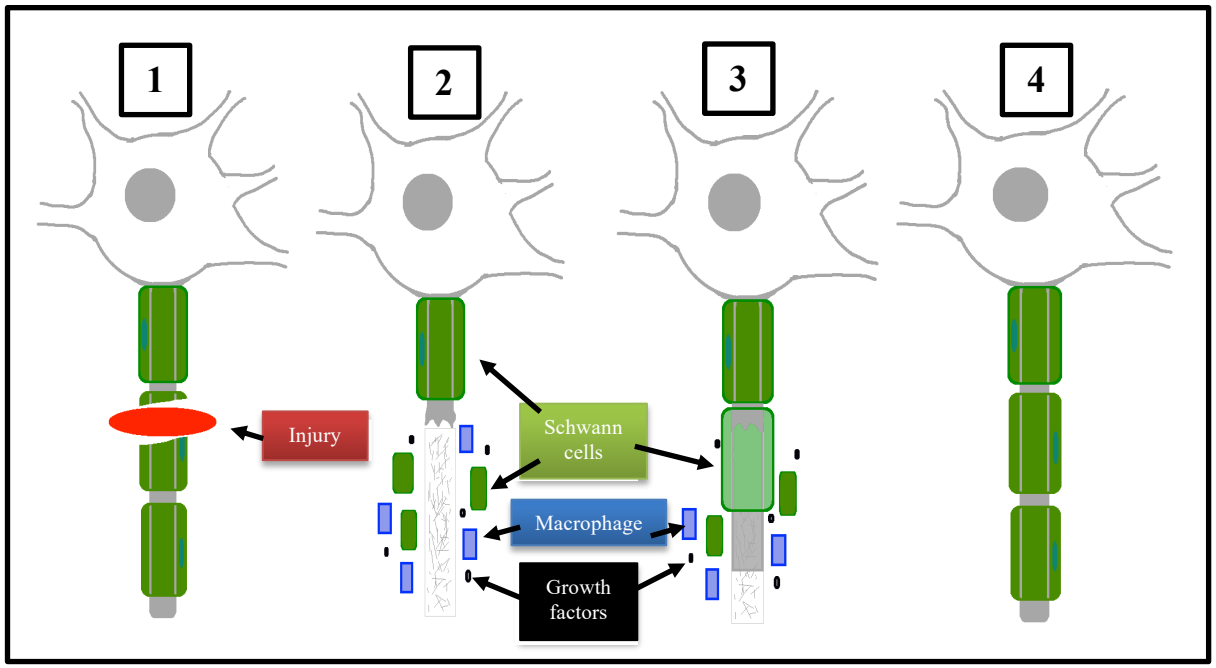

Figure 2. Peripheral Nerve Regeneration. 1 - Injury to the axon; 2 - Wallerian degeneration; 3 - Nerve reconstruction; 4 - Reinnervation of the target organ. Authors own artwork.

The rate of regeneration of an axon may vary between 1-3 mm/day. When the cone reaches the endoneurial tube, the nerve is guided, as mentioned above. The nerve goes through the process of remyelination, axonal enlargement, and finally, end-organ innervation.[14]

Unfortunately, reinnervation does not always mean functional nerve recovery. In large gap injuries, it is generally assumed to be that regenerating axons fail to reinnervate target muscles due to irreversible denervation atrophy with ultimate fat replacement.[25,26,27] Furthermore, in large gap injuries, limited sensory recovery is observed due to sensory axons failing to reach the skin, cross-reinnervation, and possibly degeneration of sensory receptors.[12]

1.4. Current Surgical Management of Nerve Gaps

Tension-free repair is the optimal technique in the repair of peripheral nerve injuries.[28] However, this method may not be feasible due to nerve retraction, fibrosis, or tissue loss generating a nerve gap. [29,31] When end-to-end coaptation of the nerve stumps is achieved under tension, the microvascular flow in the nerve is disrupted, leading to ischemia and eventually nerve fibrosis. This outcome limits fascicular recovery, leading to poor clinical outcomes.[30] When the surgeon is presented with this type of nerve damage, an alternative strategy must be applied to repair the injured nerve. Although multiple methods are available, each has its benefits and risks of complications, which must be considered before choosing the proper method of nerve repair (Table 2).

1.4.1. Peripheral Nerve Autograft Repair

Peripheral Nerve Autograft (PNA) is viewed as the "gold standard" for the nerve gap repair treatment, especially for peripheral nerve gaps >5 cm in length.[31,32] The most commonly used nerve autograft in the reconstruction of nerve gaps is the sural nerve. However, the medial and lateral cutaneous nerves of the forearm, the dorsal cutaneous branch of the ulnar nerve, the superficial and deep peroneal nerves, the intercostals nerves, and the posterior and lateral cutaneous nerves of the thigh have also been applied as the autograft.[33,34] Autografts are considered the ideal option for nerve gap repair since they are not immunogenic and supply both Schwann cells and neurotrophic factors.[35-37] However, both the surgeon and the patient must consider the limitations of the autograft technique, which include donor site morbidity, the potential of neuroma creation, and its limited availability.[31]

1.4.2. Application of the Peripheral Nerve Transfer

The Peripheral Nerve Transfer technique involves coaptation between a nearby normal donor nerve and the distal denervated nerve close to the target endplate. This approach leads to a quicker target muscle reinnervation by shortening the distance required for nerve regeneration. This method is notably valuable when the nerve injury is far from the endplate, which leads to the risk of unsatisfactory clinical outcomes.[32,38] A modified variant utilizes selected fascicles of the donor's nerve, which are coapted to the injured nerve.[11] Application of the Nerve Transfer can be utilized in both brachial plexus and proximal injuries that are far away from the target motor endplate. Furthermore, they can be used to treat significant limb trauma producing segmental impairment of nerve function as well as managing injuries with

notable scarring encompassing essential bony or vascular structures. This method prevents Autograft related morbidity; however, it may lead to the impairment of function in the donor nerve. This leads to the loss of the donor's muscles application in a possible muscle transfer. [31]

Table 2. Various Techniques of Nerve Gap Repair [31]

	Pros	Cons
Peripheral Nerve Autograft	• Nonimmunogenic • Bridge nerve gap	• Sensory loss • Neuroma formation • Scarring • Second incision • Limited supply
Nerve Transfer	• Typically avoid donor autografts and associated morbidity • Proximity of donor nerves to target motor endplates provides earlier reinnervation	• Possible loss of function from donor nerve site • Donor muscle is no longer an acceptable donor for muscle transfer
End-to-side Coaptation	• Useful when minimal sensory recovery is needed	• Will not result in motor recovery without donor axonal injury
Peripheral Nerve Allografts	• Readily accessible • Unlimited supply • Bridge nerve gap • Avoids donor site morbidity	• Potential side effects of immunosuppression
Nerve Conduits	• Readily available • Avoids donor site morbidity • Bridges a nerve gap • Barrier to scar tissue infiltration • Allows for accumulation of local neurotrophic factors • Allows to be combined with different stem cell lines e.g., BMSC, MSC	• Variable outcomes • Lack of laminin scaffold and Schwann cells • Limits its use to short nerve gaps • Potential foreign body material response

1.4.3. Technique of End-to-Side Nerve Coaptation

End-to-side repair was first described in the 1900s. It creates a coaptation between the distal stump of the injured nerve to the side of a normal nerve that is in its proximity. [39,40, 41,42,43] For the treatment of motor nerve dysfunction, donor nerves axotomy is required to induce budding into the distal stump of the injured nerve.[44] However, for sensory transfers, it has been shown to bud spontaneously without donor nerve injury. According to Ray et al., end-to-side repairs should be implemented to noncritical sensory nerve injuries only. Although this technique is beneficial for treating minimal sensory recovery, its motor recovery limitations have made this method less than dependable.[31]

1.4.4. Peripheral Nerve Allograft Technique

Peripheral Nerve Allografts can be applied in large or segmental nerve injuries, where the nerve gap is between 20-40 cm in large-caliber nerves.[32] The cadaveric tissue contains Schwann cells (SC), which play a crucial role in the remyelination of nerves but are also antigen-presenting cells. Because SC display major histocompatibility complex (MHC) II molecules, systemic immunosuppression is required until host SC can migrate into the allograft, a process that usually takes 18-24 months.[45-51]

To inhibit allograft rejection, agents such as Tacrolimus, Cyclosporine A, Azathioprine, and Prednisone have been used. The most prevalent side effects of these medications, such as infections, malignancies, and metabolic disturbances have been noted, yet are relatively uncommon due to the short duration of therapy in patients with peripheral nerve injuries. Furthermore, studies have suggested that Tacrolimus possesses a positive effect on the regeneration of the injured nerves. To reduce the antigenicity of the nerve allograft, multiple methods such as irradiation, cold preservation, and lyophilization have been practiced.[52-61]

1.4.5. Application of Nerve Conduits

Nerve Conduits can be used in the treatment of nerve gaps when a tension-free repair is unattainable. The first attempt to apply a conduit in the treatment of nerve gaps transpired in the 1880s when Gluck unsuccessfully tried to bridge a nerve gap with decalcified bone.[62] Since that time, both biological and synthetic conduits have been investigated, leading to numerous being commercially available (Table 3). The conduits' primary role is to provide axonal guidance, separate the developing axons from the neighboring tissue, restrict inflammation and fibrosis, and reduce the chances of neuroma formation. However, their application is limited

to small nerve gaps as they lack neurogenic, angiogenic, and anti-inflammatory factors, such as Schwann cells.[31]

Table 3. Key properties of the effective nerve conduit [63]

The effective nerve conduit should possess several key properties
Biocompatible- no inflammatory response
Resist tears from sutures and tissue inflammation
Flexible and soft
Semipermeable
Prevent fibrous tissue ingrowth

Biological conduits such as veins, arteries, muscles, tendons, and epineurium have been extensively researched as alternatives to standard methods. A prospective clinical evaluation of autologous vein grafts by Chiu et al. found that veins produce similar results to sural nerve digital grafts.[64] Nijhuis et al. conducted a study on the rat model with a 1.5 cm sciatic nerve defect. They reported favorable results when using vein conduits filled with muscle to prevent collapse.[65] Unlike vein grafts, skeletal muscles longitudinally oriented basal lamina enhances cell adhesion to the extracellular matrix. Fawcett et al. reported, using both the anatomical and functional criteria, that sciatic nerve repair using muscle basal lamina grafts had comparable regeneration rates to the Autograft.[66] Brandt et al. published multiple studies investigating the use of tendon as a possible bridging material for nerve gaps compared to the freeze-thawed muscle grafts. These studies concluded that the efficacy of tendon application is comparable to freeze-thawed muscle grafts. The abundant amount of tendon and the limited loss of function makes this bridging material a possible alternative.[67-69]

In recent years, significant interest has been devoted to the Epineural Sheath conduits. As a naturally occurring tissue, epineural sheath lack of Schwann cells provides the surgeon with an ideal allogenic material that does not require immunosuppression.[70,71] Furthermore, it has been reported by Yavuzer et al. that epineural sheath, using the turnover epineural sheath tube (TEST) technique, can decrease foreign body reaction and decrease inflammatory response with less fibrosis in the area of the end-to-end coaptation.[72] Similar findings were reported using the epineural sleeve technique, which was found to be superior to conventional nerve repair.[73,74] Siemionow's group has been studying the use of epineural sheath conduits as an alternative method to bridge nerve gaps. In their research, 20 mm sciatic nerve gaps were created in the rat model, followed by Epineural Tube Repair with or without Bone Marrow

Stromal Cells (BMSC). Their findings demonstrated comparable results between the epineural tube/BMSC conduits and Autograft repair.[75]

1.5. Human Mesenchymal Stem Cells

Mesenchymal Stem Cells (MSC) are stromal stem cells that can differentiate into cells of the mesodermal linage as well as cells of other embryonic lineages depending on the signal from the microenvironment. MSC can be isolated from several tissues, such as bone marrow, adipose tissue, or umbilical cord, though bone marrow remains the most commonly used source. Tissue-containing stem cells have the capability for renewal after insult from trauma, disease, or aging, with the population of stem cells being within the tissue or in stem cell reservoirs.[76] Mesenchymal stem cells are weakly immunogenic, and their neurodegenerative potential has been comprehensively investigated. Therefore, MSC may prevail as a new and promising cell-based therapy applied for the enhancement of peripheral nerve regeneration.

MSC are known to improve neuronal function by secreting neurotrophic, growth factors, and cytokines such as brain-derived neurotrophic factor (BDNF), Ciliary neurotrophic factor (CNTF), Glial cell line-derived neurotrophic factor (GDNF), Insulin-like growth factor (IGF), Interleukin 6 (IL-6) and Nerve growth factor (NGF).[77,78,79,80,81] These factors can promote differentiation, proliferation, and survival of nerve cells. For example, BDNF, through the activation of the JAK/STAT, promotes regeneration via activation of Schwann Cells rather than by directly affecting the nerve fibers.[82] IGF was discovered to improve neurite growth and branching from embryonic motoneurons, with exogenous administration improving regeneration of motor axons and promoting Schwann cells in lesions of the sciatic nerve.[83,84] NGF research has confirmed its regulation of neurotransmitters and neuropeptides synthesis of sympathetic and sensory nerves while showing protective actions on degenerating peripheral nerves.[85,86]

MSC has also been found to produce multiple extracellular matrix elements, such as fibronectin, laminin, and collagen.[87] In vivo studies have shown the supportive role of MSC in extracellular matrix production, which supports neurogenesis such as neurite development.[88,89]

Numerous authors have reported that MSC produce a variety of angiogenic cytokines, such as Vascular endothelial growth factor (VEGF), Basic fibroblast growth factor (FGF), Hepatocyte growth factor, Insulin-like growth factor 1, Monocyte chemoattractant protein (MCP)-2, and MCP-3.[90,91,92,93,94] Tang et al. provide evidence that through implantation of MSC into ischemic myocardium, an increase in VEGF, vascular density, and regional blood

flow have decreased apoptosis. It was further suggested that MSC differentiate into endothelial cells, which support angiogenesis.[95]

MSC can communicate with cells of both the innate and adaptive immune systems, leading to various responses. After in vivo administration, MSC induce peripheral tolerance and relocate to damaged tissues and inhibit pro-inflammatory cytokine release, improving the damaged cells' survival.[96]

Schwann cells produce a microenvironment that is necessary for the neurodegenerative process and maintenance of nerves. It was reported that in the vivo studies, differentiation of MSC into Schwann cells was confirmed, allowing for better axonal regeneration and remyelination in spinal cord injuries.[97] MSC not only improve the survival and proliferation of Schwann cells but also increase the expression of BDNF and NGF.[98] Furthermore, Ding et al.'s study revealed the influx of Schwann cells into the injury site, and improved survival was attributed to the effect of MSC (Figure 3).[99]

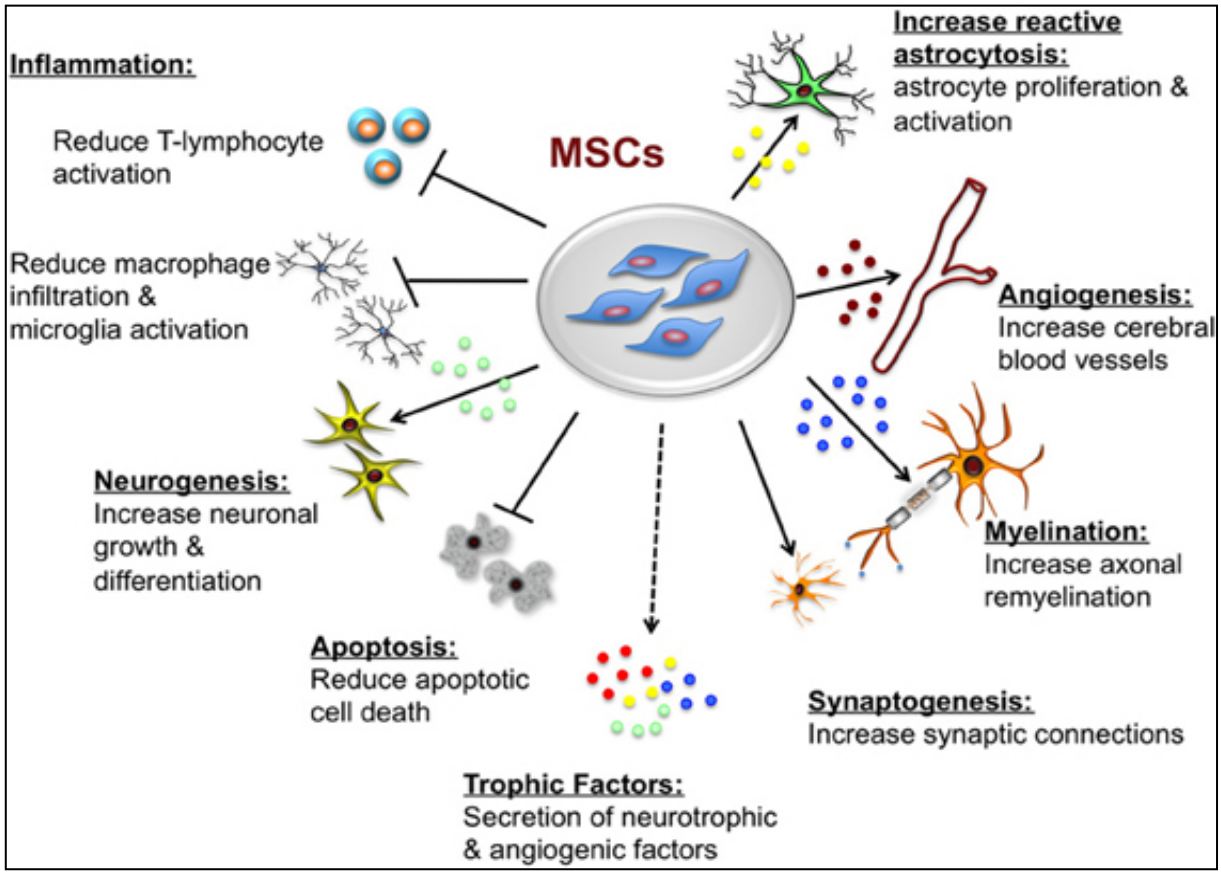

Figure 3. Mesenchymal Stem Cell Neurologic Effects [100] (Copyright © 2013 Castillo-Melendez, Yawno, Jenkin and Miller. This is an open-access article distributed under the terms of the Creative Commons Attribution License (CC BY). The use, distribution, or reproduction in other forums is permitted.

2. HYPOTHESIS AND AIMS OF THE STUDY

Nerve allografts offer an unrestricted source of nerve epineurium, which can be utilized as a bridging conduit between the two nerve stumps to support nerve recovery. Its acellular properties make it non-immunogenic, which is an important trait, especially compared to traditional nerve allografts, which require systemic immunosuppression. The neural origin is the potential advantage of the epineural conduit over other biological tubes. High Laminin B and VEGF expression provide a highly neuropermissive environment for Schwann cell attachment and axonal ingrowth.

Multiple studies have suggested the need to match the diameter of a synthetic conduit to the diameter of the nerve and confirmed detrimental effects on nerve regeneration if size discrepancy exists between the nerve and the conduit.

Mesenchymal stem cells, due to their anti-inflammatory and neuroregenerative properties, are considered a promising approach as supportive therapy for peripheral nerve injuries.

We hypothesize that the application of human Epineural Sheath Conduit (hESC) will regenerate a 20 mm long nerve defect in the experimental athymic nude rat model. Furthermore, hESC supported with human Mesenchymal Stem Cells (hMSC) will enhance axonal regeneration and will shorten the recovery time after injury.

Aims:

1. To assess *in vivo* the neuroregenerative potential of hESC supported with hMSC in 20 mm long nerve gaps assessed in the nude rat model.

2. To evaluate the neurotrophic and proangiogenic properties of hESC and hMSC in the nude rat model.

3. To assess the effect of hESC diameter modification on peripheral nerve regeneration.

3. MATERIALS AND METHODS

3.1. General Information

The experimental study was carried out from January 2015 to January 2016 at the University of Illinois at Chicago (UIC) Microsurgery Laboratory, under the supervision of Maria Siemionow, M.D., Ph.D., D.Sc.

The study protocol 13-218 was followed after obtaining prior approval from the University of Illinois at Chicago Office of Animal Care and Institutional Biosafety Committee (OACIB) (Appendix 1). Based on this decision, the University of Life Sciences in Poznań Local Ethics Committee for Animal Experiments (*Lokalna Komisja Etyczna do Spraw Doświadczeń na Zwierzętach Uniwersytet Przyrodniczy w Poznaniu*) found no contraindications to the study (Appendix 2).

3.2. Experimental Animals

A total of 36 male athymic homozygous nude rats (Crl:NIH-*Foxn1*^{rnu}, Charles River Laboratories, Wilmington, MA, US), weighing between 150-250 grams, were used in this experimental study (Figure 4). This rat strain is optimal for our research because this strain is T-cell deficient, and it presents depleted cell populations in the thymus-dependent areas of peripheral lymphoid organs. This prevents the development of an immunological reaction towards human Mesenchymal Stem Cells. The rats were housed at two animals to a hooded cage at room temperature, on a 14/10 light-dark schedule. The rats were fed *ad libitum* with irradiated rodent feed and provided with autoclaved water in bottles. The rats' treatment was in accordance with the United States Health Department guidelines and the Office of Animal Care and Institutional Biosafety Committee of the University.

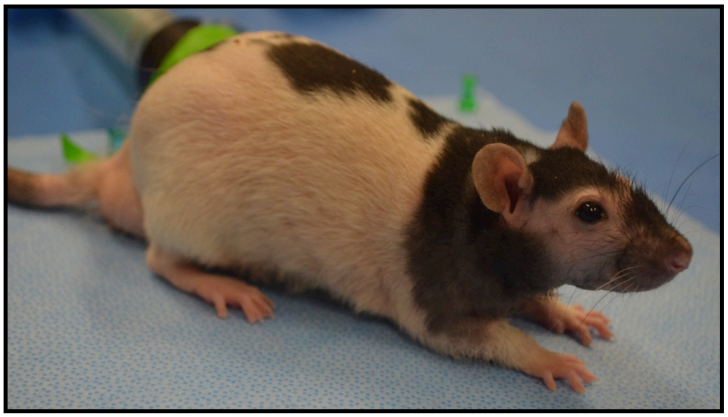

Figure 4. The Crl:NIH-*Foxn1*^{rnu} Rat: A T-cell-deficient, athymic nude model (Charles River Laboratories, USA). Author's picture.

3.3. Human Epineural Sheath Conduits

Human Sciatic nerves were obtained from the Musculoskeletal Transplant Foundation (NJ, US). In sterile conditions and on dry ice, the frozen nerves were shipped to the Microsurgery Laboratory on prearranged days. After receiving the package, the container with the nerve was placed into a Glacier Ultralow Temperature Freezer (NuAire, Plymouth, MN, US) at -86C. Once the nerve was needed in order to obtain the epineurium (usually 1-2 days after shipment), the nerve was defrosted by placing it onto a warm water circulating heating pad (T/Pump, Gaymar Industries, Orchard Park, NY, US) at 38C (Figure 5).

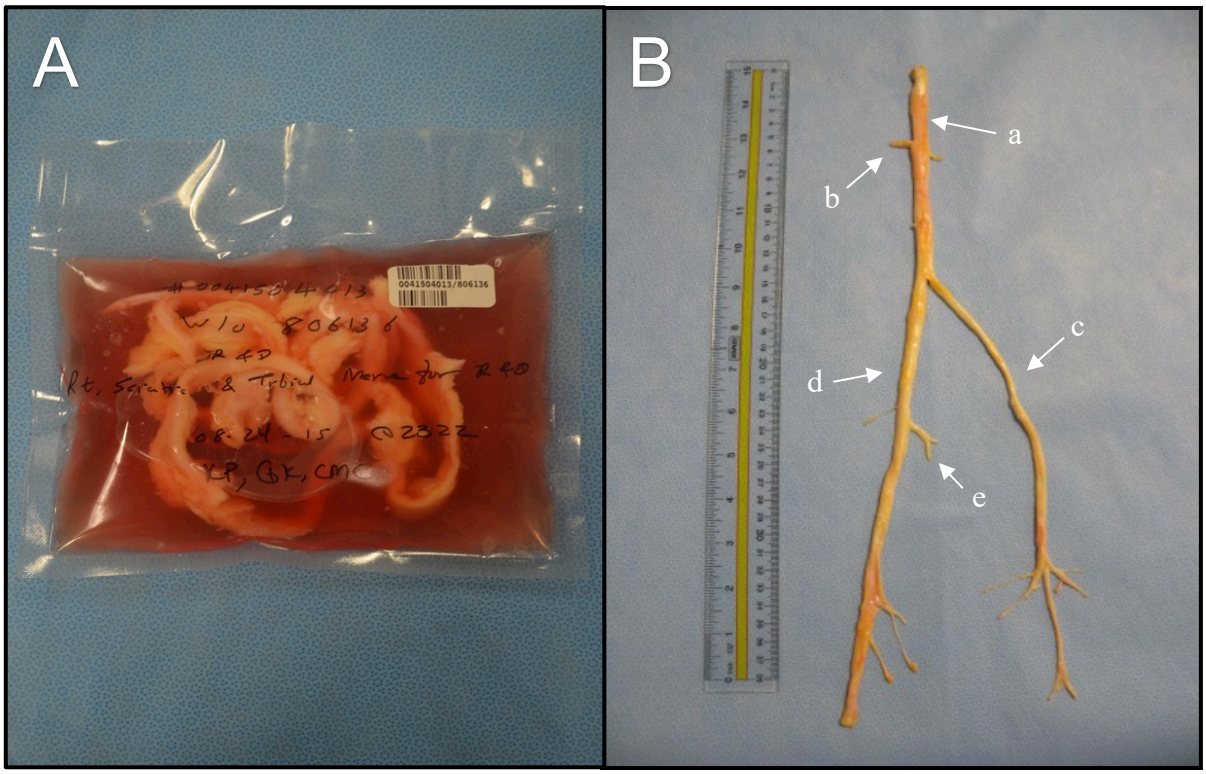

Figure 5. A- Packaged Human Sciatic and Tibial nerves purchased from the Musculoskeletal Transplant Foundation (NJ, US). B- Human Sciatic and Tibial nerve with branches: a- sciatic nerve; b- muscular branches of the sciatic nerve; c- common fibular (peroneal) nerve; d- tibial nerve; e- medial sural cutaneous nerve.

3.4. Human Mesenchymal Stem Cells

The vials of Poietics human Mesenchymal Stem Cells (hMSC) and all mediums were acquired from Lonza (Lonza Group Ltd. Basel, Switzerland). Each Poietics hMSC vial contained ≥ 750,000 cells. According to the company, hMSC were isolated from non-diabetic adult human bone marrow withdrawn from bilateral punctures of posterior iliac crests. Each MSC donor was tested and affirmed negative by Food and Drug Administration (FDA)

approved screening methods for the presence of HIV, hepatitis B, and C virus. All work was performed maintaining sterile conditions of the cell culture in accordance with the CDC-NIH manual for Biosafety and Microbiological and Biomedical Laboratories, 5th edition.

3.4.1. Thawing of Cells and Initiation of in vitro Cell Culture

To start hMSC in vitro cell propagation, the number of vessels required for culture was determined based on the surface area and the recommended cell seeding density. The suggested seeding density for hMSC is 5,000-6,000 cells per cm^2. The sterile 75cm^2 Cell Culture 3276 Corning Flasks (Corning Incorporated, Corning, NY) were used. After adding optimized medium volume to the vessels (0.2-0.4 ml per cm^2) the vessels were equilibrated in a 37°C, 5% HERAcell 150i CO_2 humidified incubator (Thermo Scientific, Waltham, MA) for at least 30 minutes.

The cryovials were wiped with isopropanol before opening. The cap was momentarily twisted a quarter turn to relieve pressure and then retighten. It was then thawed in a 37°C water bath. Cells were not thawed longer than 90 seconds, as this would result in lower cellular viability.

Using a micropipette, the thawed cell suspension was gently added to 5 ml of temperature-equilibrated medium. After washing and centrifuging at 500x g for 5 minutes, the pellet was resuspended in an equilibrated mesenchymal stem cell growth medium (MSCGM). The total number of viable and dead cells was assessed, and cell viability was determined using Trypan Blue 0.4% staining.

After adding the calculated volume of cell suspension to each culture flask, cells were placed in 37°C, 5% CO 2, and 90% humidity incubator.

3.4.2. Incubation of the Human Mesenchymal Stem Cells

Cell media and debris were aspirated from the flasks and discarded, and the adherent cell layer was washed with Dulbecco's phosphate buffered saline.

Clonetics trypsin/EDTA (CC-3232) enzyme solution was added to cover the cell layer (approx. 0.05 ml/cm2). The flask(s) was gently rocked to ensure that the trypsin solution covered the cells. Cells were incubated at room temperature for 5 minutes and then inspected using a microscope. If the cells were less than 90% detached, incubation was extended, and cells were observed every 3 minutes, however no longer than 15 minutes.

Once ≥ 90% of the cells were detached, an equal volume of temperature equilibrated MSCGM was added to each vessel in order to stop the enzymatic activity of trypsin. Cells were centrifuged at 600 x g for 5 minutes to remove the trypsin. The cell pellet was resuspended in equilibrated MSCGM, and a sample was selected for counting. After Trypan Blue 0.4% staining, the cells were counted with a hemocytometer under the microscope, and the total number of cells was calculated (Figure 6).

The following equation was used to count the total number of viable cells.

$$\text{Total number of Viable Cells} = \frac{\text{Total cell count x percent viability}}{100}$$

The cells were then incubated at 37°C, 5% CO 2, and 90% humidity. After 3 to 4 days after seeding, the medium was removed entirely and replaced with an equal volume of fresh MSCGM. Cells at the desired cell confluence of 70-80% were observed after day 6 or 7 of culture and were ready for injection into the hESC (Figure 6).

Once the required number of $3x10^6$ hMSC was collected, MSC were stained with PKH26 (Sigma-Aldrich, United Kingdom) red membrane dye. The cells were incubated with PKH26 dye in Diluent C buffer solution for 5 minutes. Following the wash in alpha-MEM medium, the cells were ready for implantation into hESC conduits.

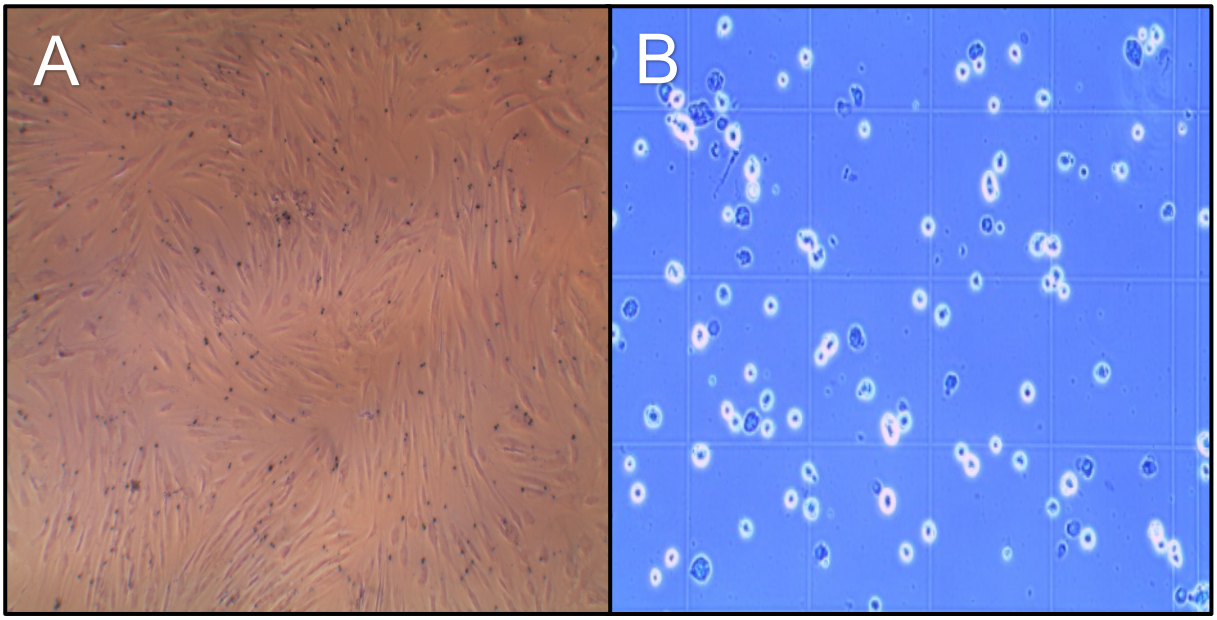

Figure 6. A- Human Bone Marrow- Derived MSC after 7 days of culturing in mesenchymal stem cell growth medium (MSCGM). B- Human Mesenchymal Stem Cells stained with Trypan Blue on a hemocytometer. The number of cells increased 5x with 70-80% viability.

3.5. Surgical Procedure

3.5.1. Conduit Preparation

For experimental groups, epineural conduits from the human sciatic nerves were prepared in aseptic conditions before surgical procedure of nerve repair. Schematic presentation of the epineural conduit creation is shown in Figure 7. A 3-4 cm section of the sciatic nerve, without branching, was resected from the nerve. The diameter of the nerve depended on the experimental group design. Using microsurgical tools under a surgical microscope (Wild 691, Leica Microsystems, Wetzlar Germany), the epineurium was separated from the fascicles in a circular motion with the help of scissors, pulling the epineurium back until fully separated. A 30G irrigator or the irrigator's protectives plastic cover was inserted into the conduit preventing it from collapsing. The conduit was then inspected for any accidental tears or damage which would preclude it from implantation. After being tailored to 2-2.5 cm in length, conduit diameter was measured, and it was placed in saline until implanted into the nerve gap (Figure 8).

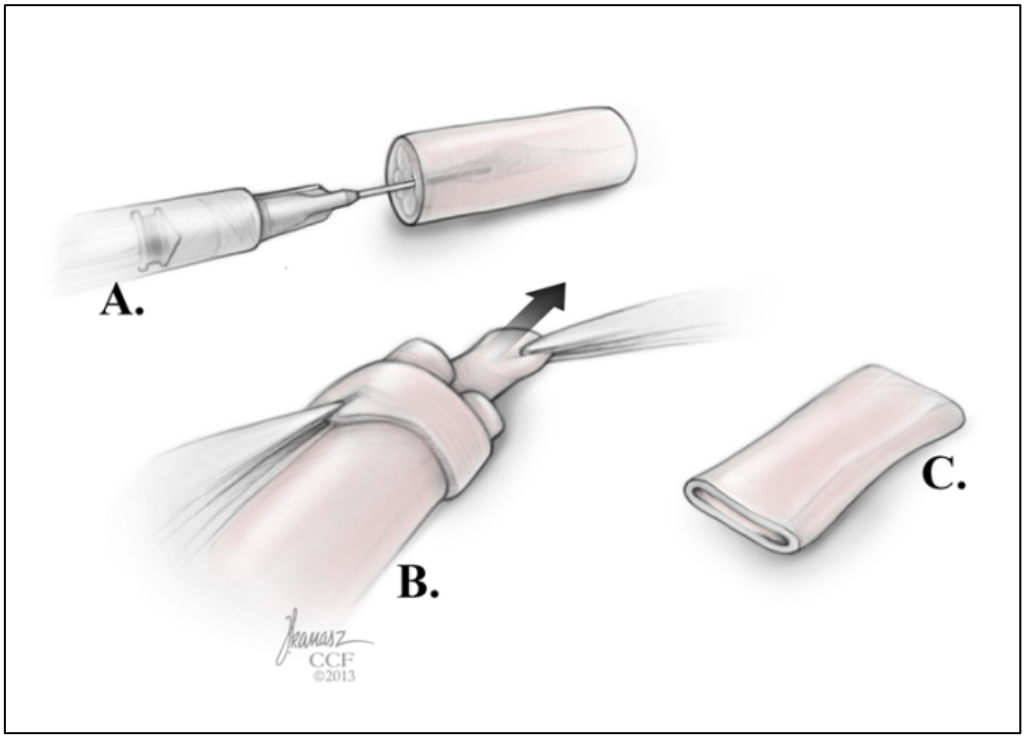

Figure 7. Removal of nerve fibers from the resected fragment of the human sciatic nerve. A- Insertion of the needle-irrigator into the interior of the resected fragment of the nerve in order to remove the nerve fibers. B- Removal of nerve fibers. C- Empty epineural sheath conduit ready for implantation. Image by Joseph Kanasz, Cleveland Clinic Center for Medical Art & Photography (used with permission from Siemionow et al. manuscript Peripheral nerve defect repair with epineural tubes supported with bone marrow stromal cells: a preliminary report. Ann Plast Surg. 2011 Jul;67(1):73-84.)[75]

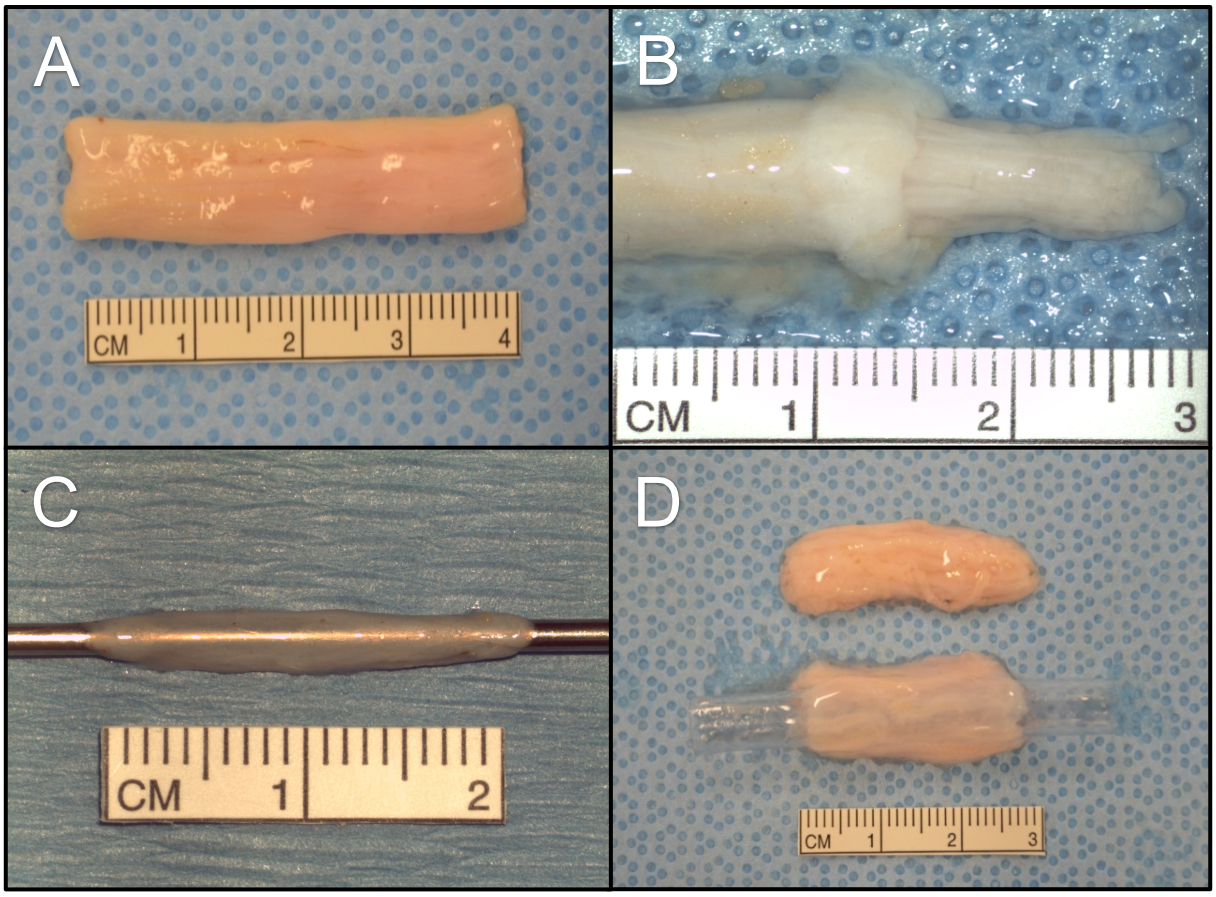

Figure 8. A- Segment of the human sciatic nerve; B- Epineurium being separated from the fascicles during harvesting of the epineural sheath; C- Epineural conduit ready for implantation to fill the nerve gap; D- Harvested empty epineural conduit with the nerve fascicles removed shown above the conduit.

3.5.2. Surgical Procedure

Each rat was weighed before surgery using a triple beam scale (700/800 series, OHAUS, Parsippany, NJ, US). For all surgical procedures and other assessments requiring anesthesia, Isoflurane (Terrell Isoflurane, Piramal Critical Care Inc., Bethlehem, PA, US) inhalation was used through the SurgiVet Vaporizer (Smiths Medical, Dublin, US). After inducing the animals in an induction chamber at 5% Isoflurane until unconscious, the rat was next placed on the surgical table. To maintain anesthesia, 1,5-2,5% Isoflurane was administered until the end of the surgery. Pain control was provided with one subcutaneous injection of Buprenorphine SR (1.2 mg/kg) 15 minutes before the first skin incision. After the animal was anesthetized, the rat was placed on the preparation table. The right hind limb was shaved, and a thin coat of hair remover lotion (Nair, Church & Dwight Co., Princeton, NJ, US) was applied. After 3-5 minutes, the area was gently wiped with a damp gauze removing the hair and lotion, followed

by a rinse using a sterile saline solution. After this step, the rat was placed on the sterile operating table.

Aseptic technique was used for all animals subjected to surgical intervention. The skin was then prepared with a 5% povidone-iodine solution (Betadine, Purdue Products L.P., Stamford, CT, US). Surgery was performed at room temperature, and animals were placed on a warm water circulating heating pad (T/Pump, Gaymar Industries, Orchard Park, NY, US) before, during, and after surgery.

A 20 mm right sciatic nerve defect was created in all experimental groups. A surgical microscope (Wild 691, Leica Microsystems, Wetzlar Germany) with x 20 magnification was used for all procedures. A 3 cm oblique incision was made to the right gluteal area and, after hemostasis, the gluteus superficialis and biceps femoris muscles were visualized. The plane between the gluteus superficialis and biceps femoris muscles was dissected, and the right sciatic nerve was visualized. The 20 mm long segment of the sciatic nerve was dissected from the surrounding connective tissue and was transected proximally using a minimally traumatic technique. Careful consideration was taken to visualize the trifurcation of the sciatic nerve distally and ensure that the distal transection was made above trifurcation. The intact 20 mm segment of the sciatic nerve was then resected.

Following excision of a 20 mm segment of the sciatic nerve in the control group without nerve repair, the surgical wound was closed. In the Autograft control and conduit groups, the conduits were implanted and coapted to the proximal and distal nerve stumps using eight interrupted 10-0 nylon sutures (Ethicon, Bridgewater, NJ, and Cincinnati, OH, US). All coaptations were conducted applying standard microsurgical techniques under the operating microscope magnification (20-40x). After completing the nerve gap repair with hESC, the conduits were filled with either 1 mL saline in control groups or $3x10^6$ hMSC in a 1 mL volume with insignificant leakage (Figure 9).

Next, the gluteus superficialis and biceps femoris muscles were approximated using a 4-0 interrupted vicryl suture (Ethicon, Bridgewater, NJ, and Cincinnati, OH, US). The skin was then once again washed using 5% povidone-iodine solution and approximated using interrupted 5-0 monocryl sutures (Ethicon, Bridgewater, NJ, and Cincinnati, OH, US). The isoflurane was then turned off. An antibiotic cream (Neosporin, Johnson & Johnson, New Brunswick, NJ, US) was placed on the incision site, and a collar was placed around the rats' neck for protection against wound biting.

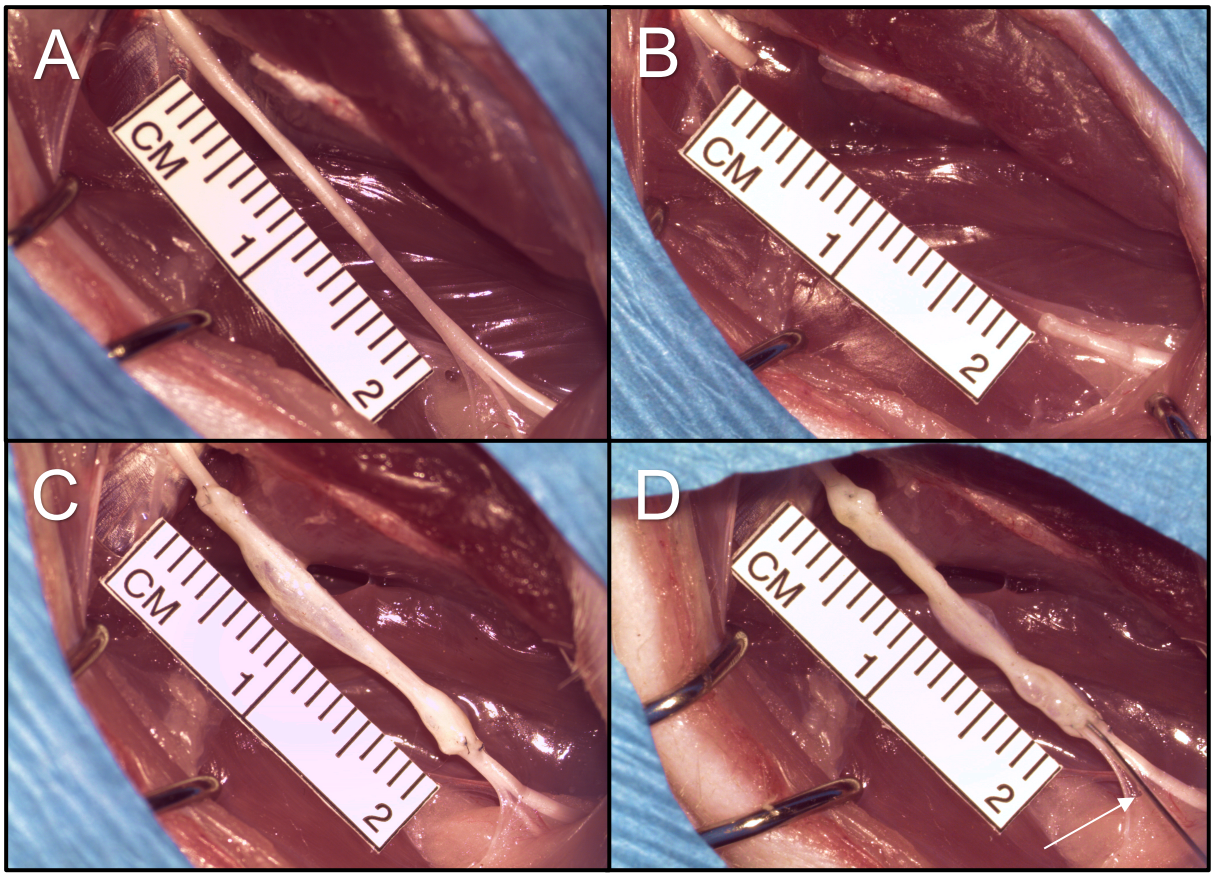

Figure 9. A- 20 mm segment of the rat sciatic nerve; B- Creation of a 20 mm gap in the rat sciatic nerve; C- Implantation of a human Epineurium Sheet Conduit into the 20 mm gap; D- Injection of either hMSC or saline into the conduit.

3.6. Experimental Groups

The study consisted of six experimental groups outlined in Table 4. Each group included six animals (n=6). Group I served as the no repair control, while Group II served as the Autograft control. Group III-IV served as the experimental groups, with the injection of saline or hMSC into the hESC. Injection of saline (1 mL) or hMSC ($3x10^6$ hMSC suspended in 1 mL of saline) was delivered from the distal coaptation site towards the proximal site of the conduit under surgical microscope to assure filling of the entire length of the conduit with saline or hMSC. Next, the injection site was compressed to prevent leakage.

The rat's sciatic nerve diameter ranges between 1 and 1.5 mm. We defined matched diameter conduits as those with a diameter less than three times (<3:1) the size of the rat sciatic nerve. For large diameter conduits, the diameter was more than five times (>5:1) when compared to the rat's nerve being repaired. In this case, only the ends of the conduits, which

were in contact with the rat's nerve epineurium, were folded on top of each other, decreasing the diameter allowing for proper coaptation to the nerve stump. The body of the conduits was unaffected by this diameter manipulation.

Table 4. Study Groups

Study Group		Experimental Design
I	Control Groups	No nerve gap repair
II		Autograft Repair
III	Experimental Groups	Application of a large diameter (>5:1) hESC filled with saline
IV		Application of a large diameter (>5:1) hESC filled with $3x10^6$ hMSC
V		Application of matched diameter (<3:1) hESC filled with saline
IV		Application of matched diameter (<3:1) hESC filled with $3x10^6$ hMSC

Group I. Following resection of 20 mm of a sciatic nerve segment, no repair of the nerve gap defect was performed

After visualizing the right sciatic nerve of the rat, a 20 mm segment of the nerve was excised, creating a gap. The nerve gap was not repaired, and no further surgical intervention was applied. The muscle edges were approximated, followed by skin closure.

Group II. Repair of the nerve defect was made using the 20 mm segment of the nerve Autograft

A 20 mm long segment of the harvested sciatic nerve Autograft was reversed 180 degrees and implanted to the site of the nerve defect. Prior to implantation, any visible branches were dissected and tied using 10-0 nylon sutures to prevent neuroma formation. The coaptation sites were sutured to the epineural surface of the proximal and distal stump of the sciatic nerve. Next, the muscle edges were approximated, followed by skin closure.

Group III. Repair of the nerve defect using the large diameter hESC filled with saline

After creating the 20 mm gap in the sciatic nerve, a large diameter hESC was implanted into the site. A large diameter hESC was defined as a conduit which diameter was at least five times greater (range between 5-8 mm) than the diameter of the repaired rat sciatic nerve (1-1.5 mm). Prior to implantation, any visible branches were dissected and tied using 10-0 nylon sutures to prevent neuroma formation. The coaptation sites were sutured to the epineural surface of the proximal and distal stump of the sciatic nerve. Next, the conduit was filled with 1 mL of saline. The muscle edges were approximated, followed by skin closure.

Group IV. Repair of the nerve defect using the large diameter hESC filled with hMSC

After creating the 20 mm gap in the sciatic nerve, a large diameter hESC was implanted into the site of defect. Prior to implantation, any visible branches were dissected and tied using 10-0 nylon sutures to prevent neuroma formation. The coaptation sites were sutured to the epineural surface of the proximal and distal stump of the sciatic nerve. Next, the conduit was filled with $3x10^6$ hMSC suspended in 1 mL of saline. Next, the muscle edges were approximated, followed by skin closure.

Group V. Repair of the nerve defect using the matched diameter hESC filled with saline

After creating the 20 mm gap in the sciatic nerve, a large diameter hESC was implanted into the site of defect. A matched diameter hESC was defined as a conduit which diameter was less than three times (range between 1-4.5 mm) that of the diameter of the repaired sciatic nerve (1-1.5 mm). Prior to implantation, any visible branches were dissected and tied using 10-0 nylon suture to prevent neuroma formation. The coaptation sites were sutured to the epineural surface of the proximal and distal stump of the sciatic nerve. Next, the conduit was filled with saline (1 mL). Next, the muscle edges were approximated, followed by skin closure.

Group VI. Repair of the nerve defect using the matched diameter hESC filled with hMSC

After creating the 20 mm gap in the sciatic nerve, a large diameter hESC was implanted into the site of defect. Prior to implantation, any visible branches were dissected and tied using 10-0 nylon sutures to prevent neuroma formation. The coaptation sites were sutured to the epineural surface of the proximal and distal stump of the sciatic nerve. The conduit was filled with $3x10^6$ hMSC suspended in 1 mL of saline. The muscle edges were approximated, followed by skin closure.

3.7. Postsurgical Supportive Treatment

Each rat was individually quarantined with a collar for the first 24 hours after the procedure. The next day the collar was taken off, and the rat was placed into the original cage. Postoperative pain control was provided with buprenorphine (0.1 mg/kg) twice daily for the first two days. Animals were physically examined daily for the first 14 days post-surgery to assess the wound site, and a daily progress note was written. The animals were observed for signs of morbidity, lack of eating or drinking, weight loss greater than 20%, inability to locomotor activities, or signs of pain or distress such as rough hair coat or hunched posture. The animals were also under the University veterinary team's care, which examined each rat once a week.

3.8. Assessment Methods

The animals were evaluated for functional recovery at 1,3,6,9, and 12 weeks after surgery. All animals were euthanized at 12-week post-surgery using euthanasia solution SomnaSol (Henry Schein, Inc., NY, US). Both gastrocnemius muscles and the sciatic nerve repair area were harvested for histological and immunological examination.

3.8.1. Clinical Assessment

Clinical Assessment was performed daily on each rat. Any rat developing any of the following clinical signs was disqualified from the study (Table 5). The veterinary staff was consulted to determine a course of action if such symptoms were noted.

Table 5. Disqualifying criteria

Disqualifying criteria	
Behavioral	Weight loss >20%
	Aggression
	Signs of pain or distress
Physical	Surgical site non-closure
	Limb auto cannibalization
	Hindlimb pressure sores

3.8.2. Functional Motor Assessment

The toe-spread test was used to assess motor nerve recovery. In an uninjured limb, the rat extends and abducts the hindfoot toes when the rat is held up by the tail. The toe-spread test was graded between 0 and 3 in the following manner: no movement = grade 0, any sign of movement of the toes = grade 1, abduction of the toes = grade 2, abduction and extension of the toes = grade 3 (Figure 10).

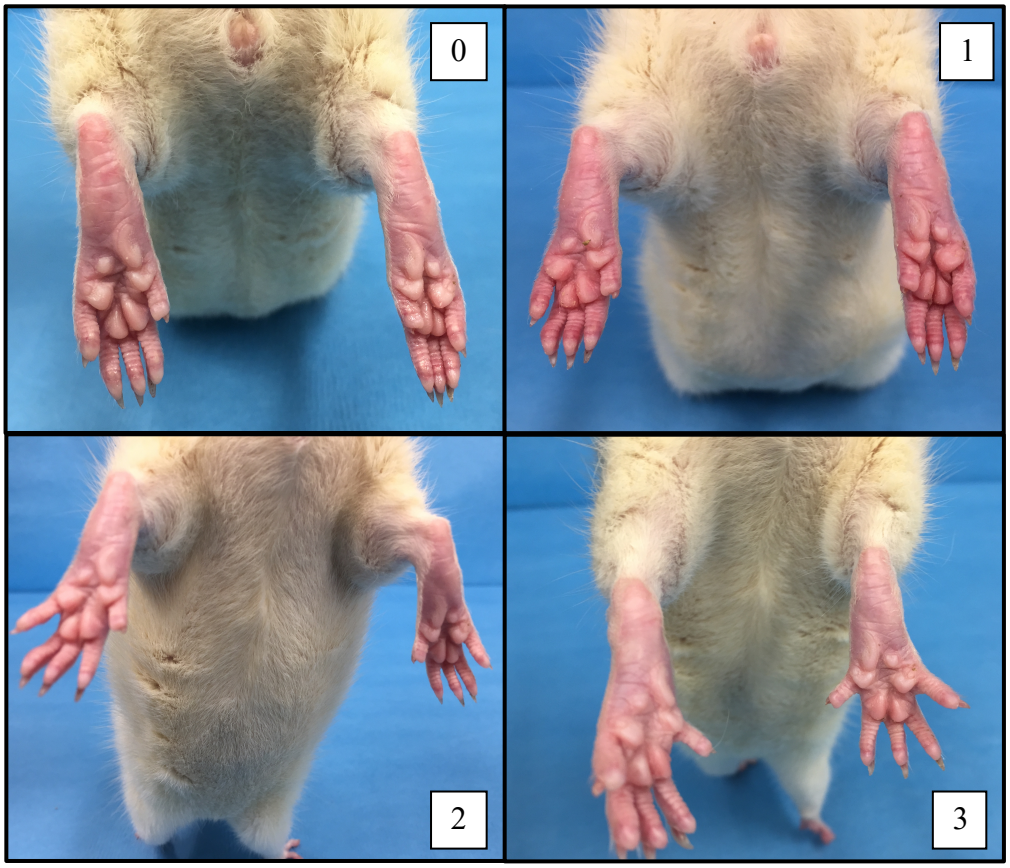

Figure 10. The toe spread assessment of rat's right hind limb at 1,3,6,9, and 12 weeks after the creation of a 20 mm nerve gap of the right sciatic nerve. The assessment of the motor recovery was measured and recorded using the following scale: 0 = no movement of the toes; 1 = any sign of movement of the toes; 2 = abduction of the toes; 3 = abduction and extension of the toe.

3.8.3. Functional Sensory Assessment

The pinprick test was used to assess the sensory nerve recovery. Using Adson's toothed forceps, pressure was applied to the skin of the right hind limb of the rat. This was performed starting from the toe to the level of the knee joint until a retraction of the limb and/or a vocal response from the painful stimulus was obtained. Attention was paid not to pinch the deep tissues and periosteum of the limb. Stimulus response was graded between 0 and 3 in the following manner: no sensation was elicited on the limb = grade 0, withdrawal response between the knee and ankle = grade 1, withdrawal response between the ankle and toes = grade 2, and withdrawal response to the pinch of the toes = grade 3 (Figure 11). The test was performed at least three times at each evaluation stage to prevent incidental false positive results.

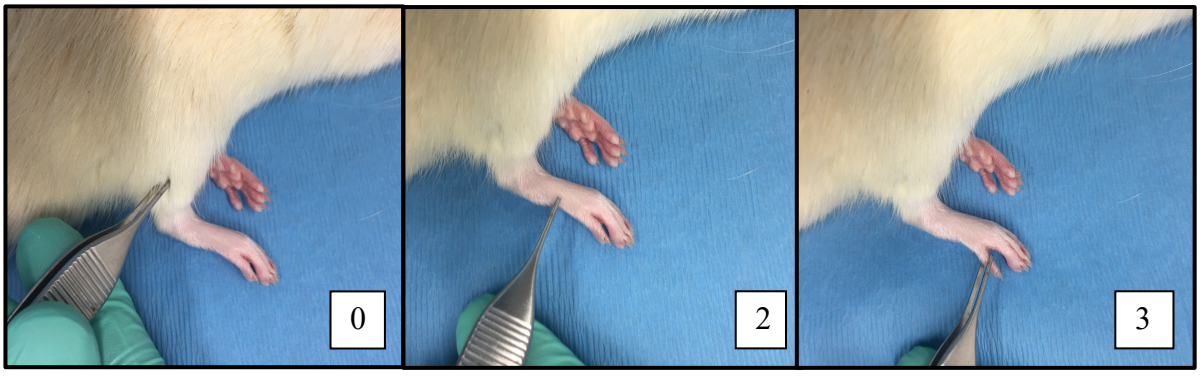

Figure 11. The pin-prick assessment of each rat using Adson's forceps at 1,3,6,9 and 12 weeks after the creation of a 20 mm nerve defect. The assessment of the sensory recovery using various surgical techniques was measured and recorded using the following scale: 0 = no sensation was elicited on the limb (picture not shown); 1 = withdrawal response between the knee and ankle; 2 = withdrawal response between the ankle and toes; 3 = withdrawal response to the pinch of the toes.

3.8.4. Assessment of Muscle Denervation Atrophy

Muscle denervation atrophy was assessed by calculating the Gastrocnemius Muscle Index (GMI). At the experiment end-point of 12 weeks after nerve defect repair, gastrocnemius muscles were harvested from both limbs- the right and the left sides, and wet-muscle weight measurements were taken.

$$\text{GMI} = \frac{\text{Right Gastrocnemius muscle weight}}{\text{Left Gastrocnemius muscle weight}}$$

3.8.5. Histomorphometric Analysis

After GMI was assessed, the muscles were fixed in formalin. Cross sections of the muscle samples were taken, and routine H&E stained paraffin sections were prepared. Six non-overlapping fields were chosen from each muscle sample, with three hundred muscle fibers assessed in total. Images were taken using a Leica DM 4000B Compound Microscope (Leica Microsystems, Wetzlar, Germany) with a Qimaging Retiga 2000R Color Digital Camera (Teledyne Photometrics, Tuscon AZ, US) and digitalized and assessed using Image-Pro Plus, Ver 6.3.0.512 (Media Cybernetics, Bethesda MD, US). Each animals' right limb muscle fiber area average was compared to the left limb muscle fiber area average, and the values were expressed as a R/L ratio.

3.8.6. Macroscopic Evaluation

After the rat's euthanasia, a 3 cm incision was made in the gluteal region of the right hind limb. The same method as described above was used to visualize the right sciatic nerve. Once the nerve and the graft were visualized, the assessment for the following was performed:

1. Adhesions or local signs of inflammation
2. Structure, shape, and integrity of the graft
3. Fascicle-like structures inside the conduit
4. Signs of atrophy of the nerve distally to the conduit
5. Vascularization of the graft

3.8.7. Immunostaining

Monoclonal antibodies and immunofluorescence technique assessed the expression of growth factors involved in nerve regeneration. Freshly dissected nerve conduit from both the proximal and distal stump was suspended and snap frozen in O.C.T. compound. Tissue slides were cut for 1 um slides and fixed for 10 minutes in acetone. Next, the sections were rinsed in tris buffered saline (TBS) (Dako) and incubated with mouse antirat vWF, VEGF (Thermo Fischer Scientific) and S-100 (Abcam, Inc.), rabbit antirat GFAP (Thermo Fisher Scientific), Laminin B and NGF (Abcam, Inc), and mouse antihuman HLA-1 and HLA-DR (Abcam, Inc.) monoclonal antibody for 30 minutes (Table 6). Incubation using secondary antibodies was performed using goat anti-mouse or goat anti-rabbit IgG Cross-Absorbed Alexa Fluor 488 (Thermo Fischer Scientific). PKH26 staining of hMSC prior to implantation assessed the

presence of hMSC in the conduit. The slides were stained with DAPI and analyzed using a Leica DM 4000B Compound Microscope (Leica Microsystems, Wetzlar, Germany) with a Qimaging Retiga 2000R Color Digital Camera (Teledyne Photometrics, Tuscon AZ, US) and digitalized and assessed using Image-Pro Plus, Ver 6.3.0.512 (Media Cybernetics, Bethesda MD, US). Assessment of immunoreactivity was scored as follows: 0 = no staining; 1 = weak; 2 = moderate; and 3 = strong.

Table 6. Immunostaining

Growth Factor	**Function**
Laminin B	Produced by Schwann cells and located and expressed in basal lamina. Promotes axonal growth in peripheral nerve injuries.
S-100	S100 released from activated Schwann cells promotes macrophages and Schwann cell migration and the release of trophic factors to the site of injury
NGF	NGF regulates neurotransmitter and neuropeptide synthesis of sympathetic and sensory nerves, promoting neurite outgrowth. It's upregulated during nerve cell recovery after injury.
GFAP	Produced by Schwann cells, and functions as a framework and supports the cytoskeleton assembly after neuronal injury.
VEGF	Expressed in the endothelial cells. It is a mitogen which enhances intraneural vascularization and peripheral nerve regeneration.
vWF	vWF regulates angiogenesis through the intracellular and extracellular pathways. It is synthesized and expressed in the endothelial cells (EC) and stored in the Weibel-Palade bodies.
HLA-1	HLA-1 is expressed on hMSC and hESC.
HLA-DR	HLA-DR is expressed on hMSC.
PKH26	PKH26 red dye staining is used for hMSC to confirm MSC presence in the conduit after injection.

3.8.8. Toluidine Blue Staining

Tissue samples of the conduit from both the proximal and distal stump of the nerve were excised, immersed, and fixed in 4% glutaraldehyde. The specimens were post-fixed using 4% aqueous osmium tetroxide and embedded in Araldite 502 following the manufacturer's instructions. Toluidine blue stain was used to stain 1 µm thick cross-sections. Six non-overlapping fields were chosen from each nerve. Images of these nerves were taken using a Leica DM 5500B Compound Microscope with a Leica DFC290 Color Digital Camera (Leica Microsystems, Wetzlar, Germany) and digitalized and evaluated using Image-Pro Plus, Ver 6.3.0.512 (Media Cybernetics, Bethesda MD, US). Each image was assessed for myelin thickens, axonal density, fiber diameter, and percentage of the myelinated nerve fibers (Figure 12).

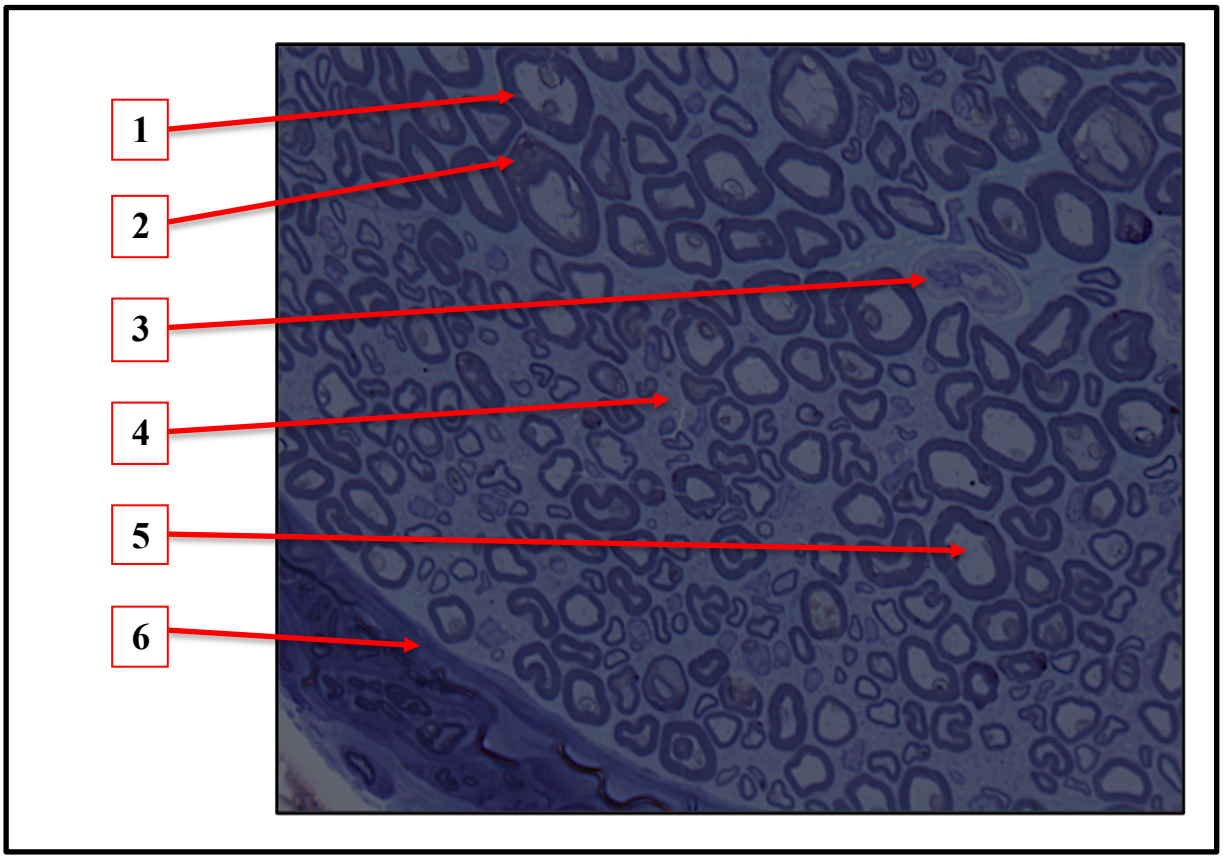

Figure 12. Image of Toluidine Blue Staining of the rat sciatic nerve. Magnification 1000x
1 - Myelin sheath; 2 - Schwann cell; 3 - Vasa nervorum; 4 - Connective tissue; 5 - Axon; 6 - Epineural sheath.

3.9. Overview

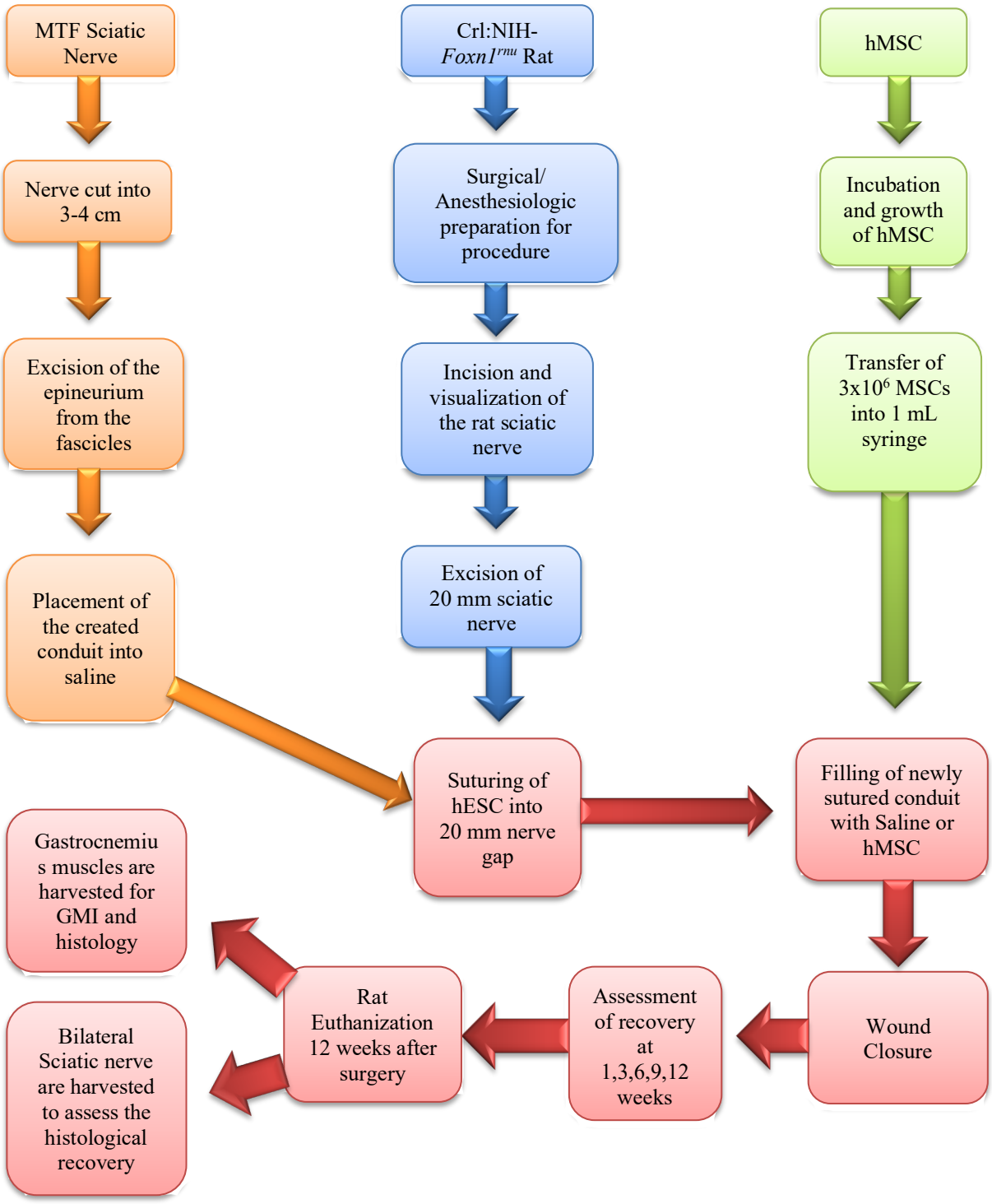

Figure 13. Overview of the experimental design of the study.

4. STATISTICAL ANALYSIS

The calculations were made using the Statistica 13 software by TIBCO. The level of significance was assessed at $\alpha = 0.05$. The result was considered statistically significant when $p < \alpha$. The normality of the distribution of variables was tested with the Shapiro-Wilk test and the equality of variance with the Levene test.

To compare the variables between the two groups, in the case of compliance with the normal distribution and equal variances, the Student's t-test was calculated for unpaired samples, and for a larger number of groups, the analysis of variance test for unpaired samples was used. If the variance was not equal, the Cochran-Cox test was calculated for the comparison between the 2 groups. For the variables measured on an ordinal scale or in the case of non-compliance with the normal distribution, the Mann-Whitney test was calculated for two groups and for a larger number of groups - the Kruskal-Wallis test with Dunn's test of multiple comparisons was applied.

5. RESULTS

5.1. Macroscopic Evaluation of the hESC

Before harvesting, each conduit was evaluated macroscopically. We found no adhesions or local signs of inflammation around the conduits. Each conduit had a well-preserved structure, shape, and integrity with good vascularization of the graft. We confirmed the presence of fascicle-like structures inside the grafts. No signs of atrophy of the nerve distally to the conduit were observed (Figure 14).

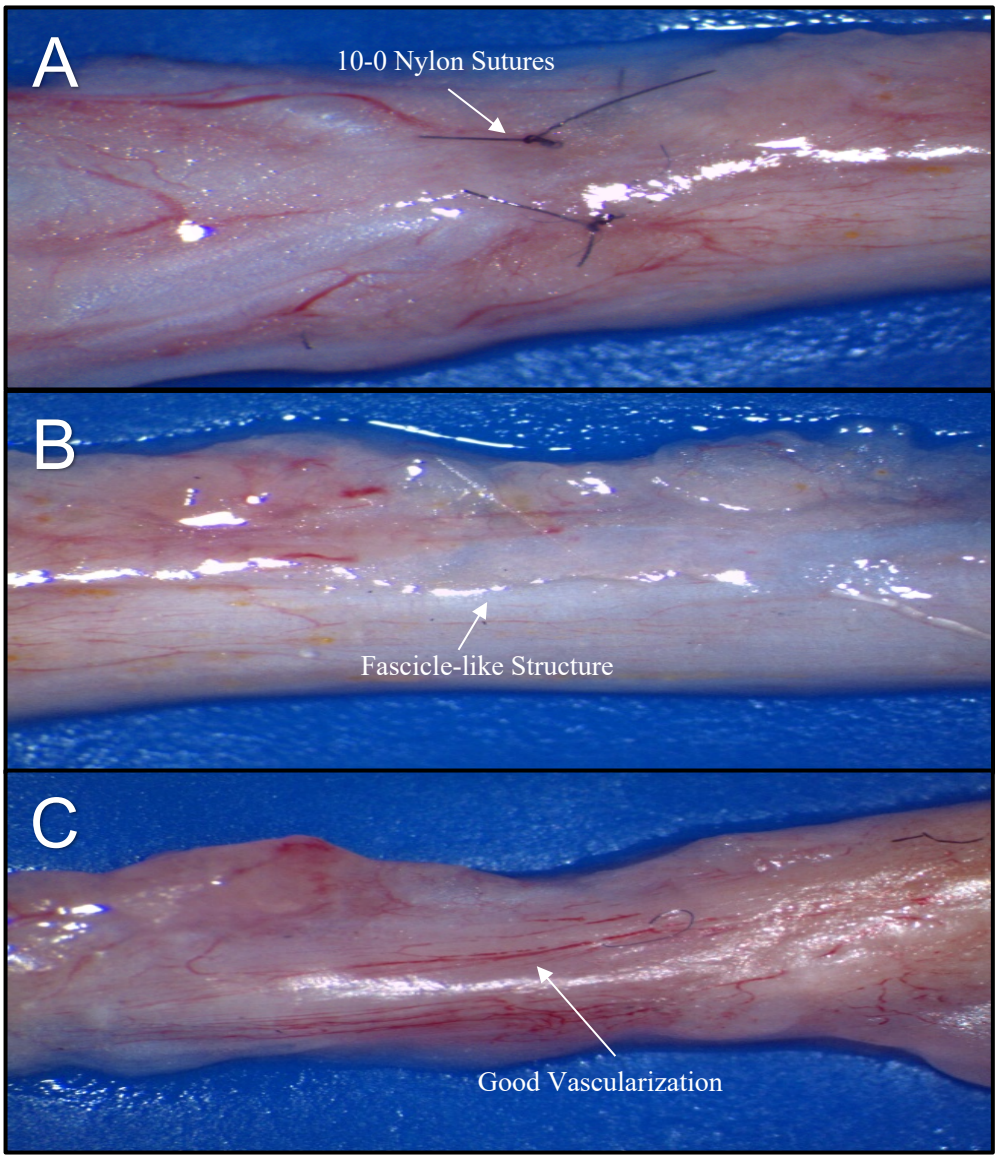

Figure 14. Macroscopic Evaluation of Matched Diameter hESC filled with hMSC at 12 weeks after nerve repair. A- Proximal end of conduit showing well-preserved structure with 10-0 suture; B- Middle of the conduit with fascicle-like structures present; C- Distal end of conduit shows good vascularization.

5.2. Functional Motor Assessment: The Toe-Spread Test

Functional Motor recovery was first noted in the Autograft and all four experimental groups at 6th week after repair. In the group without repair, recovery was first noted at 12 weeks. At 12 weeks after surgery, none of the groups fully recovered their motor function. Autograft revealed the best result (1.8 ± 0.41) followed by groups: Matched diameter hESC supported with hMSC (1.5 ± 0.55), Matched diameter hESC with saline (1 ± 0.63), Large diameter supported with hMSC (0.5 ± 0.55), Large diameter hESC with saline (0.33 ± 0.82) and finally No repair group (0.17 ± 0.41) (Figure 15, Table 7). There were significant differences when comparing the Autograft group to the Large diameter hESC with saline group and to the No repair group (p=0.001).

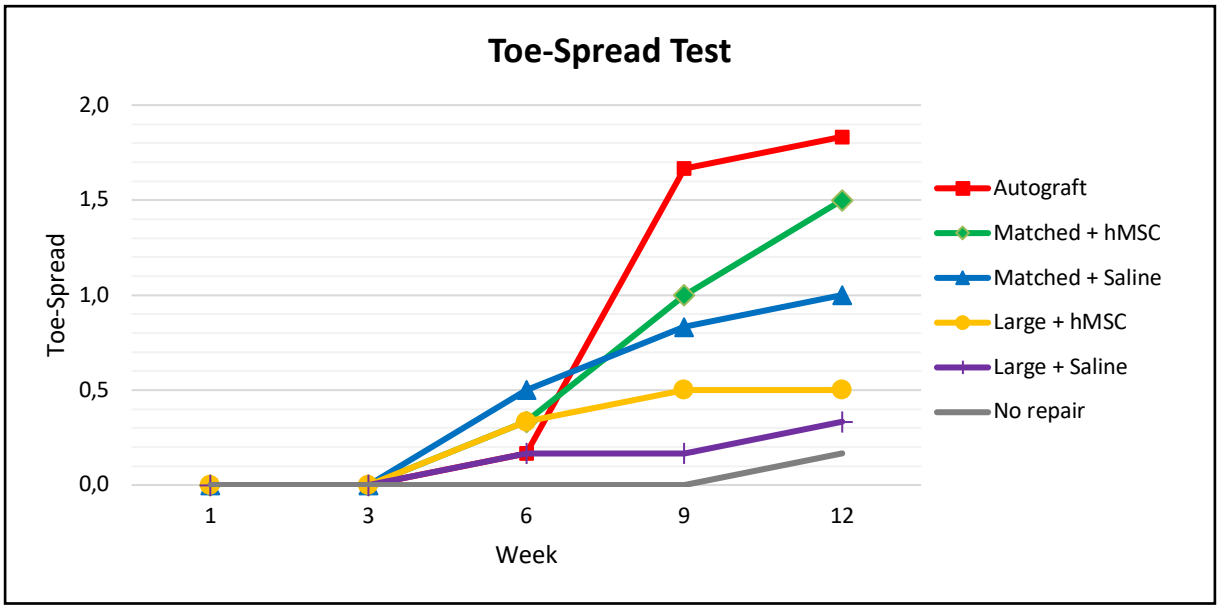

Figure 15. Results of the toe-spread test up to 12 weeks after sciatic nerve defect repairs assessed in 6 experimental groups. Steady improvement of motor function began at week 6 in all four conduit groups and Autograft. Although both Matched hESC initial results were momentarily better, by week 9, the Autograft recovery overtook the conduit groups. Signs of no repair group functional recovery were first recorded at week 12.

Table 7. Result of the toe-spread test at 12 weeks after sciatic nerve defect repair with hESC assessed in 6 experimental groups

Group	Average	SD	Median	p-value
Autograft	1,83	± 0,41	2	p=0.001
Matched + hMSC	1,5	± 0,55	1,5	p>0.05
Matched + Saline	1	± 0,63	1	p>0.05
Large + hMSC	0,5	± 0,55	0,5	p>0.05
Large + Saline	0,33	± 0,82	0	p=0.001
No Repair	0,17	± 0,41	0	p=0.001

5.3. Functional Sensory Assessment: The Pinprick Test

Sensory recovery was first noted at week 3 after repair in the Autograft and both Matched diameter groups. At week 9, all of the groups showed signs of recovery. It is worth noting that between the 6th and 9th week, the Matched Diameter hESC with saline group revealed better results compared to Matched Diameter hESC supported with hMSC group. However, at longer follow-up of 12 weeks, the Autograft group fully recovered (3 ± 0) followed by Matched diameter supported with hMSC (2.33 ± 0.52), Matched diameter hESC with saline (2 ± 0.63), Large diameter hESC supported with hMSC (1.5 ± 0.55), Large diameter hESC with saline (1 ± 0.63) and finally No repair group. (0.5 ± 0.55) (Figure 16, Table 8). We found a statistical difference when comparing the Autograft group to Large diameter with saline and No repair group ($p<0.001$).

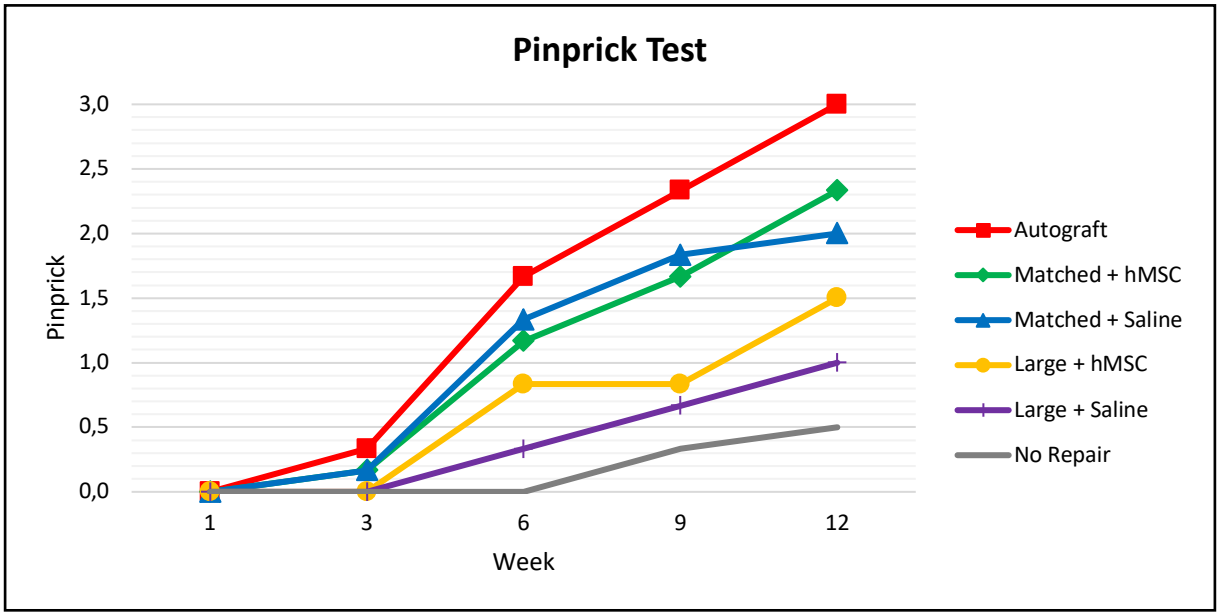

Figure 16. Results of the Pinprick Test up to 12 weeks in 6 experimental groups. Steady improvement of motor function began at week 3 in Autograft and both Matched conduit groups. By week 6, the Autograft and all four conduit groups' recovery were noted. Signs of no repair group functional recovery were first recorded at week 9.

Table 8. Result of the Pinprick Test at week 12 after sciatic nerve repair with hESC

Group	Average	SD	Median	p-value
Autograft	3	± 0	3	p<0.001
Matched + hMSC	2,33	± 0,52	2	p>0.05
Matched + Saline	2	± 0,63	2	p>0.05
Large + hMSC	1,5	± 0,55	1,5	p>0.05
Large + Saline	1	± 0,63	1	p<0.001
No Repair	0,5	± 0,55	0,5	p<0.001

5.4. Muscle Denervation Atrophy

Gastrocnemius denervation atrophy was assessed by the GMI in the six experimental groups at 12 weeks after nerve repair. The Autograft control group revealed the highest muscle ratio recovery (0.32 ± 0.03) followed by the Matched diameter hESC supported with hMSC (0.29 ± 0.03), Matched diameter hESC with saline group (0.27 ± 0.05) followed by the Large diameter hESC supported with hMSC group (0.21 ± 0.02) and Large diameter hESC filled with saline group (0.19 ± 0.02). The No Repair group showed the lowest GMI value compared with all studied groups (0.16 ± 0.03) (Figure 17).

There were statistically significant differences found between the No Repair group and Autograft, Matched diameter hESC with saline and Matched diameter hESC supported with hMSC groups, respectively. Furthermore, a significant difference was found between the Autograft and Large diameter hESC with saline group ($p < 0.001$).

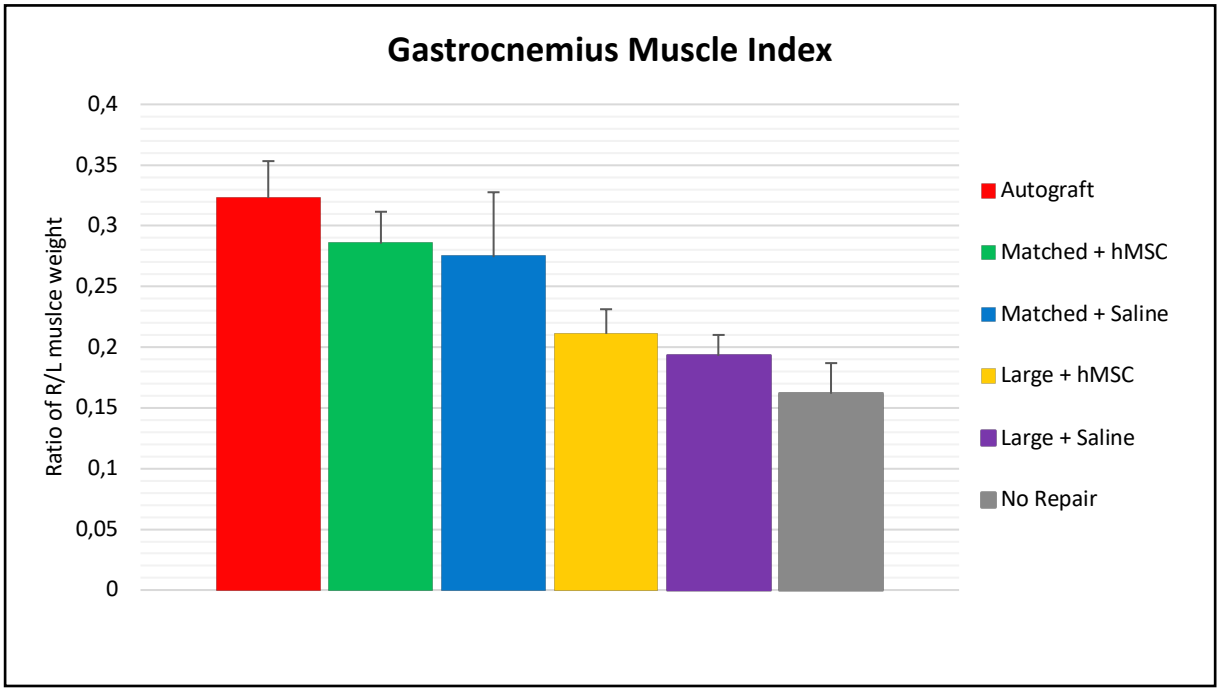

Figure 17. Gastrocnemius Muscle Index at 12 weeks with the highest muscle recovery in the Autograft group (0.32 ± 0.03) followed by the Matched hESC with hMSC treated group (0.29 ± 0.03), Matched hESC with saline (0.27 ± 0.05), Large hESC with hMSC group (0.21 ± 0.02), Large hESC with saline group (0.19 ± 0.02) and No repair group (0.16 ± 0.03).

5.5. Muscle Fiber Area Ratio

Muscle fiber area ratio was assessed in all six experimental groups at week 12 after nerve repair. The Autograft control group revealed the highest fiber area ratio (0.45 ± 0.13) followed by the Matched diameter hESC with hMSC group (0.32 ± 0.05), Matched diameter with saline group (0.27 ± 0.5), Large diameter hESC filled with hMSC group (0.21 ± 0.11) and Large diameter hESC filled with saline group (0.19 ± 0.04). The No Repair group showed the lowest muscle fiber area ratio compared with all studied groups (0.11± 0.03) (Figure 18). As in GMI, there were significant differences found between the No Repair group compared to the Autograft and both Matched diameter groups ($p < 0.001$).

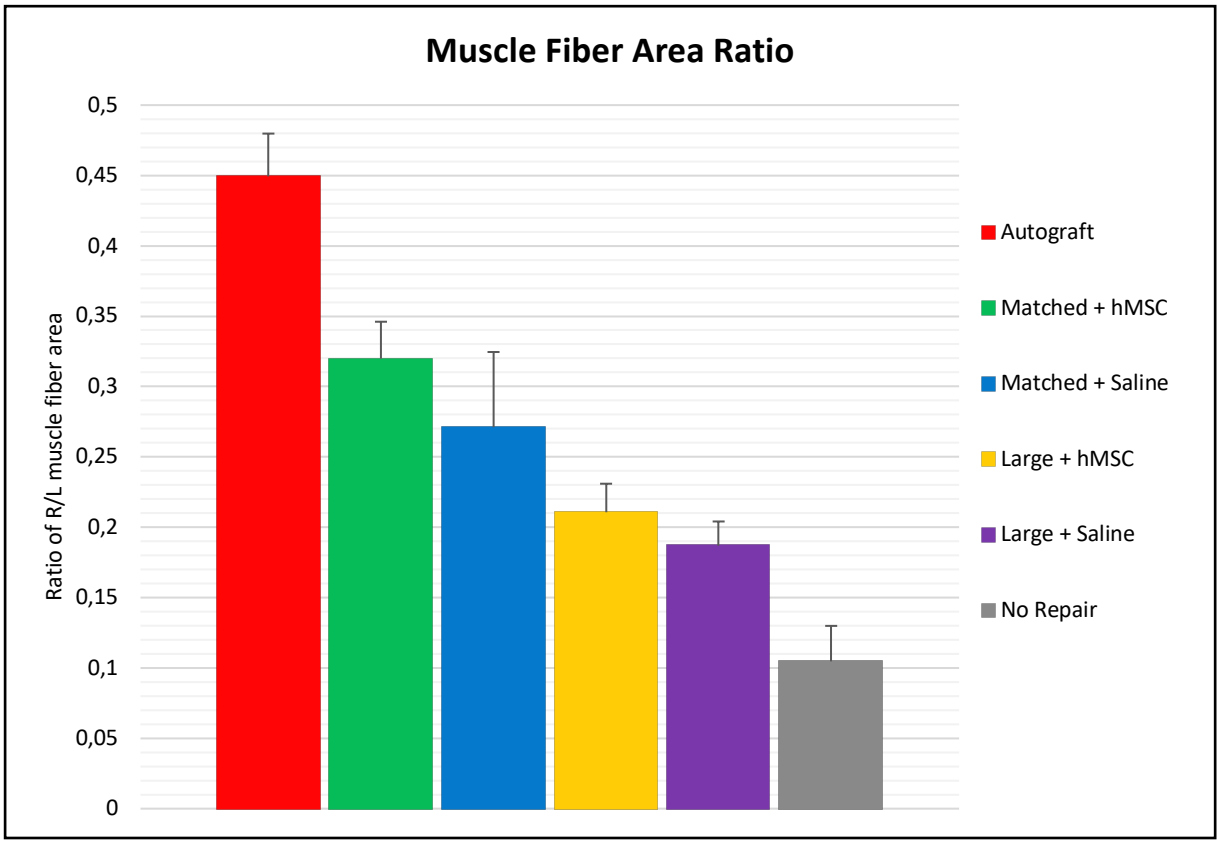

Figure 18. Muscle Fiber Area Ratio at 12 weeks after surgery with the largest fiber area in the Autograft group (0.45 ± 0.13) followed by the Matched hESC with hMSC treated group (0.32 ± 0.05), Matched hESC with saline (0.27 ± 0.5), Large hESC with hMSC group (0.21 ± 0.11), Large hESC with saline group (0.19 ± 0.04) and No repair group (0.11 ± 0.03).

5.6. Immunostaining

5.6.1. PKH26

In the two groups receiving hMSC, immunofluorescence staining confirmed the presence of the PKH26 positive cells in the proximal and distal parts of the human epineural sheath conduit. In the Matched and Large diameter groups, PKH26 expression was strong at the proximal end (mean score of 2.5 and 2, respectively), while the expression at the distal end was strong in the Matched conduit group and moderate in the Large diameter conduit group (mean score of 2.33 and 1.833, respectively). There was a lack of PKH26 expression in both saline conduit groups and the Autograft group (Figure 19). There were significant differences between Matched diameter with hMSC group and the three groups without hMSC ($p<0.001$)

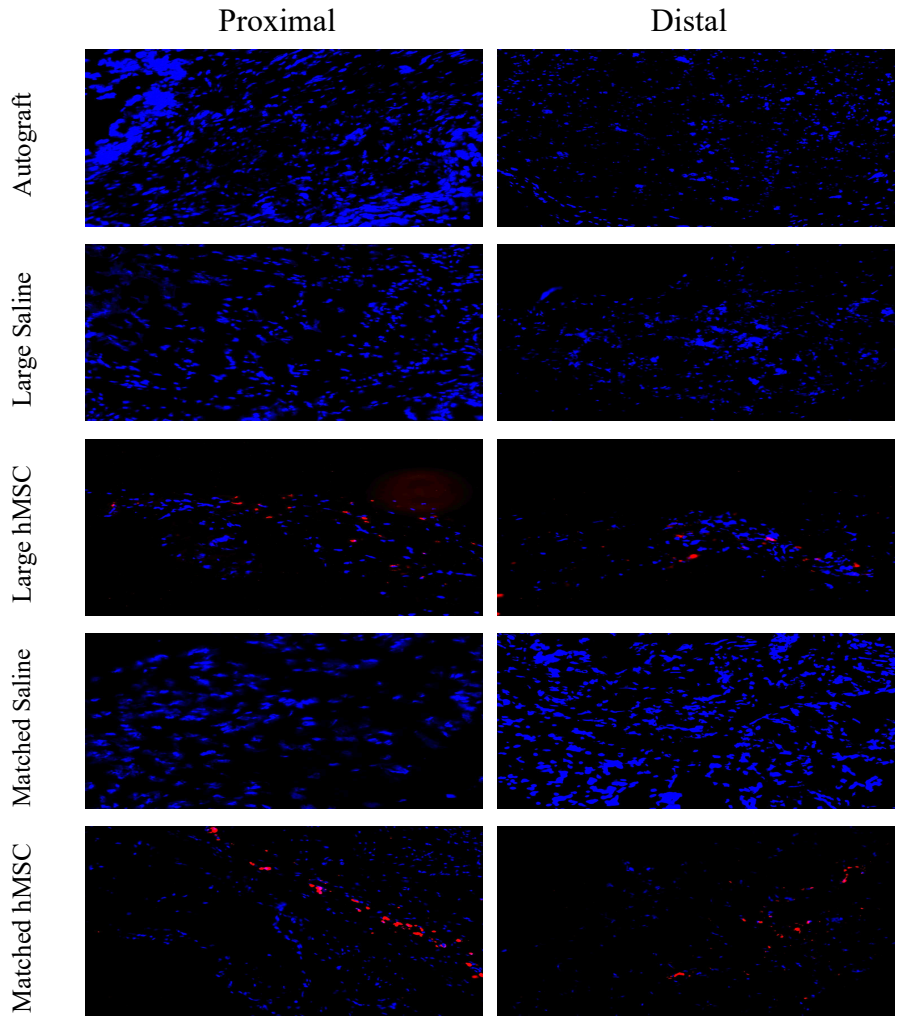

Figure 19. Expression of PKH26 markers in the proximal and distal segment of the rat epineural sheath conduit in autograft control and 4 experimental groups was assessed by immunofluorescent staining. Twelve weeks after repair, PKH26 positive cells were detectable at the proximal and distal parts of the conduit supported with hMSC. 200x magnification.

5.6.2. HLA-1

HLA-1 expression was confirmed in the two hMSC groups at both sides of the conduit. HLA-1 expression was increased at the proximal side of the conduit, where it was at a moderate level in both Matched and Large diameter groups (mean score of 1.83 and 1.5, respectively), when compared to the distal end, where the expression ranged from moderate to weak (mean score of 1.33 and 1 point, respectively). Both saline conduit groups and Autograft did not express HLA-1 (Figure 20). Statistical differences were found between the Matched diameter with hMSC and the three groups without hMSC at both ends of the conduit ($p<0.001$).

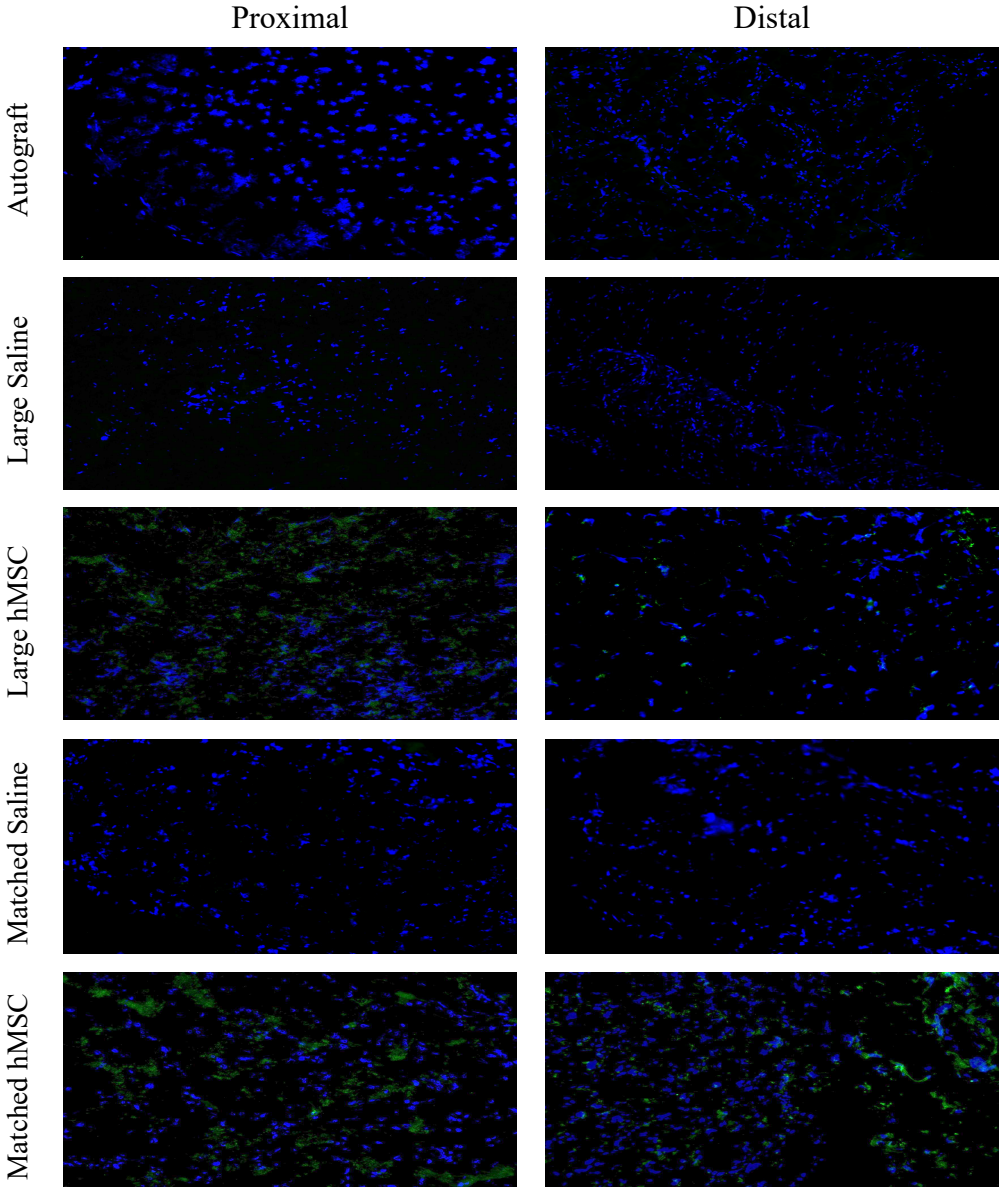

Figure 20. Expression of HLA-1 at the proximal and distal segment of the rat epineural sheath conduit in the autograft control and 4 experimental groups as assessed by the immunofluorescent staining. Twelve weeks after nerve repair, HLA-1 expression was noted only in the hMSC groups, confirming stem cell presence in the conduits. 200x magnification.

5.6.3. HLA DR

The expression of HLA-DR was confirmed in the two hMSC groups, whereas there was no expression found in the saline and autograft groups. The expression of HLA-DR in the Matched diameter conduits supported with hMSC was moderate at both sides of the transplanted conduit (mean score of 1.66 and 1.5, respectively). Statistical differences were found at each side of the conduit between the Matched diameter with hMSC group and the two saline and autograft groups ($p<0.001$).

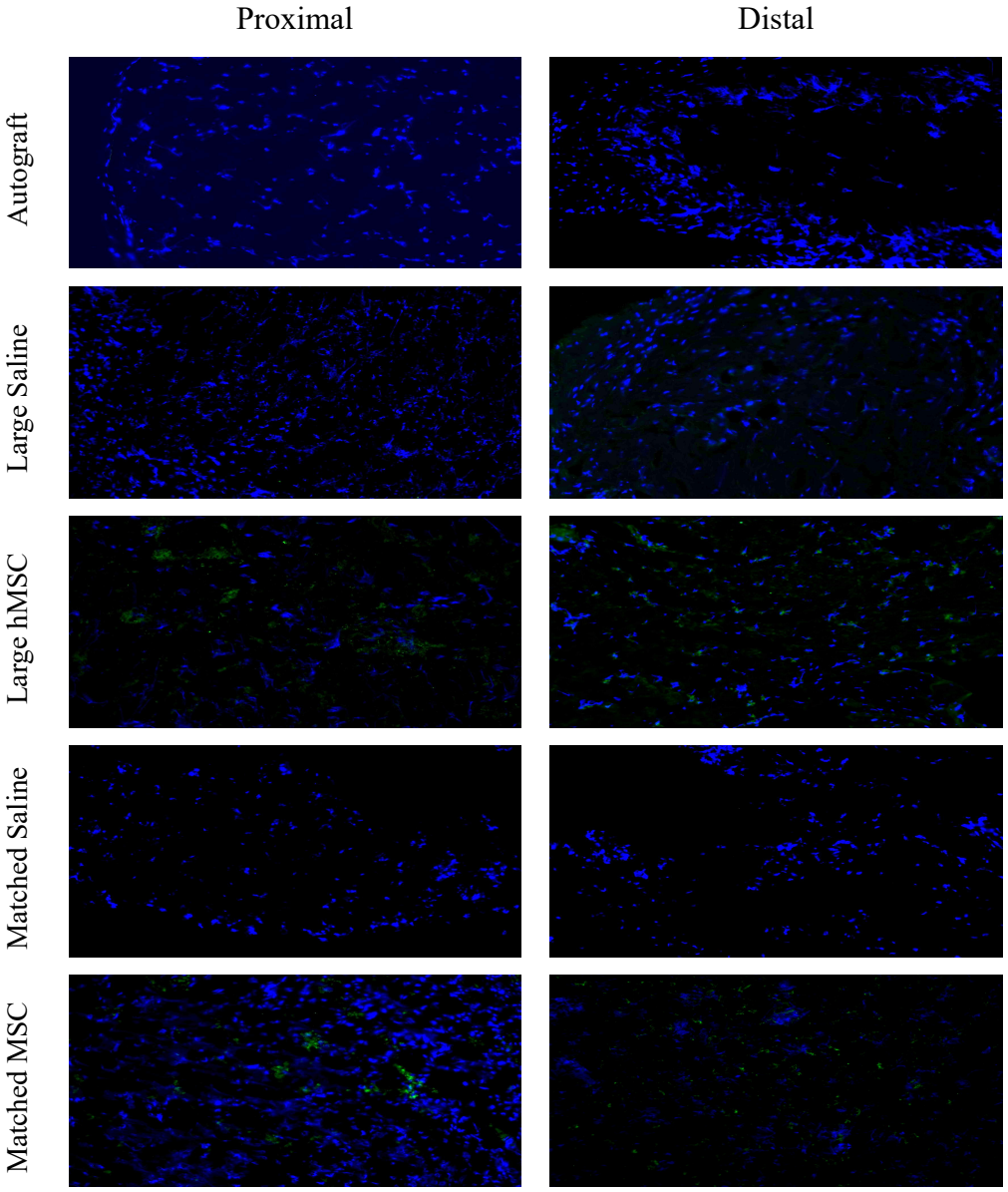

Figure 21. Expression of HLA DR at the proximal and distal segment of the rat epineural sheath conduit in the autograft control and 4 experimental groups as assessed by the immunofluorescent staining. The presence of HLA-DR was observed only in hMSC supported conduits. 200x magnification.

5.6.4. Laminin B

The Extracellular matrix competent Laminin B was up-regulated at the proximal section of the conduits when compared with the distal segments. At the proximal end, there was a significant difference in Laminin B expression between the Matched diameter conduit with hMSC (mean score 2.83) and Large diameter conduit with saline (mean score 1.33; p=0.005). No statistical differences were found at the distal end between the groups (p=0.206).

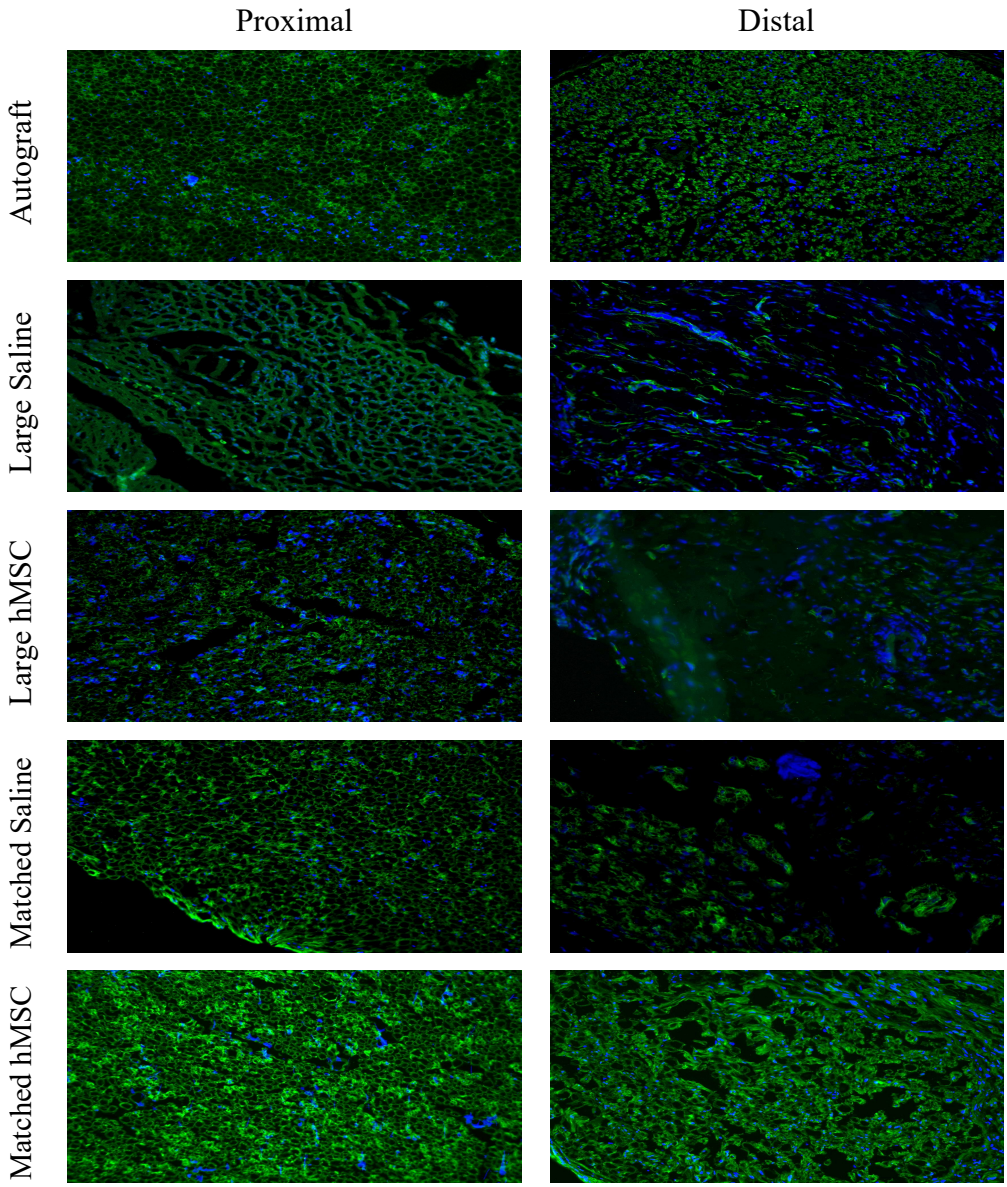

Figure 22. Expression of Laminin B in the proximal and distal segment of the rat epineural sheath conduit in autograft control and 4 experimental groups as assessed by the immunofluorescent staining. At twelve weeks after repair, increased Laminin B expression was found at the proximal side of the conduit in the Matched diameter hESC group supported with hMSC when compared with the large diameter hESC with saline group. 200x magnification.

5.6.5. S-100

The expression of the Schwann cell marker S-100 was found in all the experimental groups, with increased expression present at the proximal end of the conduits (Figure 23). A significant difference was found at the proximal end of the conduits between the Matched and Large diameter conduit filled with saline (p=0.038).

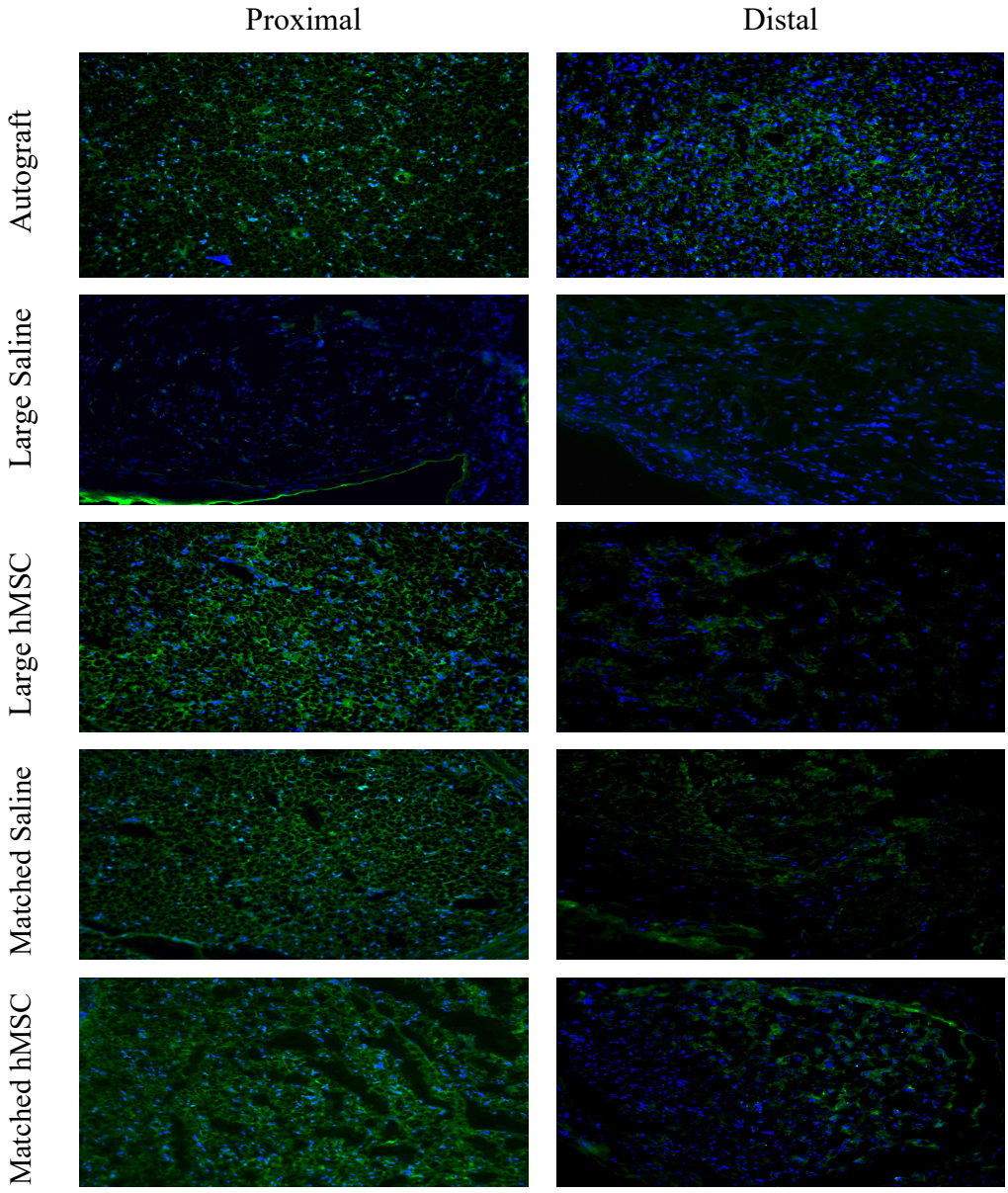

Figure 23. The expression S-100 at the proximal and distal segment of the rat epineural sheath conduit in the autograft control and 4 experimental groups as assessed by the immunofluorescent staining. At twelve weeks after nerve repair, S-100 expression in the Matched diameter hESC group supported with hMSC was comparable to the Autograft control group and scored as moderate at both - the proximal and distal segments of the conduit. In the Large diameter hESC group filled with saline, S-100 expression was weak at both – the proximal and the distal segments of the conduit. 200x magnification.

5.6.6. GFAP

The expression of GFAP found no statistical difference on the proximal (p=0.664) and distal (p=0.419) end of the conduit. The expression of this marker was weak (mean score < 1 point) in all groups on both sides of the conduit except the proximal Autograft, which noted a moderate expression (mean score 1.16) (Figure 24).

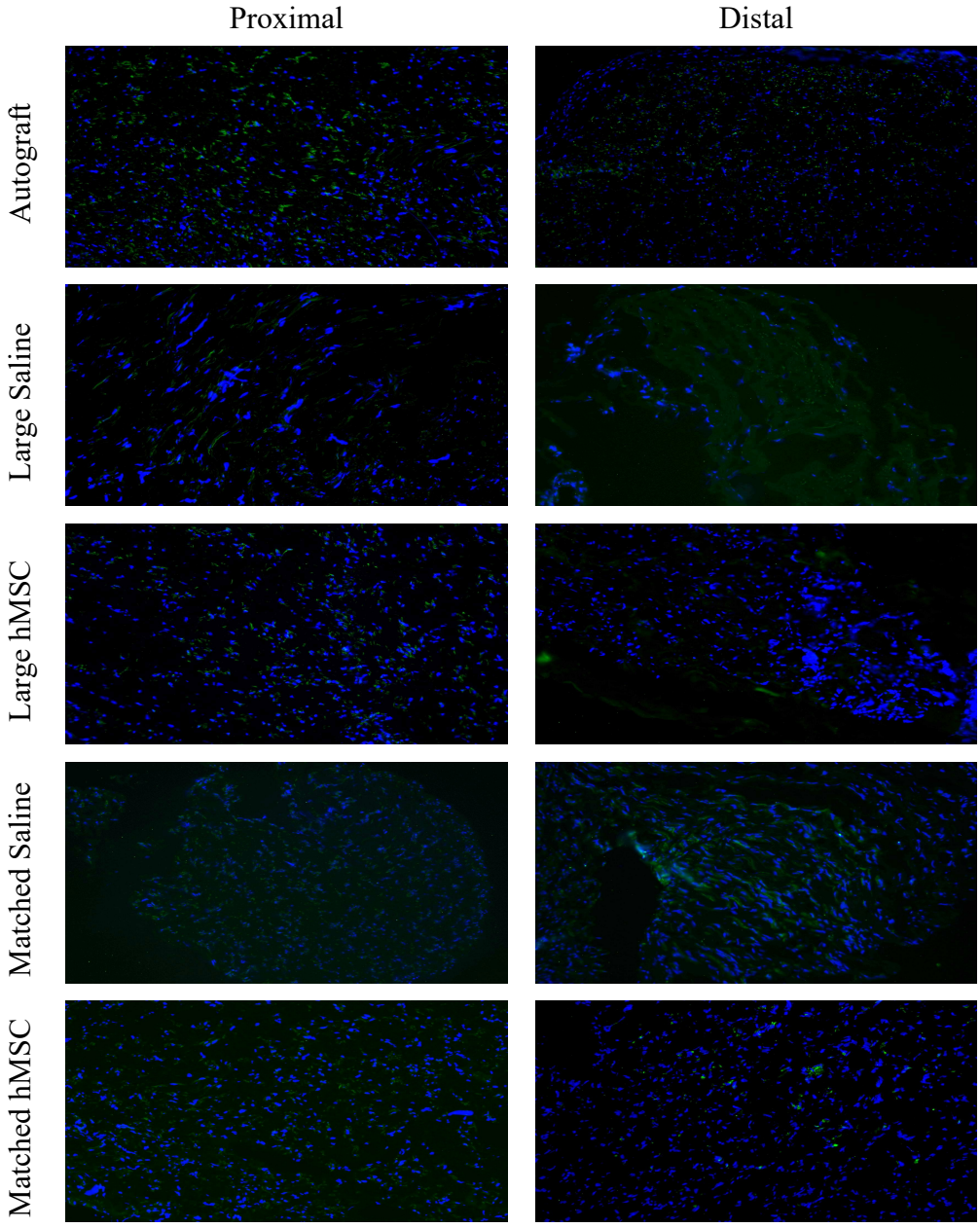

Figure 24. Expression GFAP at the proximal and distal segment of the rat epineural sheath conduit in autograft control and 4 experimental groups as assessed by the immunofluorescent staining. GFAP expression was moderate in the Autograft group at the proximal side, while in the remaining groups' expression of GFAP was weak. 200x magnification.

5.6.7. NGF

In the Autograft group, strong NFG expression was revealed at the proximal end of the conduit, followed by a moderate expression in both Matched diameter groups and Large diameter with hMSC, whereas weak expression was found in the Large diameter with saline group. There were significant differences found between the Autograft and Large diameter with saline group (p=0.006). The same pattern was observed at the distal end of the conduit; however, the expressions were lower (Figure 25). Furthermore, a significant difference was found at the proximal end of the conduits between the Matched and Large diameter conduit filled with saline (p=0.038).

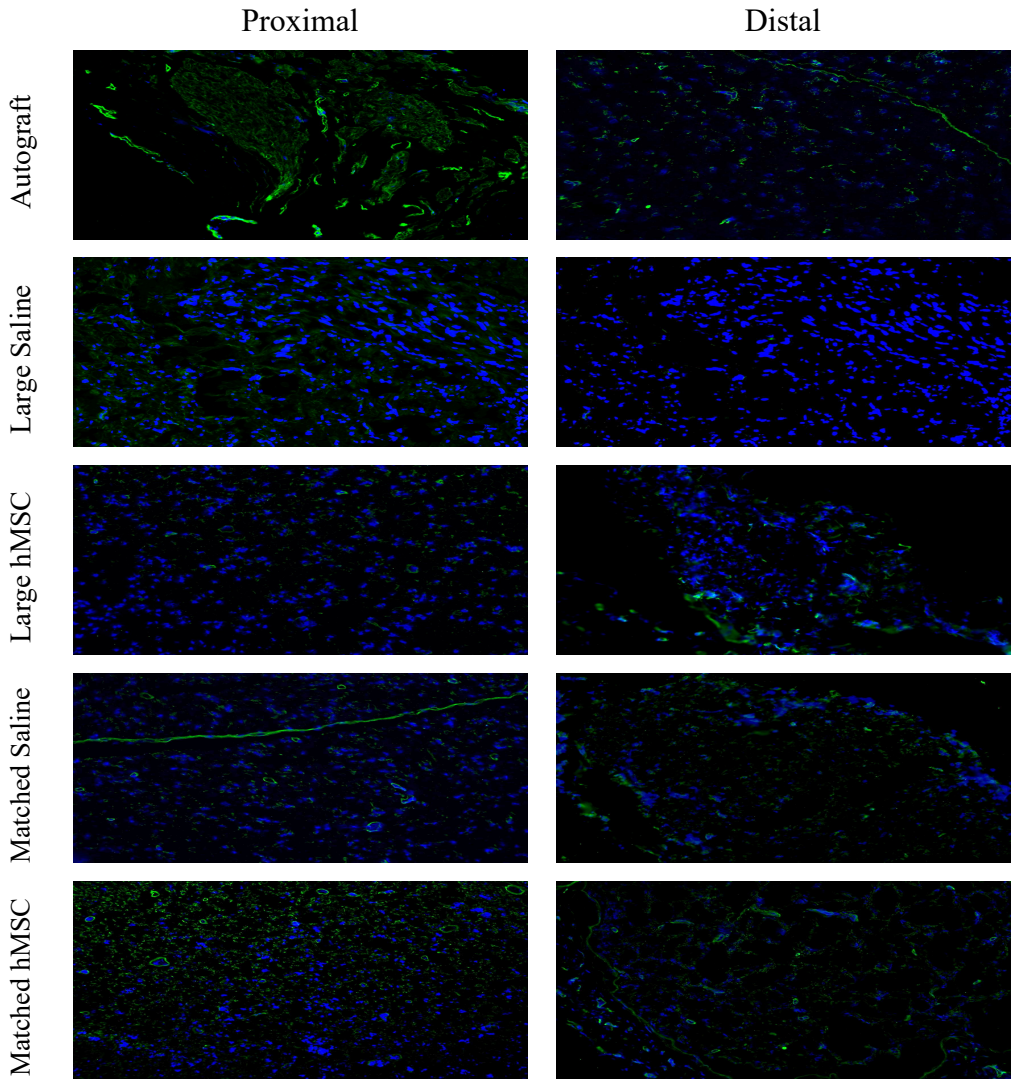

Figure 25. Expression of the NGF at the proximal and distal segment of the rat epineural sheath conduit in the autograft control and 4 experimental groups as assessed by the immunofluorescent staining. Strong expression was noted in the Autograft group. Moderate expression was observed at both sides of the conduit in the Matched diameter conduits and Large diameter hESC filled with hMSC groups with weak expression found in the Large diameter hESC filled with saline. 200x magnification.

5.6.8. vWF

The expression of vWF was weak in all five groups at the proximal end of the conduit, with no significant differences found between the groups (p=0.992). At the distal end of the Autograft, vWF expression was moderate, whereas a weak expression was found in the remaining groups. There were no statistical differences found between the groups (p=0.134).

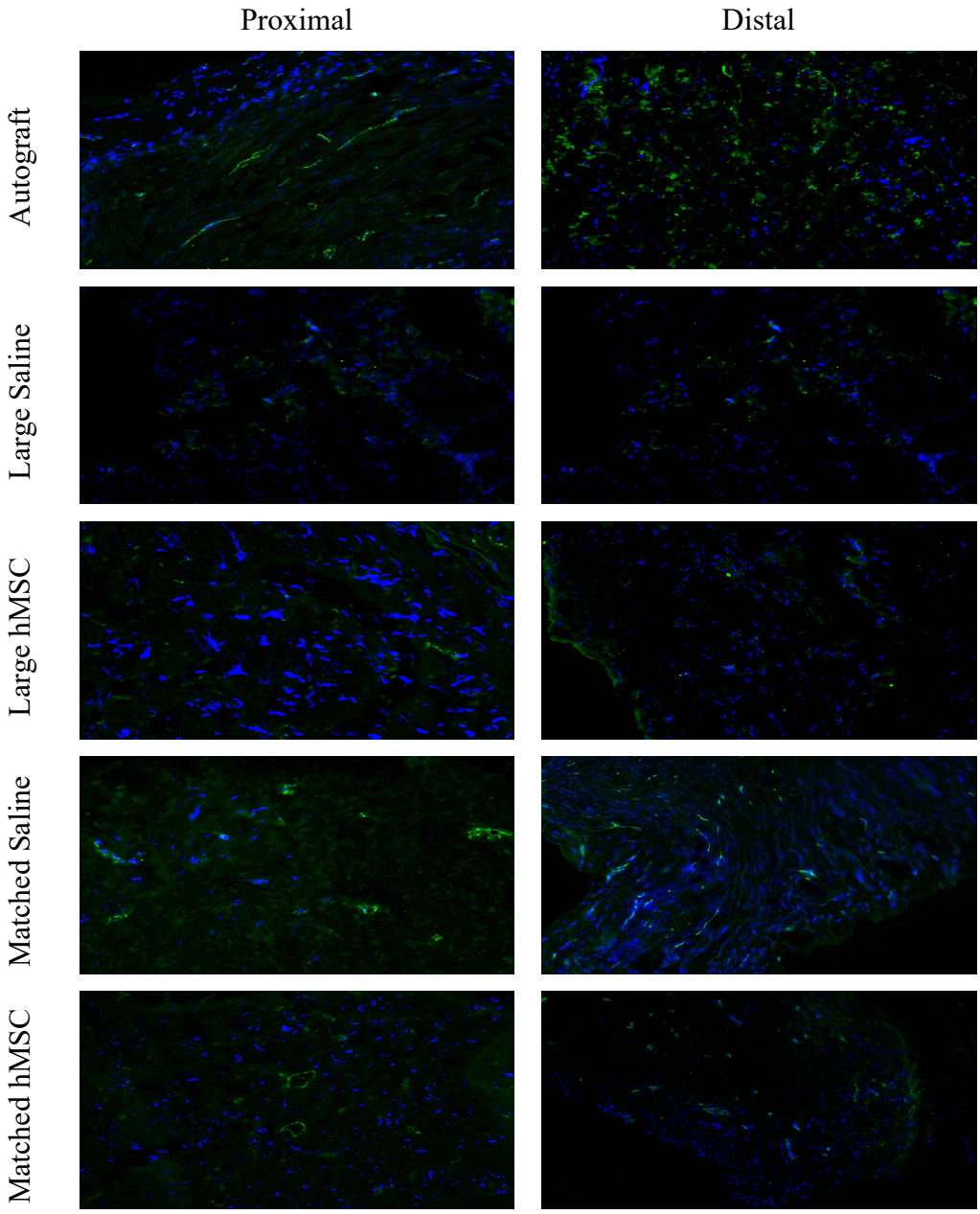

Figure 26. Expression of vWF in the proximal and distal segment of the rat epineural sheath conduit in the autograft control and 4 experimental groups as assessed by the immunofluorescent staining. The expression of vWF was weak in all five groups at the proximal end, whereas at the distal end, vWF expression was moderate in the Autograft group and was weak in the remaining groups. 200x magnification.

5.6.9. VEGF

There was a strong expression of the VEFG found at the proximal end of the conduit in all studied groups except for the Large diameter with saline group, which scored a weak expression. There was a statistically significant difference found between the Large diameter with saline group and both Autograft and Matched diameter with hMSC group (p=0.002).

Compared to the proximal side of the conduit, there was a down-regulation of the VEGF expression found at the distal end, with all of the groups scoring moderate expression except for the Large diameter with saline group, which revealed a weak expression (Figure 27). There were significant differences found in the VEGF expression when comparing the Large diameter with saline and Matched diameter with hMSC groups (p=0.007).

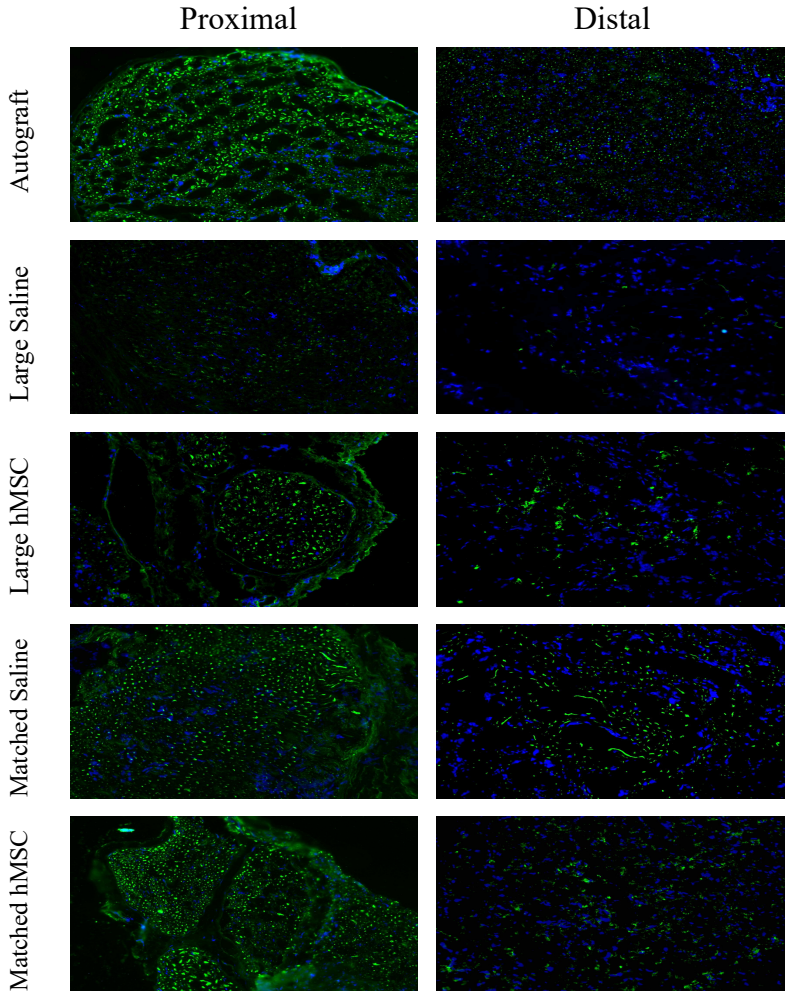

Figure 27. Expression of VEGF in the proximal and distal segment of the rat epineural sheath conduit in the autograft control and 4 experimental groups as assessed by the immunofluorescent staining. At twelve weeks after repair, there was a strong expression of VEFG found at the proximal end of the conduit in all groups studied except for the Large diameter with saline group, which revealed weak expression. At the distal end of the conduit, VEGF expression was moderate except for the Large diameter with saline group, where weak expression was observed. 200x magnification.

5.7. Myelin Thickness

Histomorphometric analysis on the proximal end of the conduit revealed increased myelin thickness in the Matched diameter with hMSC conduits (0.79 ± 0.02) compared to the Matched diameter with saline (0.67 ± 0.07), Autograft (0.65 ± 0.21), Large diameter filled with hMSC (0.59 ± 0.12) and Large diameter filled with saline (0.46 ± 0.10) (Figure 28). No statistical differences were found between the Autograft group and the four experimental groups. However, statistical difference was found between the Matched with hMSC group and Large diameter with saline group (p=0.004). Furthermore, there was a statistical difference between the Matched diameter with hMSC vs. saline group (p=0.01), Matched vs. Large diameter with hMSC groups (p=0.011), and Matched vs. Large diameter with saline groups (p=0.002).

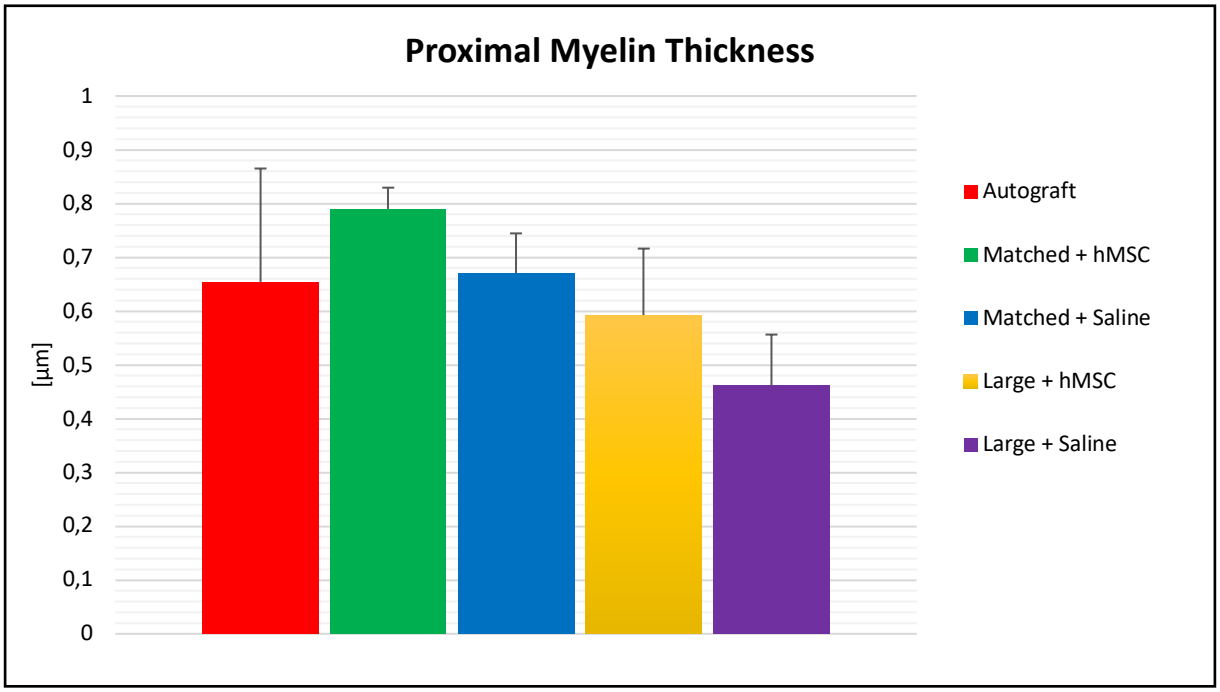

Figure 28. Myelin Thickness at the Proximal end of the hESC at 12 weeks after nerve defect repair. The myelin thickness was increased in the Matched hESC with hMSC treated group (0.79 ± 0.02) when compared to the Matched hESC with saline (0.67 ± 0.07), Autograft group (0.65 ± 0.21), Large hESC with hMSC group (0.59 ± 0.12) and Large hESC with saline group (0.46 ± 0.10), illustrating the importance of conduit diameter matching during nerve gap repair. Furthermore, the results confirm the value of the application of hMSC as a catalyst for peripheral nerve regeneration.

The analysis of the distal end of the conduits revealed a higher tendency of myelin thickness in the Matched diameter with hMSC conduits (0.65 ± 0.06) followed by the Autograft group (0.63 ± 0.10), Matched diameter hESC with saline (0.47 ± 0.07), Large diameter hESC filled with hMSC (0.38 ± 0.05) and Large diameter hESC filled with saline (0.37 ± 0.04) (Figure 29). We found a statistical difference when comparing the Autograft and Matched diameter hESC with hMSC each to the rest of the three groups ($p < 0.001$). However, we found no statistical difference when comparing the Autograft to the Matched diameter hESC with hMSC group ($p > 0.05$). Furthermore, there is a statistical difference between Matched diameter hESC with hMSC vs. saline group ($p < 0.001$), Matched vs. Large diameter with hMSC groups ($p < 0.001$), and Matched vs. Large diameter with saline groups ($p = 0.023$).

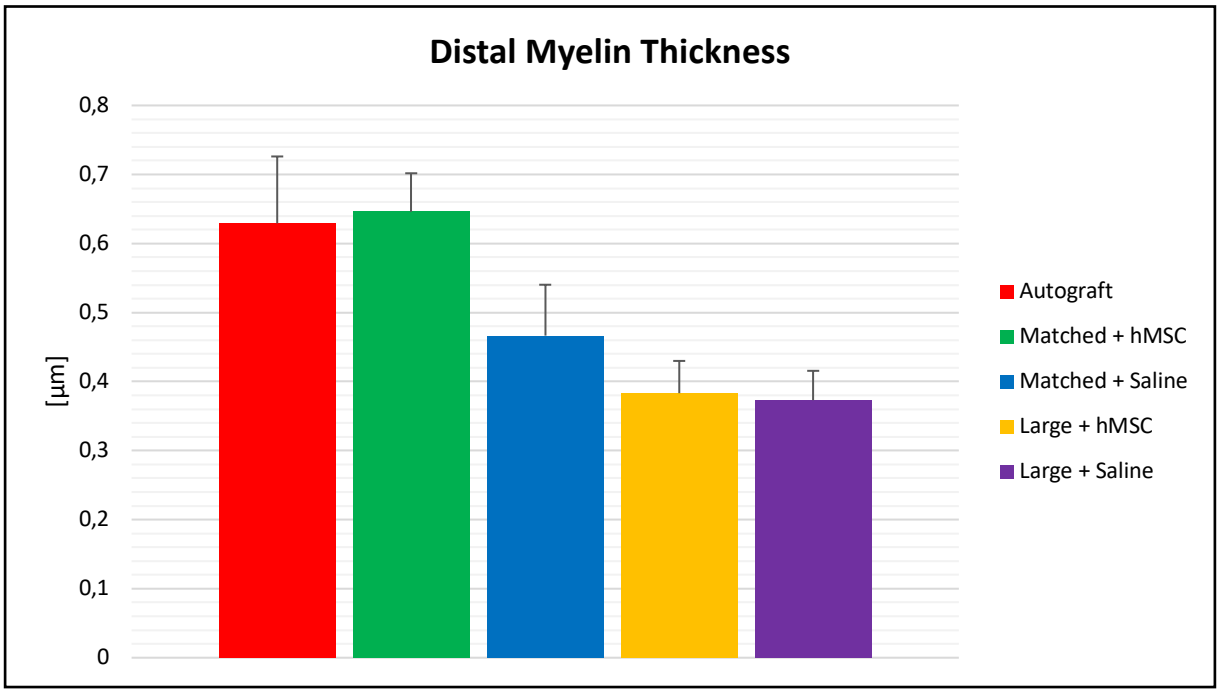

Figure 29. Myelin Thickness at the Distal end of the hESC at 12 weeks after nerve defect repair. The myelin thickness was increased in the Matched hESC with hMSC treated group (0.65 ± 0.06) when compared to the Autograft group (0.63 ± 0.10), Matched hESC with saline (0.47 ± 0.07), Large hESC with hMSC group (0.38 ± 0.05) and Large hESC with saline group (0.37 ± 0.04), confirming the importance of the conduit diameter matching during nerve gap repair and supporting the application of hMSC for enhancement of peripheral nerve regeneration.

5.8. Fiber Diameter

In the Matched diameter hESC with hMSC, the conduits revealed a larger diameter of the nerve fibers at the proximal end (4.69 ± 0.31) when compared to the Autograft group (4.32 ± 0.93), Matched diameter hESC with saline (3.99 ± 0.38), Large diameter hESC filled with saline (3.26 ± 0.91) and Large diameter hESC filled with hMSC (3.26 ± 0.20) (Figure 30). There were no significant differences between the Autograft and the Matched diameter hESC with hMSC group, however, statistical difference was found between the Matched diameter hESC with hMSC group and the two Large diameter groups (p=0.005). Furthermore, a statistical difference was noted between the Matched diameter hESC saline and hMSC group (p=0.006).

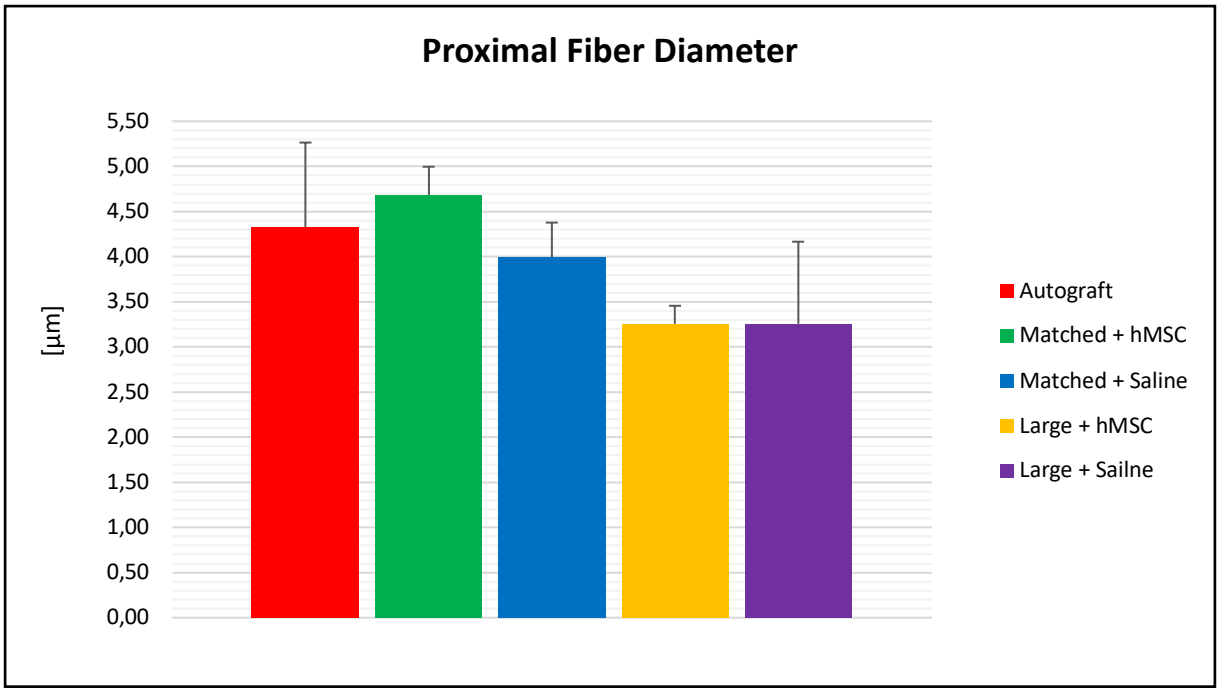

Figure 30. Fiber Diameter at the Proximal end of the hESC at 12 weeks after nerve defect repair. The largest fiber diameter was observed in the Matched hESC with hMSC treated group (4.69 ± 0.31), followed by the Autograft group (4.32 ± 0.93), Matched hESC with saline (3.99 ± 0.38), Large hESC with hMSC group (3.26 ± 0.91) and Large hESC with saline group (3.26 ± 0.20). The results confirm the importance of conduit diameter matching and support the evidence of beneficial effects of hMSC application for enhancement of peripheral nerve regeneration.

At the distal end, the conduits in groups with Matched diameter hESC with hMSC revealed the largest diameter of nerve fibers (4.04 ± 0.31) followed by the Autograft group (3.79 ± 0.69), Matched diameter hESC with saline (3.36 ± 0.19), Large diameter hESC filled with saline (3.13 ± 0.46) and Large diameter hESC filled with hMSC (3.08 ± 0.53) (Figure 31). There was no significant difference found when comparing the Autograft to Large diameter hESC with saline group and when comparing the Matched diameter hESC with hMSC group to both the Large diameter groups (p=0.003). Furthermore, a statistical difference was noted between the Matched diameter hESC saline and hMSC group (p=0.001).

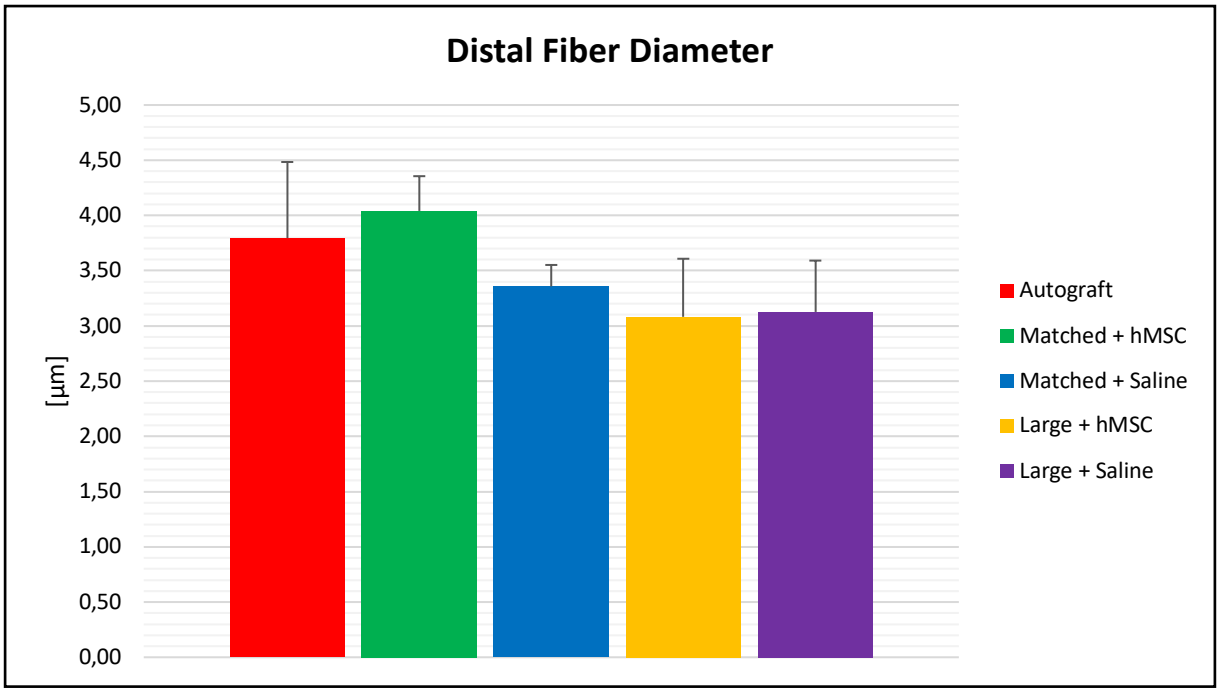

Figure 31. Fiber Diameter at the Distal end of the hESC at 12 weeks after nerve defect repair. At the distal end in all the groups, the myelin thickness values were smaller when compared to the respective proximal ends of the hESC. The largest diameter was observed in the Matched hESC with hMSC treated group (4.04 ± 0.31), followed by the Autograft group (3.79 ± 0.69), Matched hESC with saline (3.36 ± 0.19), Large hESC with saline group (3.13 ± 0.46) and Large hESC with hMSC group (3.08 ± 0.53). The results confirm the importance of conduit diameter matching during nerve gap repair in order to achieve optimal nerve recovery. Moreover, the positive impact of hMSC support was observed only in the Matched diameter groups. The Large conduit group supported with hMSC did not differ in fiber diameters when compared to the Large conduit group with saline.

5.9. Axonal Density

The proximal axonal density was observed to be most prominent in the Matched diameter hESC with hMSC conduits (371 ± 38) followed by the Autograft group (322 ± 162), Matched diameter hESC with saline (294 ± 97), Large diameter hESC filled with hMSC (240 ± 73) and Large diameter hESC filled with saline (166 ± 91) (Figure 32). Statistical differences were observed between the Large diameter hESC with saline vs. Matched diameter hESC with hMSC groups (p=0.017), Matched vs. Large diameter with hMSC (p=0.003), and Matched vs. Large diameter filled with saline (p=0.039).

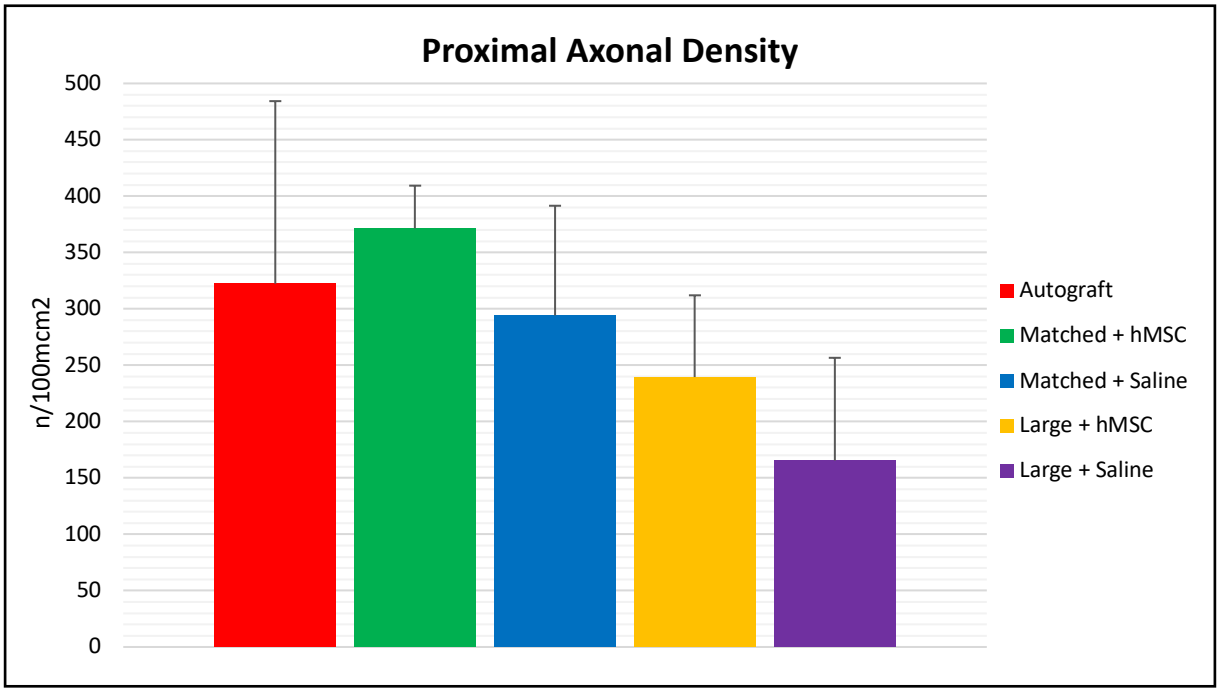

Figure 32. Axonal Density at the Proximal end of the hESC at 12 weeks after nerve defect repair. The highest axonal density was observed in the Matched hESC with hMSC treated group (371 ± 38), followed by the Autograft group (322 ± 162), Matched hESC with saline (294 ± 97), Large hESC with saline group (240 ± 73) and Large hESC with hMSC group (166 ± 91). The results confirmed a better recovery in the matched diameter conduits when compared to the groups where large diameter conduits were passed for nerve gap repair.

At the distal ends, there was a reduction in the axonal density in the four conduit groups when compared to the axonal density at the proximal end of the respective groups. The Autograft group revealed the largest axonal density at the distal end (322 ± 112) followed by the Matched diameter hESC with hMSC conduits (167 ± 47), Matched diameter hESC with saline (133 ± 81), Large diameter hESC filled with hMSC (107 ± 33) and Large diameter hESC filled with saline (71 ± 37) (Figure 33). There was a statistical difference found between the Autograft vs. Large diameter hESC with saline group (p=0.001) and Matched vs. Large diameter conduit filled with hMSC (p=0.026).

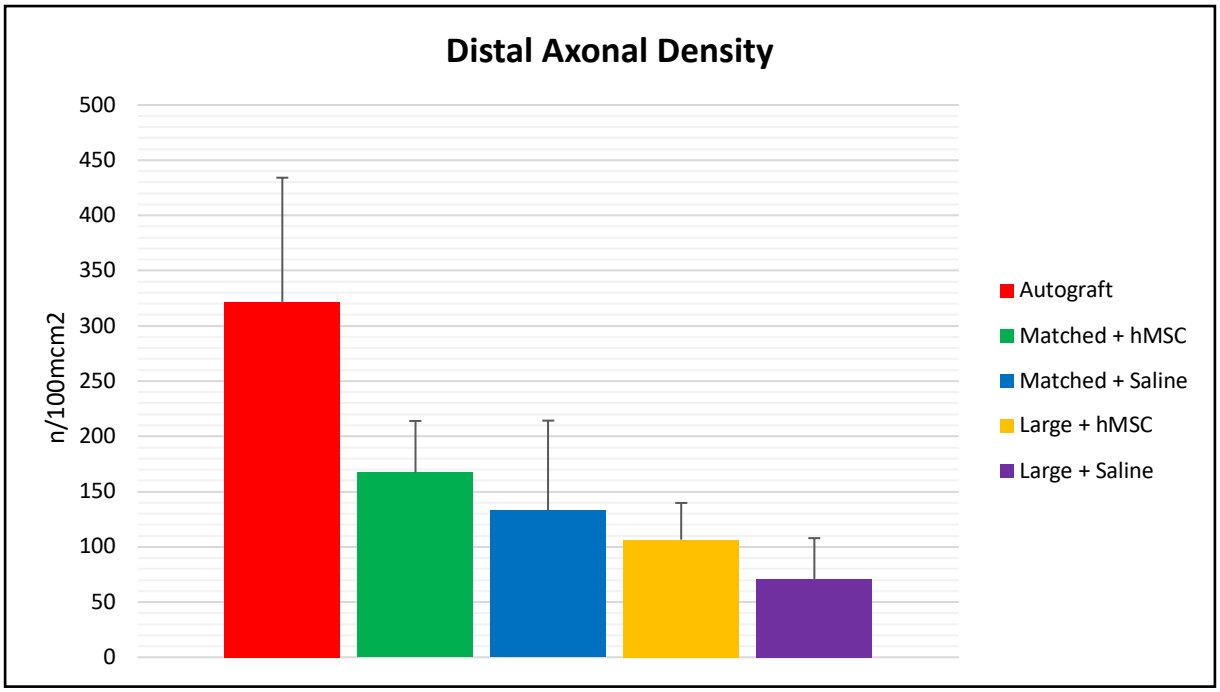

Figure 33. Axonal Density at the Distal end of the hESC at 12 weeks after nerve defect repair. The largest axonal density was observed in the Autograft group (322 ± 112), followed by the Matched hESC with hMSC group (167 ± 47), Matched hESC with saline (133 ± 81), Large hESC with hMSC group (107 ± 33), and Large hESC with saline group (71 ± 37). The Matched hESC filled with hMSC showed significantly better results when compared to the Large hESC filled with hMSC, confirming the need for conduit diameter matching during nerve gap repair.

5.10. Percent Myelinated Fibers

At the proximal end of the conduit, the Matched diameter hESC with hMSC conduits revealed the highest percent of the myelinated fibers (90% ± 4) followed by the Autograft group (85% ± 3), Matched diameter hESC with saline (84% ± 3), Large diameter hESC filled with hMSC (68% ± 10) and Large diameter hESC filled with saline (61% ± 7) (Figure 34). Statistical differences were observed between the Autograft and both Large diameter groups. Furthermore, statistical differences were noted between each of the Large diameter hESC groups when compared to the Matched diameter hESC respective groups in terms of hMSC and saline ($p < 0.001$) and Matched vs. Large conduit group filled with hMSC ($p=0.033$).

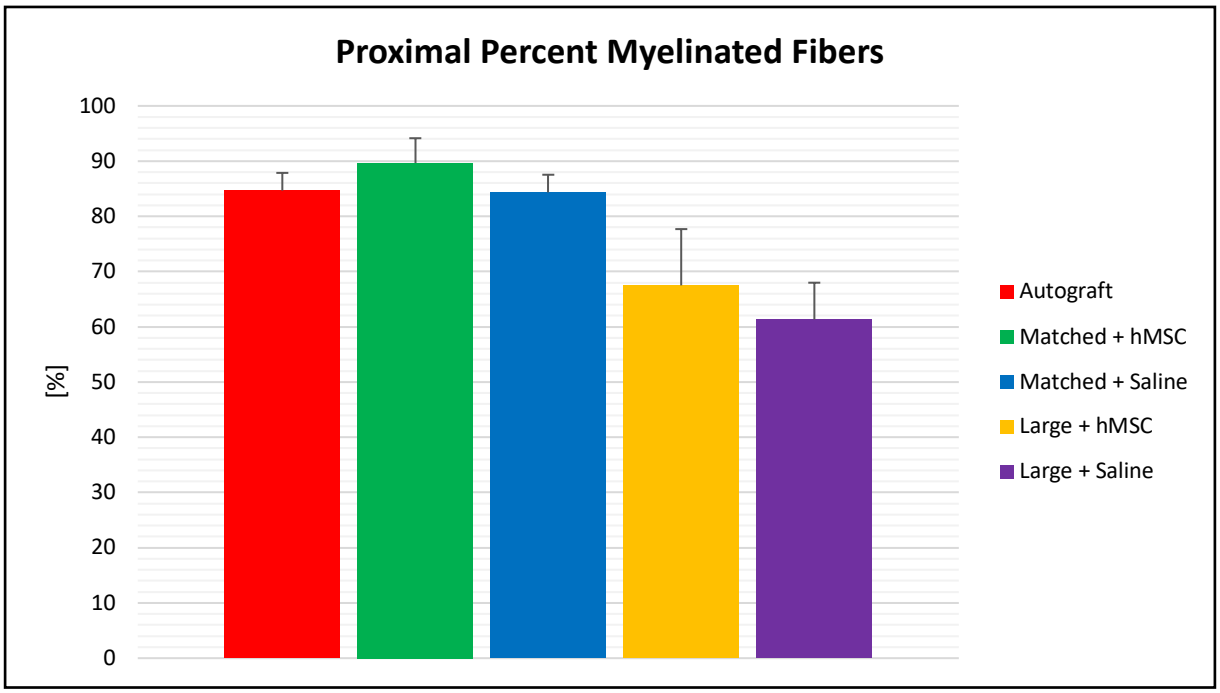

Figure 34. Percent of the Myelinated Fibers at the Proximal end of the hESC at 12 weeks after nerve defect repair. The highest ratio of myelinated fibers was found in the Matched hESC with hMSC treated group (90% ± 4), followed by the Autograft group (85% ± 3), Matched hESC with saline (84% ± 3), Large hESC with saline group (68% ± 10) and Large hESC with hMSC group (61% ± 7). The results confirm the positive impact of hMSC support in both the matched and large conduits. Furthermore, the importance of conduit matching was significant in the hMSC groups.

The Matched diameter hESC with hMSC conduits revealed the highest percent of the myelinated fibers (92% ± 3) at the distal end of the hESC followed by the Autograft group (83% ± 3), Matched diameter hESC with saline (75% ± 7), Large diameter hESC filled with hMSC (66% ± 10) and Large diameter hESC filled with saline (53% ± 9) (Figure 35). There were statistical differences found between the Large diameter hESC with saline group with the Autograft and Matched diameter hESC with hMSC group. There were also statistical differences found between Matched vs. Large diameter conduit with hMSC ($p<0.001$), Large diameter hESC conduit filled with saline vs. hMSC ($p=0.424$), Matched diameter with saline vs. hMSC ($p=0.001$), Matched vs. Large conduits filled with saline ($p<0.001$).

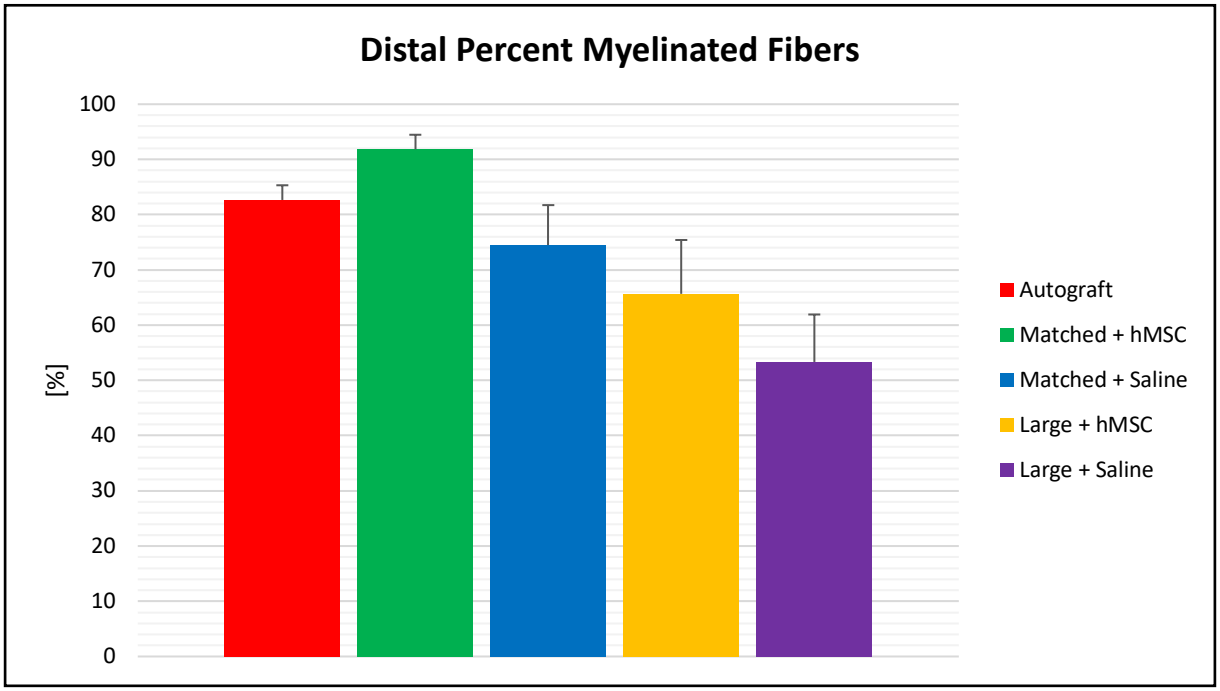

Figure 35. Percent of the Myelinated Fibers at the Distal end of the hESC at 12 weeks after nerve defect repair. The highest ratio of the myelinated fibers was found in the Matched hESC with hMSC treated group (92% ± 3), followed by the Autograft group (83% ± 3), Matched hESC with saline (75% ± 7), Large hESC with hMSC group (66% ± 10) and Large hESC with saline group (53% ± 9). The results confirmed favorable effects of both the conduit diameter matching to the injured nerve stump and the application of hMSC as a supportive therapy for enhancement of nerve regeneration.

6. DISCUSSION

Peripheral nerve injuries are among the most prevalent causes of disability globally.[101] In recent years, an increase in the incidence of peripheral nerve injuries in both the military and civilian settings has been noted, with approximately 100,000 peripheral nerve repair operations occurring in Europe and the United States annually.[9,10] Following stretch-related injuries, lacerations are the second most prevalent type of nerve injury, comprising about 30% of all severe injuries.[102] These traumatic cases impede the restoration of function and return to work and, as such, represent a substantial economic burden. Despite a considerable amount of research, the treatment of nerve injuries still represents a serious challenge for clinicians.

The primary purpose of peripheral nerve repair is to restore the function of the end-organ as fast and as well as possible while restricting the donor site and systemic morbidities. The surgeon must carefully consider multiple factors of injury to optimize the recovery. Earlier treatment of nerve injuries leads to better clinical results due to faster endplate and receptor reinnervation. Younger patients, with better regenerative ability, show better outcomes compared to the elderly. Injuries at the proximal sites of extremities result in longer regenerative distances to the distal target, limiting the chance of full recovery. Furthermore, the presence of soft and vascular tissue damage significantly slows the recovery process due to significant distortion and scarring of the affected area.[31]

Although end-to-end coaptation of a lacerated nerve is the favored method of treatment, it is not applicable in the management of nerve gaps since the coaptation of the nerve ends under tension leads to distorted microvascular flow hindering fascicular regeneration, leading to poor clinical outcomes. Terzis et al. note that even marginal tension can adversely influence the functional results after nerve repair.[28,30]

In such cases, the application of bridging material between the two nerve stumps is needed to guide the proximal end to the distal end of the nerve. The lack of nerve guidance within the space between the two stumps may result in the misdirection of the regenerating axons, generating a neuroma. In their study, Lundborg et al. have shown that a 10 mm nerve gap without guidance prevents regenerating fascicles from reaching the nerve's distal end.[103] Multiple surgical strategies have been proposed to address these problems.

One of the strategies includes nerve transfer techniques which were first proposed by Tuttle et al. in 1913.[104] In the last 20 years, multiple authors published good results employing this technique. Using the nerve transfer method, the surgeon will use an expendable healthy donor nerve that is in the proximity and will insert it into the injured nerve close to the target

end-organ, allowing to skip the injury site that is located proximately. This technique is well established in both the brachial plexus and proximal upper extremity injuries. However, this method leads to loss of function from the donor nerve site and is limited to isolated nerve injuries.[31]

In 1903, both Balance and Harris proposed a technique of end-to-side coaptation in which the distal end of the injured nerve is coapted into a healthy nerve that is in its proximity.[42,43] This method can be used when the proximal end of the injured nerve is inaccessible. Although this technique is beneficial when minimal sensory recovery is required, it will not result in motor regeneration without donor axonal injury.[31]

Nerve allografts from cadavers can be applied in large or segmental nerve injuries where other surgical methods cannot be successfully applied. Its unlimited supply, the avoidance of donor site morbidity, and its ability to bridge the nerve gap have made it a potential alternative to other methods. The use of such grafts supplies the donors Schwann Cells into the host, which support the remyelination of the nerve and also acts as an antigen-presenting cell. This later characteristic requires systemic immunosuppression. This, however, is temporary, as the host Schwann Cells migrate into the allograft, and the need for immunosuppression is usually not needed after around 24 months. Furthermore, the commonly used immunosuppressive agent FK-506 has been shown to augment neuroregeneration. Nevertheless, the potential side effects of immunosuppression must be considered when contemplating this method.[31]

Autologous nerve grafting is viewed as the gold standard in peripheral nerve gap regeneration. Its ability to supply both Schwann cells and neurotrophic factors for nerve regeneration makes it almost an ideal method of nerve reconstruction. Multiple nerves have been shown to be used as the preferred donors depending on the area of nerve injury. However, autologous grafting method has its limitations, such as neuroma formation, tissue scarring, limited availability, and prolonged surgery.[31]

In recent years, a reemergence of interest in biological and artificial conduits as an alternative therapy for peripheral nerve injuries has been observed. Conduits can be employed in the management of nerve gaps as an alternative to nerve autografts. The function of such a conduit is to provide axonal guidance, isolate the growing axons from the surrounding tissues, restrict inflammation and fibrosis, and reduce the possibility of a neuroma formation.

As the first, in the 1880s, Gluck unsuccessfully tried to apply a conduit constructed from a decalcified bone.[62] Since then, biological conduits such as veins, arteries, muscles, and tendons have been researched as a potential alternative to autografts. Using a rat model, Nijhuis et al. presented favorable results when repairing a 1.5 cm sciatic nerve defect with a vein

conduit.[65] In a prospective clinical evaluation, Chiu et al. noted that vein grafts delivered similar results when compared to the sural nerve digital grafts.[64] As an alternative, Fawcett et al. applied muscle basal lamina grafts into sciatic nerve gaps and obtained a comparable nerve regeneration to the autografts. It was suggested that favorable results were related to the longitudinally oriented basal lamina of the skeletal muscles promoting cell adhesion to the extracellular matrix.[66] Brand et al. published multiple studies concluding that the use of tendon has a comparable result to the use of freeze-thawed muscle grafts in the treatment of nerve gaps.[67,68,69]

Synthetic materials, being readily available, have also been explored as a possible alternative in peripheral nerve gap repair. Silicone conduits are constructed from non-degradable material. Their neuroregenrative potential has been studied for many years and has been shown to promote nerve recovery. However, its widespread application in the clinical setting has been hindered as the conduits become surrounded by fibrous tissue, leading to the compression of the nerve, which requires an additional procedure to remove the conduit. [105] Nevertheless, these conduits have been applied successfully in the past years. Merle et al. presented their results showing that a silicone conduit was able to regenerate a gap length of 3-5 cm in three patients with ulnar and median nerve injuries.[106]

To avoid many of these problems, researchers have focused on creating a biodegradable conduit. Materials such as collagen, polyglycolic acid, chitosan, polyester, and copolyesters have all been researched as methods in bridging a nerve gap after injury. Unfortunately, synthetic conduits have variable outcomes, limiting them to small-diameter nerves with gaps less than 3 cm in length.[107,108,109,110]

Due to the limitations of the current surgical methods of long nerve defect repair, novel therapeutic strategies are required to improve nerve regeneration. As a naturally occurring tissue surrounding the nerve, the epineurium is mainly comprised of elastin fibers and collagen I and III making it a desirable substance for the creation of a conduit. Due to its high Laminin expression, it provides a neruropermisive environment that promotes Schwann cell attachment and, therefore, supports axonal growth.

One of the natural conduits commercially available and approved for clinical cases of nerve regeneration is the Advance Nerve Graft (ANG, AxoGen Inc, Alachua, FL, US), a processed human nerve allograft.[111] Choe et al. provided evidence of successful regeneration of a nerve gap up to 50 mm using decellularized nerve allograft.[112] However, it is widely accepted that this method of treatment is limited mainly to injuries of the sensory nerves with

gaps less than 3 cm.[113] Susan Mackinnon uses ANG to reconstruct nerve gaps less than 4cm in small-diameter sensory nerves.[114]

In our study, we have successfully proven that the application of a human Epineural Sheath Conduit may be a possible substitute to the now gold standard Autograft repair as it eliminates many of the complications of autograft surgery such as sensory loss, tissue scarring, neuroma formation, and limited supply. Although some studies have shown that the application of an epineural sheath conduit has a positive effect on nerve regeneration, prevention of neuroma formation and muscle denervation atrophy, to the best of our knowledge, this is the first study reporting use of the human epineurium as a biomaterial for creation of the epineural sheath conduit (ESC) and application of the ESC in the regeneration of nerve gaps.

Macroscopically, our ESC conduits in all experimental groups showed limited signs of inflammation, well-preserved nerve structure, shape, and integrity with good vascularization. These findings are supported by Klimczak et al., who confirmed negligible immunogenic and increased proangiogenic properties of human ESC.[115] Furthermore, Yavuzer et al. reported that the epineural sheath, using the turnover epineural sheath tube (TEST) technique, can reduce the foreign material reaction and decrease the inflammatory response by limiting fibrosis of the end-to-end coaptation.[72] This suggests that the epineural conduit becomes an integral part of the recovered nerve and represents a potential advantage of the epineural conduit over synthetic materials, such as silicone conduits, which often must be removed after nerve regeneration.

Our study also provides clear evidence of the importance of diameter size matching between the injured nerve stumps and the conduits. We found a significant benefit of using the matched diameter conduits when compared to the unmatched large diameter conduit filled with hMSC when assessing the myelin thickness, axonal density, fiber diameter, and percentage of the myelinated nerve fibers at the proximal and distal ends of the conduit. When comparing conduits filled with saline, we found a statistically significant benefit of the matched diameter in the values of the proximal myelin thickness, total fascicle numbers, and percentage of the myelinated nerve fibers, while on the distal end, the benefit was noted in both the myelin thickness and percentage of the myelinated nerve fibers.

We also observed a significant advantage when assessing the Gastrocnemius Muscle Index (GMI) in both the matched conduits filled with hMSC and saline compared to their large diameter respective controls.

To the best of our knowledge, this study is the first to assess the effect of the conduit diameter size on nerve regeneration when using conduits created from the human epineurium.

Several studies have reported the need for diameter matching in the application of the synthetic conduits. Giusti et al. demonstrated that a size-matched nerve collagen conduit had better motor recovery in the rat model.[116] Another investigation published by Shin et al. compared the application of several synthetic conduits in the rat model and observed that the larger commercially available conduits had significantly inferior results in motor function recovery compared to the smaller, closer matched diameter conduits.[117] The same conclusion was reported by Kemp et al. when assessing the histomorphometric parameters.[118] We propose that there are two reasons for the large diameter epineural sheath conduits inferior results. First, the sheer amount of excess epineural tissue that can collapse on top of each other can obstruct the lumen of the conduit, limiting the advancement of the new regenerating fascicles. Thus, the disorganized structure of the large conduit limits the guidance of the new axons. Furthermore, as suggested by Moore et al., the gradient and availability of the proregenerative factors released into the conduit's microenvironment depend on its size.[119] As the volume of the conduit increases, these factors become more diluted within, limiting their neuroregenerative potential.

In this study, we have proven a significant increase in the expression of PKH26 – the membrane marker of the MSC as well as expression of HLA-1 and HLA-DR, confirming human origin of the MSC contributing to nerve regeneration. These markers were observed only in the hESC filled with hMSC when compared to the saline injected conduits. These findings suggest that at 12 weeks after injection, hMSC were still present in the conduits. Our observation is supported by Siemionow et al., who reported the presence of Bone Marrow Stromal Cells (BMSC) at 12 weeks after injection into a conduit in the rat model.[75] It is well known that MSC are immunomodulatory and are bearing low immunogenic response. Moreover, when considering the application of the hESC in the clinical setting, the autologous mesenchymal stem cells will be harvested from the patient, thus eliminating the problem of an immune response.

Furthermore, increased expression of Laminin B, a vital extracellular matrix component for axonal regeneration, which was found in all experimental groups, confirming neuroregenerative characteristics of the hESC. In addition, the regenerative potential of hESC was confirmed by increased expression of the S-100 protein, indicating the presence of Schwann cells.

Expression of the neurotrophic factor NGF was increased in the hMSC groups, which was in accordance with the Pereira Lopes et al. study, who demonstrated the expression of NGF by BMSC.[120] There was a low expression of the GFAP in all studied groups. This finding can be

supported by Siemionow et al. study, in which a significant drop in the expression of GFAP was observed between week 6 and week 12 after injury. In the same study, there was no significant drop observed in the expression of NGF between week 6 and 12.[75]

Proper blood supply is one of the crucial components of successful peripheral nerve regeneration. Our study confirmed the expression of both vWF and VEGF in the hESC conduits. VEGF expression in the two hMSC supported groups was higher compared to the saline injected conduits. Although the highest level of vWF expression was found in the matched diameter conduit supported with hMSC group, there was no significant difference between the groups indicating the positive effect of the epineurium on the conduit vascularization. Assessment of the VEFG expression revealed a significant VEGF increase in both the Autograft and the Matched diameter with hMSC group when compared with the Large diameter with saline group. Our results are supported by numerous studies that have reported improved angiogenesis in ischemia damaged muscle tissues after MSC transplantation.[95,121] In nerve regeneration, Petrova et al. showed a positive impact of MSC on the density of blood vessels in the endoneurium.[122] Furthermore, after treating a 10 mm sciatic nerve gap in the rat model using a conduit supported with human adipose-derived MSC, Kingham et al. found increased angiogenesis in the regenerating nerve.[123] Increased expression of VEFG was also noted by Fan et al., who discovered improved angiogenesis after applying Schwann-like cells differentiated from the bone marrow-derived mesenchymal stem cells.[124] Our results, supported by the current literature, suggest that mesenchymal stem cells play a key role in angiogenesis during peripheral nerve regeneration.

Our study found no clear benefit of hMSC therapy when applied to the large conduits, noting only a positive impact on the percentage of the myelinated nerve fibers. Furthermore, expression of other growth factors revealed low scores in both large conduit groups when compared to the Autograft and the two matched conduit groups. This may be due to the fact that the same number of hMSC was injected to both the matched and the large conduits; thus, it showed an enhanced regenerative effect in the matched conduits but no significant effect in the large conduits. Therefore, in future studies, it will be interesting to test higher doses of MSC in large diameter conduits and observe if there is a dose-dependent effect on nerve regeneration.

When comparing the matched diameter conduits in terms of the effect of hMSC, we found a clear benefit of MSC application for enhancement of nerve regeneration at both the proximal and the distal ends of the conduit as confirmed by increased myelin thickness, nerve diameter, and percentage of the myelinated nerve fibers. All these parameters revealed a higher score in the matched conduit with hMSC compared to the conduits injected with saline. Our results are

supported by other investigators studies, including a study by Yang et al., who used the rat sciatic nerve injury model and demonstrated an improvement in histological and functional recovery confirmed by an increase in the expression of S100, BDNF, CNF, and BFGF, when silk fibronin nerve conduits were supported with bone marrow-derived mesenchymal stem cells.[125] Additionally, Zhao et al. using a 10 mm sciatic nerve injury model in mice, documented better axonal growth, walking track results, and target muscle preservation in animals reconstructed with nerve grafts supported with bone marrow mesenchymal stem cells.[126]

Furthermore, Siemionow et al. assessed the application of epineural sheath conduits for the repair of large nerve gaps using conduits that matched in the diameter size to the size of the injured nerves. In their study, Siemionow et al. confirmed the feasibility of the application of epineural sheath conduits for the restoration of a 6 cm long nerve defect in a large animal- the sheep median nerve model.[127] Although more research is still needed, we propose that our human epineural sheath conduit has a potential application for the large nerve gap repair, in which currently available synthetic conduits have failed to succeed.

Peripheral nerve gap regeneration is a complex process requiring guidance of the proximal sprouting nerve. Our study offers ample evidence that our novel naturally occurring conduit created from the human epineurium provides the necessary guidance for nerve regeneration when conduit diameter is matched with the diameter of the repaired nerve. As a naturally occurring tissue surrounding the nerve, the epineural conduit is not prone to inflammation, has a well-preserved neural-like structure, shape, and integrity when implanted into the nerve gap. Furthermore, when supported with human Mesenchymal Stem Cells, our Epineural Sheath conduit provides the favorable neuroregenerative microenvironment to support the successful regeneration of a 20 mm nerve gaps.

With its abundant supply, accessibility, and the lack of immune reaction, the epineural sheath conduit, supported with hMSC, introduces a new promising alternative to the Autograft technique, which is representing the current gold standard of the peripheral nerve gap repair. Although more research is warranted to define the storage and preservation protocols of the conduits and the optimization of mesenchymal stem cells harvesting, we believe that human epineural conduit can be used in the future as the "off-the-shelf" product allowing for fast and straightforward clinical application for reconstruction of peripheral nerve defects after trauma.

7. CONCLUSIONS

1. We have successfully established the application of allogeneic hESC in the repair of peripheral nerve defects tested for 12 weeks in the nude rat experimental model, as confirmed by the following findings:
   - hESC supported with hMSC enhanced regeneration of the peripheral nerve defects and accelerated the recovery of nerve function
   - hESCs may eliminate several side effects related to the harvesting of autologous grafts.
   - Our novel hESC provides a potential alternative option to the autograft repair technique.
2. hESCs supported with hMSC demonstrated increased expression of the neurotrophic factors and proangiogenic properties at 12 weeks after nerve gap repair in the nude rat model.
3. Adjusting the hESC diameter in relation to the cross-sectional area of the repaired nerve has a significant effect on the quality of nerve regeneration and function of the peripheral nerves.

8. ABSTRACT

Introduction: Due to the limitations of current surgical methods of long nerve defect repair, new therapeutic approaches are needed to enhance nerve regeneration. Nerve allografts offer an unlimited source of epineural tissue, which allows to create epineural conduits, which can be matched to the recipient's injured nerve diameter and length to support nerve regeneration. Due to their anti-inflammatory and neuroregenerative properties, mesenchymal stem cells are considered a promising approach as supportive therapy for the enhancement of nerve regeneration following peripheral nerve injuries. Thus, we propose a novel therapeutic approach for nerve gap regeneration by applying human Epineural Sheath Conduits (hESC) supported with human Mesenchymal Stem Cells (hMSC).

Aim:

1. To assess *in vivo* the neuroregenerative potential of hESC supported with hMSC in 20 mm long nerve gaps in the nude rat model.
2. To evaluate the neurotrophic and proangiogenic properties of hESC and hMSC in the nude rat model.
3. To assess the effect of hESC diameter modification on peripheral nerve regeneration.

Methods: Restoration of 20 mm sciatic nerve defect with hESC created from human sciatic nerve supported with hMSC was tested in 6 experimental groups: Group 1: no repair control (n=6), Group 2: autograft control (n=6), Group 3: large diameter hESC filled with 1 mL saline (n=6), Group 4: large diameter hESC supported with $3x10^6$ hMSC (n=6), Group 5: matched diameter hESC filled with 1 mL saline (n=6), Group 6: matched diameter hESC supported with $3x10^6$ hMSC (n=6). We defined matched diameter conduits as those with a diameter less than three times (<3:1) the size of the rat's sciatic nerve. For the large diameter conduits, the diameter was more than five times bigger (>5:1) when compared to the rat's nerve diameter under repair. Functional tests of toe-spread and pinprick were performed at 1, 3, 6, 9, 12 weeks after nerve repair. At 12 weeks, nerve samples were collected for immunofluorescence staining (PKH26, HLA-1, HLA-DR, NGF, GFAP, Laminin B, S-100, VEGF, vWF) and histomorphometric analysis of myelin thickness, axonal density, fiber diameter, and percentage of the myelinated nerve fibers. Muscle samples were collected for assessment of the Gastrocnemius Muscle Index (GMI) and for the muscle fiber area ratio measurements.

Results: Macroscopic evaluation of epineural conduit repair site at 12 weeks confirmed preservation of a normal nerve shape without scar tissue formation, adhesions, or local signs of inflammation, and good vascularization was observed in all groups. The greatest sensory and motor recovery following application of hESC was observed in Group 2, followed by Group 6, Group 5, Group 4, Group 3, and Group 1 (pinprick 3.0 vs. 2.33 vs. 2.0 vs. 1.5 vs. 1.0

vs. 0.5; toe-spread 1.83 vs. 1.5 vs. 1.0 vs. 0.5 vs. 0.33 vs. 0.17, respectively). GMI and muscle fiber area ratio revealed the highest values for Group 2 (0.323/0.449) followed by Group 6 (0.285/0.320), Group 5 (0.274/0.271), Group 4 (0.211/0.211) Group 3 (0.192/0.87) and Group 1 (0.161/0.0105). MSC cells stained with PKH26 prior to conduit implantation, as well as HLA-1 and HLA-DR immunofluorescence staining, were detectable only in conduits filled with hMSC, thus confirming the presence of hMSC of human origin. A stronger expression of Laminin B was found in the proximal segments of the hESC when compared to the distal segments. Increased expression of Laminin B was noted at the proximal end of the conduit in Group 6 when compared to Group 3. Expression of S-100 in Group 6 was comparable to Group 2, with a moderate expression detected at both the proximal and distal segments of the conduit. A strong expression of VEFG was noted in the proximal end of the conduit in all groups, except for Group 3, which revealed weak expression. At the distal end of the hESC, VEGF expression was moderate, except for Group 3, which revealed a weak expression. The histomorphometric analysis of the distal end of the conduit revealed higher values of myelin thickness in Group 6 (0.65) followed by group 2 (0.63), Group 5 (0.47), Group 4 (0.38), and Group 4 (0.37). The largest diameters of nerve fibers were found in Group 6 (4.04), followed by Group 2 (3.79), Group 5 (3.36), Group 3 (3.13), and Group 4 (3.08). The largest distal axonal density was observed in Group 2 (322), followed by Group 6 (167), Group 5 (133), Group 4 (107), and Group 3 (71). The highest values for the percentage of distal myelinated fibers were assessed in Group 6 (92%), followed by Group 2 (83%), Group 5 (75%), Group 4 (66%), and Group 3 (53%).

Conclusions:

1. We confirmed the successful application of allogeneic hESC in the repair of peripheral nerve defects tested for 12 weeks in the nude rat experimental model:

- hESC supported with hMSC enhance regeneration of the peripheral nerve defects and accelerate the recovery of nerve function
- hESCs may eliminate several side effects related to harvesting of autologous grafts.
- Our novel hESC provides a potential alternative option to the autograft repair technique.

2. hESCs supported with hMSC demonstrate increased expression of the neurotrophic factors and proangiogenic properties at 12 weeks after nerve gap repair in the nude rat model.
3. Adjusting the hESC diameter in relation to the cross-sectional area of the repaired nerve has a significant effect on the quality of nerve regeneration and function of the peripheral nerves.

9. STRESZCZENIE

Zastosowanie konduitu z ludzkiej pochewki epineuralnej wypełnionej komórkami mezenchymalnymi jako nowej metody regeneracji długich ubytków nerwów obwodowych w modelu doświadczalnym szczura

Wstęp: Ze względu na ograniczenia obecnych technik rekonstrukcji długich ubytków nerwów obwodowych, potrzebne są nowe metody wspomagające regenerację nerwów. Allograft stanowi nieograniczone źródło nanerwia (epineurium), które może być wykorzystane do utworzenia konduitu, dopasowanego do średnicy i długości uszkodzonego nerwu pacjenta. Mezenchymalne komórki macierzyste, z uwagi na swoje właściwości przeciwzapalne i neuroregeneracyjne, uważane są za obiecującą terapię wspomagającą regenerację nerwów obwodowych po urazach. W związku z tym, proponujemy nowatorskie podejście terapeutyczne wspomagajace regeneracji ubytków nerwów obwodowych przez zastosowanie konduitu utworzonego z ludzkiej pochewki epienuralnej (hESC), wypelnionego ludzkimi mezenchymalnymi komórkami macierzystymi (hMSC).

Cele pracy:

1. Ocena *in vivo,* potencjału neuroregeneracyjnego hESC wypełnionego *hMSC* w rekonstrukcji 20 mm ubytkow nerwów kulszowych w modelu doświadczalnym szczura (nude rat model).
2. Ocena właściwości neurotroficznych i proangiogennych hESC i hMSC w regeneracji nerwu kulszowego w modelu doświadczalnym szczura (nude rat model).
3. Ocena wpływu modyfikacji średnicy hESC na regenerację nerwów.

Metoda: U 36 szczurów utworzono 20 mm ubytek nerwu kulszowego. Zwierzęta podzielono na sześć grup eksperymentalnych: grupa 1: bez naprawy ubytku (n=6), grupa 2: naprawa ubytku Autograftem (n=6), grupa 3: naprawa ubytku przy użyciu hESC z dużą średnicą + 1mL sól fizjologiczna (n=6), grupa 4: hESC z dużą średnicą + $3x10^6$ hMSC (n=6), grupa 5: hESC z dopasowaną średnicą + 1mL sól fizjologiczna (n=6) oraz grupa 6: hESC z dopasowaną średnica +$3x10^6$ hMSC (n=6). Zdefiniowaliśmy dopasowanie średnicy jako mniejszej niż trzykrotna (<3:1) średnica nerwu kulszowego szczura. hESC o dużej średnicy były pięciokrotnie większe (> 5:1) od średnicy naprawianego nerwu szczura. Następnie badano funkcje czucia (ang. pinprick) i ruchu (ang. toe-spread) w 1,3,6,9 i 12 tygodniu po zabiegu. Po

12 tygodniach próbki nerwu wybarwiono błękitem toluidynowym celem analizy histomorfometrycznej (grubości mieliny, gęstości aksonów, średnicy włókien i odsetek zmielinizowanych włókien nerwowych) i ekspresji immunofluorescencyjnej (PKH26, HLA-1, HLA-DR, NGF, GFAP, Laminin B, S-100, VEGF, vWF). Próbki mięśni pobrano do oceny indeksu wagi oraz powierzchni włókien m. brzuchatego łydki (GMI) po prawej i lewej stronie.

Wyniki: Ocena makroskopowa konduitów po 12 tygodniach potwierdziła zachowanie prawidłowego kształtu nerwu bez tworzenia tkanki bliznowatej, zrostów lub miejscowych objawów zapalenia. Ponadto, uzyskano dobre unaczynienie we wszystkich grupach. Znamienną poprawę funkcji czuciowej i ruchowej zaobserwowano w grupie 2, a następnie kolejno w grupach 6, 5, 4, 3 i 1 (pin-prick 3 vs 2.33 vs 2 vs 1.5 vs 1 vs 0.5 i toe-spread 1.83 vs 1.5 vs 1.0 vs 0.5 vs 0.33 vs 0.13). Wskaźnik GMI i stosunek powierzchni włókien mięśniowych między prawy a lewym m. brzuchatym wykazał najwyższe wartości dla grupy 2 (0,323/ 0,449), a następnie grupy 6 (0,285/0,320), grupy 5 (0,274/0,271), grupy 4 (0,211/0,211) grupy 3 (0,192/0,87) i grupy 1 (0,161/0,0105). Komórki MSC barwione PKH26 przed implantacją konduitu były wykrywalne wyłącznie w proksymalnej i dystalnej części konduitów wypełnionych hMSC. Obecność HLA-1 i HLA-DR obserwowano w proksymalnym i dystalnym odcinku konduitu co potwierdza obecność MSC pochodzenia ludzkiego. W części proksymalnej konduitu stwierdzono wyższy stopień ekspresji Lamininy B niż w części dystalnej. Zwiększoną ekspresję Lamininy B odnotowano w proksymalnej stronie konduitu w grupie 6 w porównaniu z grupą 3. Ekspresja S-100 była umiarkowana i porównywalna w grupie 6 z Grupą 2 zarówno w proksymalnym, jak i dystalnym odcinku konduitu. Silną ekspresję VEFG stwierdzono w obrębie proksymalnej części konduitu we wszystkich badanych grupach, z wyjątkiem grupy 3, która ujawniła słabą ekspresję. Ekspresja VEGF była umiarkowana w dystalnym odcinku hESC z wyjątkiem grupy 3, gdzie obserwowano słabą ekspresję. Analiza histomorfometryczna dystalnego odcinka konduitu wykazała wyższe wartości grubości mieliny w grupie 6 (0,65), a następnie w grupie 2 (0,63), grupie 5 (0,47), grupie 4 (0,38) i grupie 4 (0,37). Największe średnice włókien nerwowych zaobserwowano w grupie 6 (4,04), następnie w grupie 2 (3,79), grupie 5 (3,36), grupie 3 (3,13) i grupie 4 (3,08). Największą liczbę aksonów zaobserwowano w grupie 2 (322), a następnie w grupie 6 (167), grupie 5 (133), grupie 4 (107) i grupie 3 (71). Najwyższy odsetek zmielinizowanych włókien stwierdzono w grupie 6 (92%), następnie w grupie 2 (83%), grupie 5 (75%), grupie 4 (66%) i grupie 3 (53%).

Wnioski:

1. Potwierdzono skuteczność zastosowania allogennego hESC w rekonstrukcji ubytków nerwów po 12 tygodniach w modelu doświadczalnym szczura (nude rat model):

– komórki mezenchymalne wypełniające hESC wspomagają regenerację ubytków nerwów obwodowych i prowadzą do przyspieszenia powrotu funkcji nerwu;
– hESC eliminują wiele objawów ubocznych autogennych przeszczepów nerwów;
– hESC jest nową alternatywną metodą rekonstrukcji ubytków nerwów obwodowych.

2. W modelu doświadczalnym szczura, hESC wzbogacone hMSC wykazują istotne właściwości neuroregeneracyjne i proangiogenne po 12 tygodniach od naprawy nerwu.
3. Dopasowanie średnicy hESC względem przekroju nerwu ma istotny wpływ na jakość regeneracji i funkcji nerwów obwodowych.

10. LIST OF FIGURES

11. LIST OF TABLES

12. REFERENCES

[1] Lodish H, Berk A, Zipursky SL, et al. Molecular Cell Biology. 4th edition. New York: W. H. Freeman; 2000. Chapter 21, Nerve Cells.

[2] Verkhratsky A, Ho MS, Zorec R, Parpura V. The Concept of Neuroglia. Adv Exp Med Biol. 2019;1175:1-13.

[3] Salzer JL, Zalc B. Myelination. Curr Biol. 2016;26(20):R971-R975.

[4] Manzano GM, Giuliano LM, Nóbrega JA. A brief historical note on the classification of nerve fibers. Arq Neuropsiquiatr. 2008;66(1):117-119.

[5] Ushiki T, Ide C. Three-dimensional architecture of the endoneurium with special reference to the collagen fibril arrangement in relation to nerve fibers. Arch Histol Jpn. 1986;49(5):553-563.

[6] Reina MA, Colman Peyrano E, Diamantopoulos J, De Andrés JA (2015) Ultrastructure of the Perineurium. In: Reina M., De Andrés J, Hadzic A, Prats-Galino A, Sala-Blanch X, van Zundert A (eds) Atlas of Functional Anatomy for Regional Anesthesia and Pain Medicine. Springer, Cham.

[7] Peltonen S, Alanne M, Peltonen J. Barriers of the peripheral nerve. *Tissue Barriers*. 2013;1(3):e24956.

[8] Noble J, Munro CA, Prasad VS, Midha R. Analysis of upper and lower extremity peripheral nerve injuries in a population of patients with multiple injuries. J Trauma. 1998;45(1):116-122.

[9] Daly W, Yao L, Zeugolis D, Windebank A, Pandit A. A biomaterials approach to peripheral nerve regeneration: bridging the peripheral nerve gap and enhancing functional recovery. J R Soc Interface. 2012;9(67):202-221.

[10] Kelsey J, Praemer A, Nelson L, Feldberg A, Rice D. Upper extremity disorders: frequency, impact, and cost. New York: Churchill-Livingstone;1997. p.26-42.

[11] Campbell WW. Evaluation and management of peripheral nerve injury. Clin Neurophysiol. 2008;119(9):1951-1965.

[12] Burnett MG, Zager EL. Pathophysiology of peripheral nerve injury: a brief review. Neurosurg Focus. 2004;16(5):E1.

[13] Aguayo AJ, Peyronnard JM, Bray GM. A quantitative ultrastructural study of regeneration from isolated proximal stumps of transected unmyelinated nerves. J Neuropathol Exp Neurol. 1973;32(2):256-270.

[14] Menorca RM, Fussell TS, Elfar JC. Nerve physiology: mechanisms of injury and recovery. Hand Clin. 2013;29(3):317-330.

[15] Lunn ER, Brown MC, Perry VH. The pattern of axonal degeneration in the peripheral nervous system varies with different types of lesion. Neuroscience. 1990;35(1):157-165.

[16] Tetzlaff W, Bisby MA. Neurofilament elongation into regenerating facial nerve axons. Neuroscience. 1989;29(3):659-666.

[17] Seckel BR. Enhancement of peripheral nerve regeneration. Muscle Nerve. 1990;13(9):785-800.

[18] Lasek RJ, Hoffman PN: The neuronal cytoskeleton, axonal transport and axonal growth, in Goldman R, Pollard T, Rosenbaum J (cds): Microtubules and Related Proteins. Cell Motility, Book C. Cold Spring Harhor Coference on Cell Proliferation. New York, Cold Spring Harbor, 1976, vol 3, p 1021-1049

[19] Raivich G, Bohatschek M, Da Costa C, et al. The AP-1 transcription factor c-Jun is required for efficient axonal regeneration. Neuron. 2004;43(1):57-67.

[20] Seijffers R, Allchorne AJ, Woolf CJ. The transcription factor ATF-3 promotes neurite outgrowth. Mol Cell Neurosci. 2006;32(1-2):143-154.

[21] Jankowski MP, Miller L, Koerber HR. Increased Expression of Transcription Factor SRY-box-Containing Gene 11 (Sox11) Enhances Neurite Growth by Regulating Neurotrophic Factor Responsiveness. Neuroscience. 2018;382:93-104.

[22] Huebner EA, Strittmatter SM. Axon regeneration in the peripheral and central nervous systems. Results Probl Cell Differ. 2009;48:339-351.

[23] Gilley J, Coleman MP. Endogenous Nmnat2 is an essential survival factor for maintenance of healthy axons. PLoS Biol. 2010 Jan 26;8(1):e1000300.

[24] Brazill JM, Li C, Zhu Y, Zhai RG. NMNAT: It's an NAD^+ synthase… It's a chaperone… It's a neuroprotector. Curr Opin Genet Dev. 2017;44:156-162.

[25] Fu SY, Gordon T. The cellular and molecular basis of peripheral nerve regeneration. Mol Neurobiol. 1997;14(1-2):67-116.

[26] Gordon T. The biology, limits, and promotion of peripheral nerve regeneration in rats and human. Nerves And Nerve Injuries Eds: Tubbs RS, Rizk E, Shoja M, Loukas M, and Spinner RJ. Elsevier, 2015, Vol. 2 Ch 61, pp. 993–1019.

[27] Gordon T, English AW. Strategies to promote peripheral nerve regeneration: electrical stimulation and/or exercise. Eur J Neurosci. 2016;43(3):336-350.

[28] Terzis J, Faibisoff B, Williams B. The nerve gap: suture under tension vs. graft. Plast Reconstr Surg. 1975 Aug;56(2):166-70.

[29] Millesi H. The nerve gap. Theory and clinical practice. Hand Clin. 1986;2(4):651-663.

[30] Driscoll PJ, Glasby MA, Lawson GM. An in vivo study of peripheral nerves in continuity: biomechanical and physiological responses to elongation. J Orthop Res. 2002;20(2):370-375.

[31] Ray WZ, Mackinnon SE. Management of nerve gaps: autografts, allografts, nerve transfers, and end-to-side neurorrhaphy. Exp Neurol. 2010;223(1):77-85.

[32] Sachanandani NF, Pothula A, Tung TH. Nerve gaps. Plast Reconstr Surg. 2014 Feb;133(2):313-319.

[33] Mackinnon S.E., Dellon L.E., 1988. Surgery of the Peripheral Nerve. Thieme, New York.

[34] Norkus T, Norkus M, Ramanauskas T. Donor, recipient and nerve grafts in brachial plexus reconstruction: anatomical and technical features for facilitating the exposure. Surg Radiol Anat. 2005;27(6):524-530.

[35]Hudson AR, Morris J, Weddell G, Drury A. Peripheral nerve autografts. J Surg Res. 1972;12(4):267-274.

[36] Belkas JS, Shoichet MS, Midha R. Peripheral nerve regeneration through guidance tubes. Neurol Res. 2004;26(2):151-160.

[37] Martini R. Expression and functional roles of neural cell surface molecules and extracellular matrix components during development and regeneration of peripheral nerves. J Neurocytol. 1994;23(1):1-28.

[38] Tung TH, Mackinnon SE. Nerve transfers: indications, techniques, and outcomes. J Hand Surg Am. 2010;35(2):332-341.

[39] Papalia I, Cardaci A, d'Alcontres FS, Lee JM, Tos P, Geuna S. Selection of the donor nerve for end-to-side neurorrhaphy. J Neurosurg. 2007;107(2):378-382.

[40] Papalia I, Geuna S, D'Alcontres FS, Tos P. Origin and history of end-to-side neurorrhaphy. Microsurgery. 2007;27(1):56-61.

[41] Matsuyama T, Mackay M, Midha R. Peripheral nerve repair and grafting techniques: a review. Neurol Med Chir (Tokyo). 2000;40(4):187-199.

[42] Ballance CA, Ballance HA, Stewart P. Remarks on the Operative Treatment Of Chronic Facial Palsy Of Peripheral Origin. Br Med J. 1903;1(2209):1009-1013.

[43] Harris, W, Low, V. "On The Importance Of Accurate Muscular Analysis In Lesions Of The Brachial Plexus; And The Treatment Of Erb's Palsy And Infantile Paralysis Of The Upper Extremity By Cross-Union Of The Nerve Roots." The British Medical Journal, vol. 2, no. 2234, 1903, pp. 1035–1038.

[44] Brenner MJ, Dvali L, Hunter DA, Myckatyn TM, Mackinnon SE. Motor neuron regeneration through end-to-side repairs is a function of donor nerve axotomy. Plast Reconstr Surg. 2007;120(1):215-223.

[45] Gulati AK. Immune response and neurotrophic factor interactions in peripheral nerve transplants. Acta Haematol. 1998;99(3):171-174.

[46] Gulati AK, Cole GP. Nerve graft immunogenicity as a factor determining axonal regeneration in the rat. J Neurosurg. 1990;72(1):114-122.

[47] Lassner F, Schaller E, Steinhoff G, Wonigeit K, Walter GF, Berger A. Cellular mechanisms of rejection and regeneration in peripheral nerve allografts. Transplantation. 1989;48(3):386-392.

[48] Mackinnon S, Hudson A, Falk R, Bilbao J, Kline D, Hunter D. Nerve allograft response: a quantitative immunological study. Neurosurgery. 1982;10(1):61-69.

[49] Pollard JD, Gye RS, McLeod JG. An assessment of immunosuppressive agents in experimental peripheral nerve transplantation. Surg Gynecol Obstet. 1971;132(5):839-845.

[50] Trumble TE, Shon FG. The physiology of nerve transplantation. Hand Clin. 2000;16(1):105-122.

[51] Yu LT, Rostami A, Silvers WK, Larossa D, Hickey WF. Expression of major histocompatibility complex antigens on inflammatory peripheral nerve lesions. J Neuroimmunol. 1990;30(2-3):121-128.

[52] Anderson PN, Turmaine M. Peripheral nerve regeneration through grafts of living and freeze-dried CNS tissue. Neuropathol Appl Neurobiol. 1986;12(4):389-399.

[53] Campbell JB, Bassett AL, Boehler J. Frozen-Irradiated Homografts Shielded with Microfilter Sheaths In Peripheral Nerve Surgery. J Trauma. 1963;3:303-311.

[54] Evans PJ, Mackinnon SE, Best TJ, et al. Regeneration across preserved peripheral nerve grafts. Muscle Nerve. 1995;18(10):1128-1138.

[55] Hiles RW. Freeze dried irradiated nerve homograft: a preliminary report. Hand. 1972;4(1):79-84.

[56] Lawson GM, Glasby MA. A comparison of immediate and delayed nerve repair using autologous freeze-thawed muscle grafts in a large animal model. The simple injury. J Hand Surg Br. 1995;20(5):663-700.

[57] Marmor L. The repair of peripheral nerves by irradiated homografts. Clin Orthop Relat Res. 1964;34:161-169.

[58] Martini AK. The lyophilized homologous nerve graft for the prevention of neuroma formation (animal experiment study). Handchir Mikrochir Plast Chir. 1985;17(5):266-269.

[59] Singh R, Lange SA. Experience with homologous lyophilised nerve grafts in the treatment of peripheral nerve injuries. Acta Neurochir (Wien). 1975;32(1-2):125-130.

[60] Wilhelm K. Briding of nerve defects using lyophilized homologous grafts. Handchirurgie. 1972;4(1):25-30.

[61] Wilhelm K, Ross A. Homeoplastic nerve transplantation with lyophilized nerve. Arch Orthop Unfallchir. 1972;72(2):156-67.

[62] IJpma FF, Van De Graaf RC, Meek MF. The early history of tubulation in nerve repair. J Hand Surg Eur Vol. 2008;33(5):581-586.

[63] Kehoe S, Zhang XF, Boyd D. FDA approved guidance conduits and wraps for peripheral nerve injury: a review of materials and efficacy. Injury. 2012;43(5):553-572.

[64] Chiu DT, Strauch B. A prospective clinical evaluation of autogenous vein grafts used as a nerve conduit for distal sensory nerve defects of 3 cm or less. Plast Reconstr Surg. 1990;86(5):928-934.

[65] Nijhuis TH, Bodar CW, van Neck JW, et al. Natural conduits for bridging a 15-mm nerve defect: comparison of the vein supported by muscle and bone marrow stromal cells with a nerve autograft. J Plast Reconstr Aesthet Surg. 2013;66(2):251-259.

[66] Fawcett JW, Keynes RJ. Muscle basal lamina: a new graft material for peripheral nerve repair. J Neurosurg. 1986;65(3):354-363.

[67] Brandt J, Dahlin LB, Kanje M, Lundborg G. Spatiotemporal progress of nerve regeneration in a tendon autograft used for bridging a peripheral nerve defect. Exp Neurol. 1999;160(2):386-393.

[68] Brandt J, Dahlin LB, Kanje M, Lundborg G. Functional recovery in a tendon autograft used to bridge a peripheral nerve defect. Scand J Plast Reconstr Surg Hand Surg. 2002;36(1):2-8.

[69] Brandt J, Dahlin LB, Lundborg G. Autologous tendons used as grafts for bridging peripheral nerve defects. J Hand Surg Br. 1999;24(3):284-290.

[70] Mackinnon SE, Hudson AR, Falk RE, Hunter DA. The nerve allograft response--an experimental model in the rat. Ann Plast Surg. 1985;14(4):334-339.

[71] Mackinnon SE, Hudson AR, Falk RE, Kline D, Hunter D. Peripheral nerve allograft: an immunological assessment of pretreatment methods. Neurosurgery. 1984;14(2):167-171.

[72] Yavuzer R, Ayhan S, Latifoğlu O, Atabay K. Turnover epineural sheath tube in primary repair of peripheral nerves. Ann Plast Surg. 2002;48(4):392-400.

[73] Tetik C, Ozer K, Ayhan S, Siemionow K, Browne E, Siemionow M. Conventional versus epineural sleeve neurorrhaphy technique: functional and histomorphometric analysis. Ann Plast Surg. 2002;49(4):397-403.

[74] Lubiatowski P, Unsal FM, Nair D, Ozer K, Siemionow M. The epineural sleeve technique for nerve graft reconstruction enhances nerve recovery. Microsurgery. 2008;28(3):160-167.

[75] Siemionow M, Duggan W, Brzezicki G, et al. Peripheral nerve defect repair with epineural tubes supported with bone marrow stromal cells: a preliminary report. Ann Plast Surg. 2011;67(1):73-84.

[76] Pittenger MF, Mackay AM, Beck SC, et al. Multilineage potential of adult human mesenchymal stem cells. Science. 1999;284(5411):143-147.

[77] Chen X, Li Y, Wang L, et al. Ischemic rat brain extracts induce human marrow stromal cell growth factor production. Neuropathology. 2002;22(4):275-279.

[78] Chen Q, Long Y, Yuan X, et al. Protective effects of bone marrow stromal cell transplantation in injured rodent brain: synthesis of neurotrophic factors. J Neurosci Res. 2005;80(5):611-619.

[79] Kan I, Barhum Y, Melamed E, Offen D. Mesenchymal stem cells stimulate endogenous neurogenesis in the subventricular zone of adult mice. Stem Cell Rev Rep. 2011;7(2):404-412.

[80] Nicaise C, Mitrecic D, Pochet R. Brain and spinal cord affected by amyotrophic lateral sclerosis induce differential growth factors expression in rat mesenchymal and neural stem cells. Neuropathol Appl Neurobiol. 2011;37(2):179-188.

[81] Djouad F, Charbonnier LM, Bouffi C, et al. Mesenchymal stem cells inhibit the differentiation of dendritic cells through an interleukin-6-dependent mechanism. Stem Cells. 2007;25(8):2025-2032.

[82] Lin G, Zhang H, Sun F, et al. Brain-derived neurotrophic factor promotes nerve regeneration by activating the JAK/STAT pathway in Schwann cells. Transl Androl Urol. 2016;5(2):167-175.

[83] Rauskolb S, Dombert B, Sendtner M. Insulin-like growth factor 1 in diabetic neuropathy and amyotrophic lateral sclerosis. Neurobiol Dis. 2017;97(Pt B):103-113.

[84] Messi ML, Delbono O. Target-derived trophic effect on skeletal muscle innervation in senescent mice. J Neurosci. 2003;23(4):1351-1359.

[85] Lindsay RM, Harmar AJ. Nerve growth factor regulates expression of neuropeptide genes in adult sensory neurons. Nature. 1989;337(6205):362-364.

[86] Verge VM, Richardson PM, Wiesenfeld-Hallin Z, Hökfelt T. Differential influence of nerve growth factor on neuropeptide expression in vivo: a novel role in peptide suppression in adult sensory neurons. J Neurosci. 1995;15(3 Pt 1):2081-2096.

[87] Nakayama T, Momoki-Soga T, Inoue N. Astrocyte-derived factors instruct differentiation of embryonic stem cells into neurons. Neurosci Res. 2003;46(2):241-249.

[88] Aizman I, Tate CC, McGrogan M, Case CC. Extracellular matrix produced by bone marrow stromal cells and by their derivative, SB623 cells, supports neural cell growth. J Neurosci Res. 2009;87(14):3198-3206.

[89] Li QM, Fu YM, Shan ZY, et al. MSCs guide neurite directional extension and promote oligodendrogenesis in NSCs. Biochem Biophys Res Commun. 2009;384(3):372-377.

[90] Chen J, Li Y, Katakowski M, et al. Intravenous bone marrow stromal cell therapy reduces apoptosis and promotes endogenous cell proliferation after stroke in female rat. J Neurosci Res. 2003;73(6):778-786.

[91] Kinnaird T, Stabile E, Burnett MS, et al. Marrow-derived stromal cells express genes encoding a broad spectrum of arteriogenic cytokines and promote in vitro and in vivo arteriogenesis through paracrine mechanisms [published correction appears in Circ Res. 2005 Aug 5;97(3):e51]. Circ Res. 2004;94(5):678-685.

[92] Kamihata H, Matsubara H, Nishiue T, et al. Implantation of bone marrow mononuclear cells into ischemic myocardium enhances collateral perfusion and regional function via side supply of angioblasts, angiogenic ligands, and cytokines. Circulation. 2001;104(9):1046-1052.

[93] Nagaya N, Fujii T, Iwase T, et al. Intravenous administration of mesenchymal stem cells improves cardiac function in rats with acute myocardial infarction through angiogenesis and myogenesis. Am J Physiol Heart Circ Physiol. 2004;287(6):H2670-H2676.

[94] Tang YL, Zhao Q, Qin X, et al. Paracrine action enhances the effects of autologous mesenchymal stem cell transplantation on vascular regeneration in rat model of myocardial infarction. Ann Thorac Surg. 2005;80(1):229-237.

[95] Tang YL, Zhao Q, Zhang YC, et al. Autologous mesenchymal stem cell transplantation induce VEGF and neovascularization in ischemic myocardium. Regul Pept. 2004;117(1):3-10.

[96] Uccelli A, Moretta L, Pistoia V. Mesenchymal stem cells in health and disease. Nat Rev Immunol. 2008;8(9):726-736.

[97] Zaminy A, Shokrgozar MA, Sadeghi Y, Noroozian M, Heidari MH, Piryaei A. Mesenchymal stem cells as an alternative for Schwann cells in rat spinal cord injury. Iran Biomed J. 2013;17(3):113-122.

[98] Wang J, Ding F, Gu Y, Liu J, Gu X. Bone marrow mesenchymal stem cells promote cell proliferation and neurotrophic function of Schwann cells in vitro and in vivo. Brain Res. 2009;1262:7-15.

[99] Ding P, Yang Z, Wang W, Wang J, Xue L. Transplantation of bone marrow stromal cells enhances infiltration and survival of CNP and Schwann cells to promote axonal sprouting following complete transection of spinal cord in adult rats. Am J Transl Res. 2014;6(3):224-235.

[100] Castillo-Melendez M, Yawno T, Jenkin G, Miller SL. Stem cell therapy to protect and repair the developing brain: a review of mechanisms of action of cord blood and amnion epithelial derived cells. Front Neurosci. 2013;7:194

[101] Gin-shaw S.L., Jorden R.C. 2002. Multiple trauma. In: Rosen's Emergency Medicine, Concepts and Clinical Practice. Marx R. (Ed). New York: Mosby. pp. 242-254.

[102] Jacques L, Kline DG: Response of the peripheral nerve to physical injury, Crockard A, Hayward R, Hoff JT (eds): Neurosurgery: The Scientific Basic of Clinical Practice, ed 3. London: Blackwell, 2000, Vol 1, pp 516-525

[103] Lundborg G, Dahlin LB, Danielsen N, et al. Nerve regeneration across an extended gap: a neurobiological view of nerve repair and the possible involvement of neuronotrophic factors. J Hand Surg Am. 1982;7(6):580-587.

[104] Tuttle H. Exposure of the brachial plexus with nerve transplantation. JAMA 61(1913): 15-17.

[105] Siemionow M, Uygur S, Ozturk C, Siemionow K. Techniques and materials for enhancement of peripheral nerve regeneration: a literature review. Microsurgery. 2013;33(4):318-328.

[106] Merle M, Dellon AL, Campbell JN, Chang PS. Complications from silicon-polymer intubulation of nerves. Microsurgery. 1989;10(2):130-133.

[107] Mackinnon SE, Dellon AL. Clinical nerve reconstruction with a bioabsorbable polyglycolic acid tube. Plast Reconstr Surg. 1990;85(3):419-424.

[108] Mackinnon SE, Dellon AL. A study of nerve regeneration across synthetic (Maxon) and biologic (collagen) nerve conduits for nerve gaps up to 5 cm in the primate. J Reconstr Microsurg. 1990;6(2):117-121.

[109] Meek MF, Coert JH. Clinical use of nerve conduits in peripheral-nerve repair: review of the literature. J Reconstr Microsurg. 2002;18(2):97-109.

[110] Meek MF, Coert JH. US Food and Drug Administration/Conformit Europe-approved absorbable nerve conduits for clinical repair of peripheral and cranial nerves. Ann Plast Surg. 2008;60(1):110-116.

[111] Kornfeld T, Vogt PM, Radtke C. Nerve grafting for peripheral nerve injuries with extended defect sizes. Wien Med Wochenschr. 2019;169(9-10):240-251.

[112] Cho MS, Rinker BD, Weber RV, et al. Functional outcome following nerve repair in the upper extremity using processed nerve allograft. J Hand Surg Am. 2012;37(11):2340-2349.

[113] Grinsell D, Keating CP. Peripheral nerve reconstruction after injury: a review of clinical and experimental therapies. Biomed Res Int. 2014;2014:698256.

[114] Mackinnon SE. Technical use of synthetic conduits for nerve repair. J Hand Surg Am. 2011;36(1):183.

[115] Klimczak A, Siemionow M, Futoma K, Jundzill A, Patrzalek D. Assessment of immunologic, proangiogenic and neurogenic properties of human peripheral nerve epineurium for potential clinical application. Histol Histopathol. 2017;32(11):1197-1205.

[116] Giusti G, Shin RH, Lee JY, Mattar TG, Bishop AT, Shin AY. The influence of nerve conduits diameter in motor nerve recovery after segmental nerve repair. Microsurgery. 2014 Nov;34(8):646-52.

[117] Shin RH, Friedrich PF, Crum BA, Bishop AT, Shin AY. Treatment of a segmental nerve defect in the rat with use of bioabsorbable synthetic nerve conduits: a comparison of commercially available conduits. J Bone Joint Surg 2009;91:2194–2204.

[118] Kemp SW, Syed S, Walsh SK, Zochodne DW, Midha R. Collagen nerve conduits promote enhanced axonal regeneration, schwann cell association, and neovascularization compared to silicone conduits. Tissue Eng Part A 2009;8:1975–1988.

[119] Moore AM, Kasukurthi R, Magill CK, Farhadi HF, Borschel GH, Mackinnon SE. Limitations of conduits in peripheral nerve repairs. Hand (N Y). 2009;4(2):180-186.

[120] Pereira Lopes FR, Camargo de Moura Campos L, Dias Corrêa J Jr, et al. Bone marrow stromal cells and resorbable collagen guidance tubes enhance sciatic nerve regeneration in mice. Exp Neurol. 2006;198(2):457-468.

[121] Shevchenko EK, Makarevich PI, Tsokolaeva ZI, et al. Transplantation of modified human adipose derived stromal cells expressing VEGF165 results in more efficient angiogenic response in ischemic skeletal muscle. J Transl Med. 2013;11:138.

[122] Petrova ES, Isaeva EN, Kolos EA, Korzhevskii DE. Vascularization of the Damaged Nerve under the Effect of Experimental Cell Therapy. Bull Exp Biol Med. 2018;165(1):161-165.

[123] Kingham PJ, Kolar MK, Novikova LN, Novikov LN, Wiberg M. Stimulating the neurotrophic and angiogenic properties of human adipose-derived stem cells enhances nerve repair. Stem Cells Dev. 2014;23(7):741-754.

[124] Fan L, Yu Z, Li J, Dang X, Wang K. Schwann-like cells seeded in acellular nerve grafts improve nerve regeneration. BMC Musculoskelet Disord. 2014;15:165.

[125] Yang Y, Yuan X, Ding F, et al. Repair of rat sciatic nerve gap by a silk fibroin-based scaffold added with bone marrow mesenchymal stem cells. Tissue Eng Part A. 2011;17(17-18):2231-2244.

[126] Zhao Z, Wang Y, Peng J, et al. Repair of nerve defect with acellular nerve graft supplemented by bone marrow stromal cells in mice. Microsurgery. 2011;31(5):388-394.

[127] Siemionow M, Cwykiel J, Uygur S, et al. Application of epineural sheath conduit for restoration of 6-cm long nerve defects in a sheep median nerve model. Microsurgery. 2019;39(4):332-339.

13. APPENDIX 1- University of Illinois at Chicago Office of Animal Care and Institutional Biosafety Committee Protocol Approval

UIC UNIVERSITY OF ILLINOIS AT CHICAGO

Office of Animal Care and Institutional
Biosafety Committee (OACIB) (M/C 672)
Office of the Vice Chancellor for Research
206 Administrative Office Building
1737 West Polk Street
Chicago, Illinois 60612

1/21/2015

Maria Siemionow
Orthopaedic Surgery
M/C 844

Dear Dr. Siemionow:

The protocol indicated below was reviewed in accordance with the Animal Care Policies and Procedures of the University of Illinois at Chicago and **renewed on 1/21/2015.**

Title of Application: **Novel Human Epineural conduit for Restoration of Long Nerve Defects in Rat Model**
ACC NO: **13-218**
Original Protocol Approval: **2/13/2014 (3 year approval with annual continuation required).**
Current Approval Period: **1/21/2015 to 1/21/2016**

Funding: ***Portions of this protocol are supported by the funding sources indicated in the table below.***
Number of funding sources: 1

Funding Agency	**Funding Title**			**Portion of Funding Matched**
Musculoskeletal Transplant Foundation	*Novel Engineered Human Epineural Conduit for Restoration of Long Nerve Defects*			*Portion of Grant is matched Matched for rat studies- linked to 13-230 for sheep*
Funding Number	**Current Status**	**UIC PAF NO.**	**Performance Site**	**Funding PI**
N/A	*Funded*	*2014-06351*	*UIC*	*Maria Sieminonow*

This institution has Animal Welfare Assurance Number A3460.01 on file with the Office of Laboratory Animal Welfare, NIH. **This letter may only be provided as proof of IACUC approval for those specific funding sources listed above in which all portions of the grant are matched to this ACC protocol.**

Thank you for complying with the Animal Care Policies and Procedures of the UIC.

Sincerely,

Bradley Merrill, PhD
Chair, Animal Care Committee

BM/*kg*
cc: BRL, ACC File

Phone (312) 996-1972 • Fax (312) 996-9088

14. APPENDIX 2- Local Ethics Committee for Animal Experiments (*Lokalna Komisja Etyczna do Spraw Doświadczeń na Zwierzętach Uniwersytet Przyrodniczy w Poznaniu*) decision

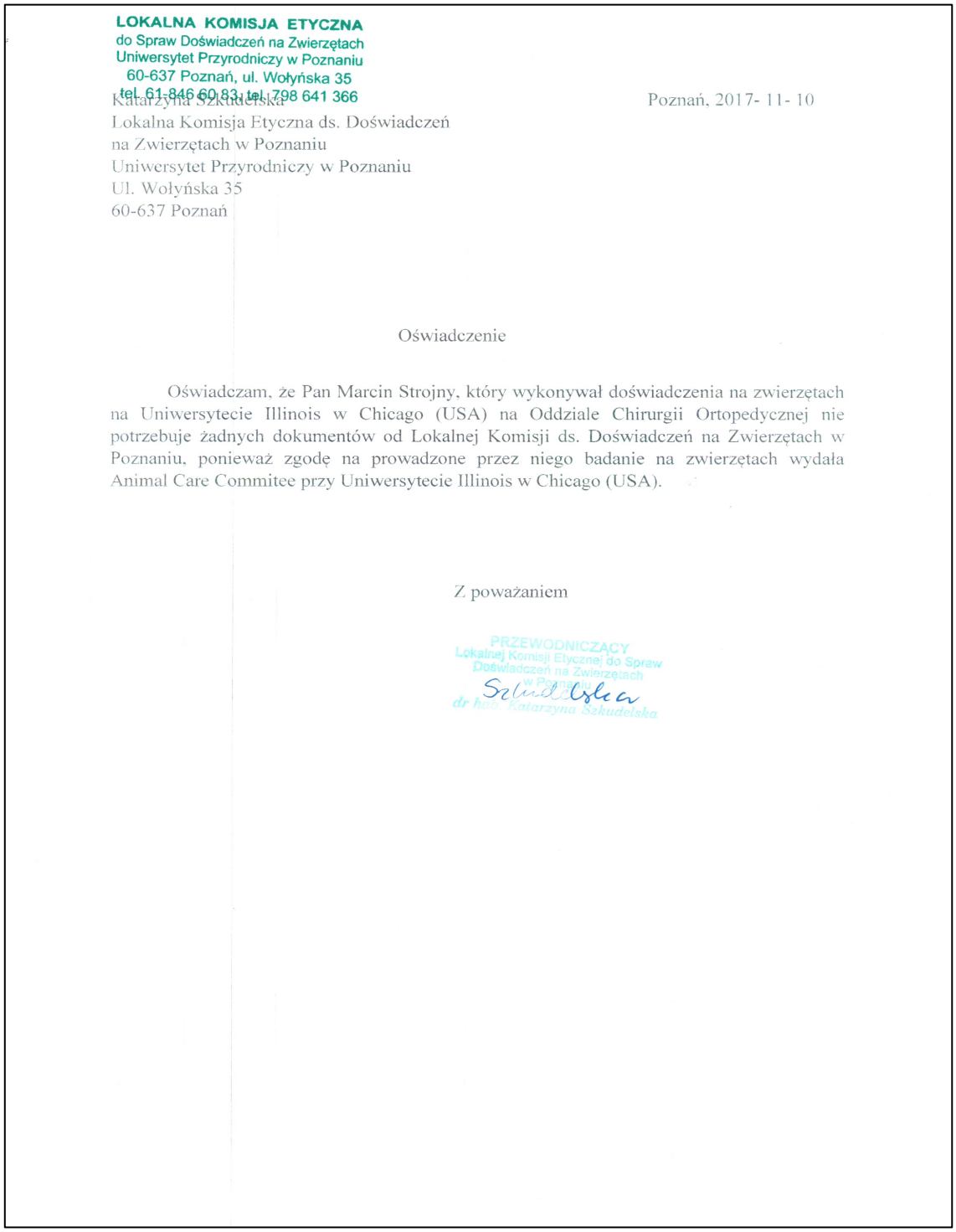

LOKALNA KOMISJA ETYCZNA
do Spraw Doświadczeń na Zwierzętach
Uniwersytet Przyrodniczy w Poznaniu
60-637 Poznań, ul. Wołyńska 35
tel. 61-846 60 83, tel. 798 641 366

Katarzyna Szkudelska
Lokalna Komisja Etyczna ds. Doświadczeń
na Zwierzętach w Poznaniu
Uniwersytet Przyrodniczy w Poznaniu
Ul. Wołyńska 35
60-637 Poznań

Poznań, 2017- 11- 10

Oświadczenie

Oświadczam, że Pan Marcin Strojny, który wykonywał doświadczenia na zwierzętach na Uniwersytecie Illinois w Chicago (USA) na Oddziale Chirurgii Ortopedycznej nie potrzebuje żadnych dokumentów od Lokalnej Komisji ds. Doświadczeń na Zwierzętach w Poznaniu, ponieważ zgodę na prowadzone przez niego badanie na zwierzętach wydała Animal Care Commitee przy Uniwersytecie Illinois w Chicago (USA).

Z poważaniem

PRZEWODNICZĄCY
Lokalnej Komisji Etycznej do Spraw
Doświadczeń na Zwierzętach
w Poznaniu
dr hab. Katarzyna Szkudelska